CLEARINGHOUSE FOR FEDERAL SCIENTIFIC AND TECHNICAL INFORMATION CFSTI
DOCUMENT MANAGEMENT BRANCH 410.11

LIMITATIONS IN REPRODUCTION QUALITY

ACCESSION # 603957

- [x] 1. WE REGRET THAT LEGIBILITY OF THIS DOCUMENT IS IN PART UNSATISFACTORY. REPRODUCTION HAS BEEN MADE FROM BEST AVAILABLE COPY.
- [x] 2. A PORTION OF THE ORIGINAL DOCUMENT CONTAINS FINE DETAIL WHICH MAY MAKE READING OF PHOTOCOPY DIFFICULT.
- [ ] 3. THE ORIGINAL DOCUMENT CONTAINS COLOR, BUT DISTRIBUTION COPIES ARE AVAILABLE IN BLACK-AND-WHITE REPRODUCTION ONLY.
- [ ] 4. THE INITIAL DISTRIBUTION COPIES CONTAIN COLOR WHICH WILL BE SHOWN IN BLACK-AND-WHITE WHEN IT IS NECESSARY TO REPRINT.
- [ ] 5. LIMITED SUPPLY ON HAND: WHEN EXHAUSTED, DOCUMENT WILL BE AVAILABLE IN MICROFICHE ONLY.
- [ ] 6. LIMITED SUPPLY ON HAND: WHEN EXHAUSTED DOCUMENT WILL NOT BE AVAILABLE.
- [ ] 7. DOCUMENT IS AVAILABLE IN MICROFICHE ONLY.
- [ ] 8. DOCUMENT AVAILABLE ON LOAN FROM CFSTI (TT DOCUMENTS ONLY).
- [ ] 9.

PROCESSOR:

TSL-107-10 64

COPY 2 of 3 COPIES

AIR FORCE INSTITUTE OF TECHNOLOGY

AIR UNIVERSITY
UNITED STATES AIR FORCE

SCHOOL OF ENGINEERING

WRIGHT-PATTERSON AIR FORCE BASE, OHIO

AF-WP-O-SEP 63 3M

AN EVALUATION OF SELECTED DESCRIBING
FUNCTIONS OF CONTROL SYSTEM
NONLINEARITIES

THESIS

GGC/EE/64-16

Robert R. Rankine, Jr.
Captain USAF

AF-WP-O-AUG 64 30

GGC/EE/64-16

AN EVALUATION OF SELECTED DESCRIBING FUNCTIONS OF CONTROL SYSTEM NONLINEARITIES

THESIS

Presented to the Faculty of the School of Engineering of
the Air Force Institute of Technology
Air University
in Partial Fulfillment of the
Requirements for the Degree of
Master of Science

By

Robert Richey Rankine, Jr., B.S.E.E.
Captain USAF
Graduate Guidance and Control

June 1964

Preface

Although this study was begun with the thought in mind of providing an unbiased evaluation of various describing-function generating schemes (unbiased, since I had no hand in any of them), it has ended up as an introduction to a describing-function generating scheme of my own, as well. I should not really call the corrected-conventional describing function my own, since it is really only an unconventional, "corrected" form of the conventional describing function developed by Kochenburger and others, and its <u>only</u> theoretical justification is that it is based on the conventional technique. Let me assure you, however, that the basic linear functions, used as being representative for the purpose of the study, were chosen <u>before</u> the idea of correcting the conventional describing function came to me, and therefore they in no way (intentionally, at least) were chosen because they favor the corrected-conventional technique. As a matter of fact, I first realized the possible benefit of such a correction while trying to improve on another unconventional technique presented by Gibson called the new rms describing function. And it was on his examples that I first had success.

I wish to express my appreciation for the encouragement, guidance, and assistance that my Faculty Thesis Advisor, Professor J. J. D'Azzo provided me, as well as for the original topic. I, furthermore, would like to thank Mr. R. O. Anderson of the Flight Control Division (R & TD) for sponsoring my work and also providing guidance and advice. Some of the greatest tangible assistance, though, came from Mr. H. E. Petersen of the Analysis Branch of the Digital Com-

puter Division (R&TD) who programmed and ran the describing function equations on the digital computer so that they could be plotted, and Mr. David K. Bowser of the Control Criteria Branch of the Flight Dynamics Laboratory, Flight Control Division (R&TD), who envisioned, programmed, and ran the digital computer verification of the analog computer results. Last, but not least, I thank my wife for typing this thesis.

Robert R. Rankine, Jr.

Abstract

A describing function is an amplitude-dependant generalized transfer function of a nonlinearity which can be used to represent the nonlinearity when its input is approximately sinusoidal. The simpler and more prominent or accurate describing-function generating schemes include (1) the conventional, (2) the minimum average error, (3) the equivalent gain, (4) the new rms, and (5) the corrected-conventional. An evaluation of these various schemes, based on the accuracy with which the describing functions they produce can predict the amplitude and frequency of self-sustained oscillations in a nonlinear system, reveals that the corrected-conventional describing functions are more accurate for single-valued nonlinearities.

Contents

Contents

AN EVALUATION OF SELECTED DESCRIBING FUNCTIONS OF CONTROL SYSTEM NONLINEARITIES

I. Introduction

A "generalized transfer function" is an approximately equivalent linear transfer function of a nonlinearity. It is used to represent the nonlinearity in control system analysis, but is applicable only when the input to the nonlinearity is sinusoidal. If the nonlinearity is independent of the input frequency, ω, and is solely dependent on the input amplitude, X, the generalized transfer function is known as a "describing function" or more specifically, a "sinusoidal describing function" (Ref 4:405). One derives the describing function of a particular nonlinearity by using some scheme to choose a sinusoid that will closely represent the output of the nonlinearity in some sense (Ref 7:153). The describing function then becomes the ratio of the amplitude and phase of the chosen output sinusoid to the amplitude and phase of the input sinusoid; that is,

$$\text{Describing Function} = N = \frac{\text{Amplitude and Phase of the Equivalent Sinusoidal Output of the Nonlinearity}}{\text{Amplitude and Phase of the Sinusoidal Input to the Nonlinearity.}} \qquad (1)$$

The foregoing definition of "describing function" is far more general than that usually encountered in literature on the subject. In the past, definitions of the function have usually encompassed only the describing function scheme developed by Kochenburger

(Ref 8:270ff) and others,[1] based on the Fourier Series representation of the output of the nonlinearity. Many other schemes for representing nonlinearities have been developed since Kochenburger's work, however, and limiting the definition to this "conventional" describing function is apt to cause confusion when one tries to define the others. Thus, the term "describing function" will be used in its most general sense in this paper, and the describing function originated by Kochenburger, which represents the output of the nonlinearity by the first harmonic of the Fourier Series expansion of the output waveform, will be referred to as the "conventional describing function."

Since there are many schemes for producing describing functions, the question arises: "Which, if any, is best?" The purpose of this paper is to answer that question.

The Problem

The problem is to evaluate comprehensively the accuracy with which the various describing functions can predict the amplitude and frequency of self-sustained oscillations in a nonlinear feedback control system. When this is done, it may be possible to choose a describing-function generating scheme which produces describing functions superior to all of the others, or it may be found that each type of nonlinearity favors a different scheme. In either case, the con-

[1] Kochenburger in the United States, Dutilh in France, and Goldfarb in Russia are generally given equal credit for having discovered the method since their works were made known about the same time.

trol system engineer shall be able to obtain greater accuracy in predicting the effects of a nonlinearity in a feedback control system as a result of this study. This paper is not intended to be a primer on the describing function method of analysis, but, rather, a comprehensive evaluation of a few of the describing functions which may be used in that analysis. Therefore, if the reader is unfamiliar with the general describing function technique for stability and limit cycle determination by direct polar (i.e., Nyquist) plots, it is recommended that he first consult the references (e.g., Ref 1:442-444).

Describing Function Generating Schemes to be Studied. Since it would be difficult, if not impossible, to research and include every scheme for generating describing functions ever invented, only the more simple and prominent or accurate methods will be included. These are (1) the conventional describing function originated by Kochenburger which expands the output of the nonlinearity in a Fourier series and uses the first Fourier harmonic as the equivalent sinusoidal output (Ref 8:270ff); (2) the minimum average error describing function originated by Gibson which, as its name indicates, minimizes the average error between the equivalent sinusoid and the output of the nonlinearity (Ref 2:381); (3) the equivalent gain originated by Prince which uses the maximum amplitude of the output of the nonlinearity as the amplitude of the equivalent sinusoid (Ref 10:217); (4) the new rms describing function originated by Gibson which is based on equating the rms value of the actual nonsinusoidal output of

the nonlinearity to the rms value of the equivalent sinusoidal output (Ref 3:1321); and (5) the corrected-conventional describing function developed by the author which includes the effects of Fourier harmonics higher than the first by taking as the amplitude of the equivalent output sine wave, the square root of the sum of the squares of the amplitudes of the first and third Fourier harmonics.

One of the more prominent methods of improving the accuracy of the conventional describing function, the use of Johnson's correction terms (Ref 6:169ff), will not be included. The calculation of the amplitude correction term is too complex to be very practical to the engineer. One important result obtained by Johnson, however, will be understood throughout this study: that the first correction term for the fundamental frequency is zero, and that therefore the describing function frequency prediction is generally quite accurate. Because of this fact, this study will be primarily aimed at improving the accuracy of the amplitude prediction; nevertheless, variations in the predicted frequencies will result when hysteresis is studied by the different schemes.

Nonlinearities to be Studied. In order to study how well a particular describing-function generating scheme can produce a describing function which accurately predicts a system oscillation, it is necessary to choose a number of nonlinearities to which to apply the scheme. The most often encountered nonlinearities are considered the most important, and the following nonlinearities are, in the opinion of the author, the most often encountered: (1) dead zone, (2) saturation, (3) dead zone combined with saturation, (4) the

ideal relay, (5) the relay combined with hysteresis, (6) the relay combined with dead zone, and (7) the relay combined with both dead zone and hysteresis. Each of these nonlinearities has an output which is both odd periodic and odd harmonic for sinusoidal inputs, or at least can be considered so by phase-shifting the axes.[2] Each of the 5 describing-function generating schemes chosen will be applied to each of the above 7 nonlinearities producing 35 different describing functions to be studied.

Linear Systems to be Studied. It is also necessary to choose some arbitrary, representative linear feedback systems into which to introduce the nonlinearities. These were chosen on the bases (1) that the frequency at which the direct polar plot of the system forward transfer function crosses the negative real axis be within the limits of the analog computer and its recording devices, so that the predictions can be checked experimentally without a lot of time scaling, and (2) that the system open loop transfer function be of higher than second order so that the describing function method is preferable over the phase plane method of analysis.[3] (Also, the system open loop transfer functions must be of higher than second order before self-

[2]A function is said to be odd periodic if $f(t)=-f(-t)$.
A function is said to be odd harmonic if $f(t)=-f(t+T/2)$, where T is the period.

[3]For a description of phase plane analysis see the references (Ref 12:65ff).

sustained oscillations can occur with nonlinearities that do not introduce a phase shift.) Nine different linear forward transfer functions to be used in unity feedback systems were chosen on these bases. They are described qualitatively in Table I on the following page. The table also indicates the nonlinearities with which each was coupled. Since there are to be five describing functions investigated for each nonlinearity, the scope of the problem involves 220 amplitude and frequency predictions, and, since each system must be checked on the analog computer as a basis for evaluation of the accuracy of the predictions, 44 analog computer runs.

Analysis of the Problem

Assumptions. The basic assumptions which one must make in order to use the describing function method of analysis to determine the amplitude and frequency of self-sustained oscillations are (1) that the system is unforced and does not vary with time, (2) that the nonlinearity is separable and is not frequency dependent,[4] and (3) that the linear transfer function provides sufficient low-pass filtering to permit excluding the higher harmonics from consideration (Ref 2:348). These assumptions are quite good for the nonlinearities and linear systems to be studied, and they are also generally true in practice. Since these assumptions are well understood by users of the describing function method, they will not be further belabored.

[4]Some authors extend the describing function to frequency dependent nonlinearities as well; however, as indicated in the definition on page 1, it would then be a "generalized transfer function" not a "describing function."

Table I

Qualitative Description of the Nine Linear
Forward Transfer Functions to Be Studied.

Linear Forward Transfer Functions				Nonlinearities Applied
Type*	Order**	Stability	Approximate (Direct Polar Plot) Real Axis Crossing***	
0	3	Unstable	- 3	
1	3	Unstable	- 3	
2	3	Unstable	- 3	
2	3	Unstable	-10	Saturation, Saturation with Dead Zone, Ideal Relay, Relay with Hysteresis, Relay with Dead Zone, Relay with Dead Zone and Hysteresis.
0	5	Unstable	-10	
1	5	Unstable	-10	
2	5	Unstable	-10	
3	3	Conditionally Stable #	- 3	Dead Zone
3	3	Conditionally Stable #	-10	

*Type 0, 1, and 2 systems are called position, velocity, and acceleration control systems, respectively, by some authors. The numbers 0, 1, and 2 refer to the power of the separable s, the Laplacian operator, in the denominator of the linear transfer function.

**The number of poles minus the number of zeros.

***The gain of each system was set for one of the two distinct crossings listed in order to provide a wide variation in the amplitudes of the sustained oscillations.

It is necessary to use a conditionally stable system in order to reach a stable limit cycle with a dead zone nonlinearity.

The new rms describing function has not been extended, as yet, to the analysis of nonlinearities with memory (Ref 2:384). In the author's opinion, however, this scheme can be applied quite easily to nonlinearities with memory that result in a phase shift of the output wave that can be calculated algebraically, such as for the hysteresis nonlinearities included in this paper. If the axes are shifted through the proper phase, the output of the nonlinearity becomes an odd-harmonic, odd-periodic function, and the new rms describing function method can easily be applied to determine the magnitude of the describing function. Furthermore, the shift in phase becomes the phase angle of the resulting new rms describing function.

The idea behind the corrected-conventional describing function is that perhaps the effect of harmonics higher than the first in the Fourier Series expansion of the output of the nonlinearity, each receiving a different degree of attenuation through the linear portion of the system, can be approximated by including the unattenuated effect of the third harmonic only.[5] This effect is "averaged in" by the same method one would use to obtain the combined effective rms value of two sine waves of different frequencies when the rms value of each is known. The square root of the sum of the squares of the first and third Fourier harmonics is therefore taken as the amplitude of the equivalent sinusoidal output of the nonlinearity, rather than just the first harmonic as in the conven-

[5] This explanation assumes that the output of the nonlinearity is odd harmonic in which case the third harmonic is the first harmonic above the fundamental.

tional describing function. It would seem that the corrected-conventional describing function would tend to overcompensate for the error caused by higher harmonics, especially as the order of the system is increased. However, the magnitude of the corrected-conventional describing function is generally less than that of the new rms describing function, thus making it applicable to a wider range of intermediate-order systems than the new rms describing function which tends to overcompensate (Ref 3:1321).

Criteria. It would be nice if the engineer could be guarenteed that one of the describing function schemes could provide him with predictions that were always within ten percent of the actual value and generally within three percent of the actual value of the amplitude and frequency of the self-sustained oscillations. To prove rigorously that a certain describing function generating scheme would always provide describing functions which were within ten percent of the true outcome would certainly be a complex and difficult, if not impossible, task. It is possible to postulate, however, based on the more or less arbitrary selection of linear systems for this experiment, that a particular method generally provides predictions which are within three percent of the true outcome, and/or is generally better than the other methods of prediction.

Procedure. The preceding criteria intrinsically call for a comparison of some kind between the various describing-function generating schemes. This was done in the following manner: (1) each of the 35 describing functions previously mentioned was derived,

(2) the direct polar plots of the linear systems and the negative inverse plots of the describing functions were compared to determine the intersection points, (3) the stable intersections were interpreted as predictions of the amplitude and frequency of self-sustained oscillations in the unforced, closed-loop system employing the nonlinearity, (4) the predictions were tabulated along with experimental data obtained by simulation of the actual nonlinear system on the analog computer, and (5) the experimental results were used as a basis of comparison of the accuracy of the various describing functions so that a preferable describing-function generating scheme could be selected.

By this procedure a "best" method of describing each of the selected nonlinearities will be postulated. In this way some guidelines will be added to the describing function method of nonlinear circuit analysis so that the control engineer may obtain quantitative as well as qualitative results from his work. In addition, the various methods of transient-response prediction which depend on the accuracy of the describing function may be improved.[6]

[6] For example, computing the closed-loop frequency response of nonlinear systems as described in the references (Ref 12:195-208).

II. Linear Systems

Table I in Chapter I qualitatively describes the forward transfer functions of the linear systems selected as representative of those often encountered in practice for the purpose of study. Since the conclusions and recommendations postulated in the last chapter of this paper are largely dependent on just how arbitrary and representative the linear systems are, this entire chapter is devoted to their description.

General Block Diagrams

The general block diagram of the linear systems discussed in the introduction is shown in Figure 1(a) below. Figure 1(b) shows the same system with a nonlinearity introduced. The nomenclature indicated in Figure 1(b) will be used throughout the remainder of this paper.

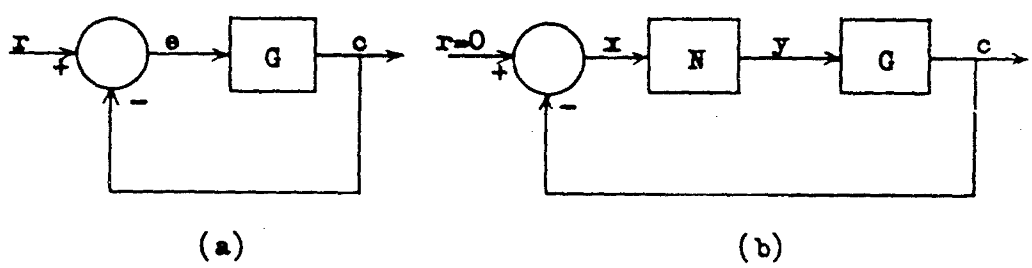

Figure 1

Unity feedback systems: (a) linear, (b) nonlinear, where G = linear forward transfer function, N = describing function which represents the nonlinearity when $x(t) = X \sin \omega t$.

Linear Transfer Functions

Three third-order and three fifth-order linear forward transfer functions were originally chosen to be used in this study. Their transfer functions are as follows, each written in two common forms:

$$G_1(s) = \frac{180}{(s+1)(s+2)(s+3)} \quad \text{or}$$

$$G_1(j\omega) = \frac{30}{(1+j\omega)(1+j0.5\omega)(1+j0.333\omega)} \tag{2}$$

$$G_2(s) = \frac{18}{s(s+1)(s+2)} \quad \text{or}$$

$$G_2(j\omega) = \frac{9}{j\omega(1+j\omega)(1+j0.5\omega)} \tag{3}$$

$$G_3(s) = \frac{4.76(s+0.1)}{s^2(s+1)^2} \quad \text{or}$$

$$G_3(j\omega) = \frac{0.476(1+j10\omega)}{(j\omega)^2(1+j\omega)^2} \tag{4}$$

$$G_4(s) = \frac{4650.3}{(s+1)(s+2)(s+3)(s+4)(s+5)} \quad \text{or}$$

$$G_4(j\omega) = \frac{38.75}{(1+j\omega)(1+j0.5\omega)(1+j0.333\omega)(1+j0.25\omega)(1+j0.2\omega)} \tag{5}$$

$$G_5(s) = \frac{301}{s(s+1)(s+2)(s+3)(s+4)} \quad \text{or}$$

$$G_5(j\omega) = \frac{12.54}{j\omega(1+j\omega)(1+j0.5\omega)(1+j0.333\omega)(1+j0.25\omega)} \tag{6}$$

$$G_6(s) = \frac{242.9(s+0.1)}{s^2(s+1)^2(s+5)^2} \quad \text{or}$$

$$G_6(j\omega) = \frac{0.9717(1+j10\omega)}{(j\omega)^2(1+j\omega)^2(1+j0.2\omega)^2} \tag{7}$$

In a block diagram arrangement such as that of Figure 1(a), Eqs (2), (3), and (4) become type 0, 1, and 2 systems, respectively. They are third order because their denominators are of order three higher than their numerators. Furthermore, their gains have been adjusted so that they cross the real axis of their direct polar plots at approximately -3. (See Figures 2, 3, and 4 at the end of this chapter.) Similarly, Eqs (5), (6), and (7) become type 0, 1, and 2 systems, respectively. They are fifth order because their denominators are of order five higher than their numerators. Their gains have been adjusted so that they cross the real axis of their direct polar plots at approximately -10. (See Figures 5, 6, and 7 at the end of this chapter.) These transfer functions are believed to be somewhat representative, since they, as most well-designed control systems, have no more than three to five dominant (closed-loop) roots, and also, the three types of systems generally encountered in practice are included. Furthermore, by establishing two separate real axis crossing points for each order group, both "large" and "small" (relatively speaking) limit cycle amplitudes can be obtained when the nonlinearities are introduced. However, in order to determine if the difference in accuracy between the predictions for $G_1(s)$, $G_2(s)$, and $G_3(s)$ and the predictions for $G_4(s)$, $G_5(s)$, and $G_6(s)$ was due to limit cycle amplitude or system order, the gain of $G_3(s)$ in Eq (4) was increased, allowing it to cross the real axis of the direct polar plot at the same point as $G_6(s)$ in Eq (7). Thus a seventh linear transfer function was introduced for study:

$$G_{3A}(s) = \frac{16.57(s+0.1)}{s^2(s+1)^2} \quad \text{or} \quad G_{3A}(j\omega) = \frac{1.657(1+j10\omega)}{(j\omega)^2(1+j\omega)^2} \tag{8}$$

The direct polar plot of this function is similar to that of Figure 4, except that the real axis crossing occurs at -10.339 instead of -2.975.

Eqs (2) through (8) comprise a set of representative linear functions into which to introduce the nonlinearities. Upon analysis of these systems, however, it was found that none would produce stable oscillations with a dead zone nonlinearity. Therefore, in order to study the accuracy with which each type of dead zone describing function can predict the amplitude and frequency of self-sustained oscillations, it is necessary to first devise a linear system which will produce stable oscillations when dead zone is introduced. Eqs (9) and (10) below are the forward transfer functions of two such systems.

$$G_7(s) = \frac{248.626(s+1)^2}{s^3(s+10)^2} \quad \text{or} \quad G_7(j\omega) = \frac{2.48626(1+j\omega)^2}{(j\omega)^3(1+j0.1\omega)^2} \tag{9}$$

$$G_{7A}(s) = \frac{828.753(s+1)^2}{s^3(s+10)^2} \quad \text{or}$$

$$G_{7A}(j\omega) = \frac{8.28753(1+j\omega)^2}{(j\omega)^3(1+j0.1\omega)^2} \tag{10}$$

As can be seen from an analysis of Figures 8(a) and (b) at the end of this chapter, these conditionally stable, type 3, third-order linear systems will exhibit stable oscillations when coupled with a dead zone nonlinearity. (The direct polar plot of $G_{7A}(s)$ is similar to that in Figure 8(a), except that the real axis crossings occur at -0.606833 and -10, instead of at -0.20605 and -3 as shown for system $G_7(s)$.)

Eqs (2) through (10) are the forward transfer functions of the so-called arbitrary, representative linear systems into which the nonlinearities covered in this study were introduced, with the exceptions noted. In future discussions in this paper, the linear functions of Eqs (2) through (10) will often be referred to by their subscripted symbols; i.e., $G_1(s)$ or $G_{3A}(j\omega)$, as has been done in several places in this chapter. With the linear systems thus established and understood, the next step is to generate some describing functions for the nonlinearities mentioned in Chapter I. This will be done in the next chapter.

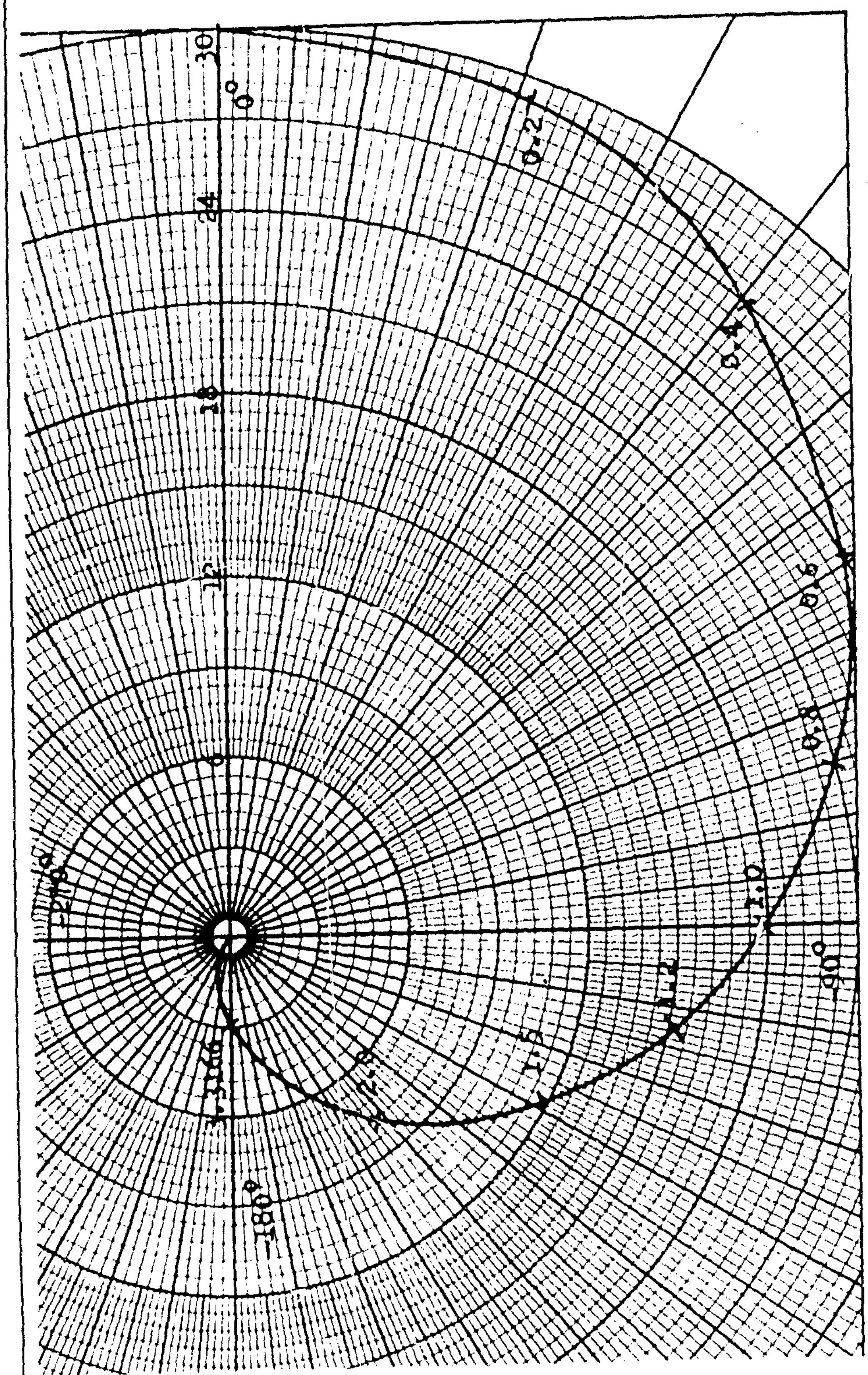

Figure 2

Direct polar plot of Eq (2): $G_1(j\omega) = \dfrac{30}{(1+j\omega)(1+j0.5\omega)(1+j0.333\omega)}$

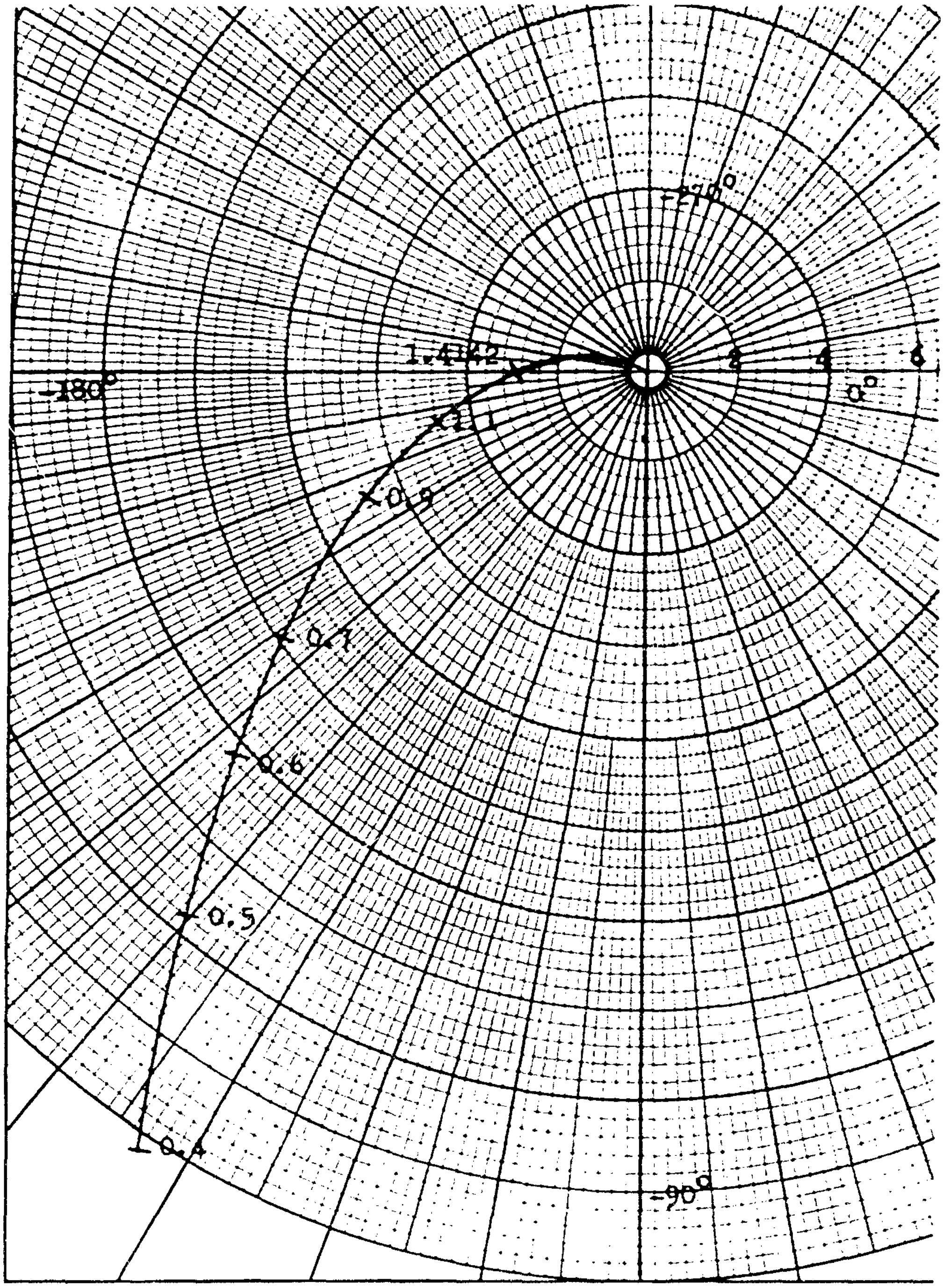

Figure 3

Direct polar plot of Eq (3): $G_2(j\omega) = \dfrac{9}{j\omega(1+j\omega)(1+j0.5\omega)}$

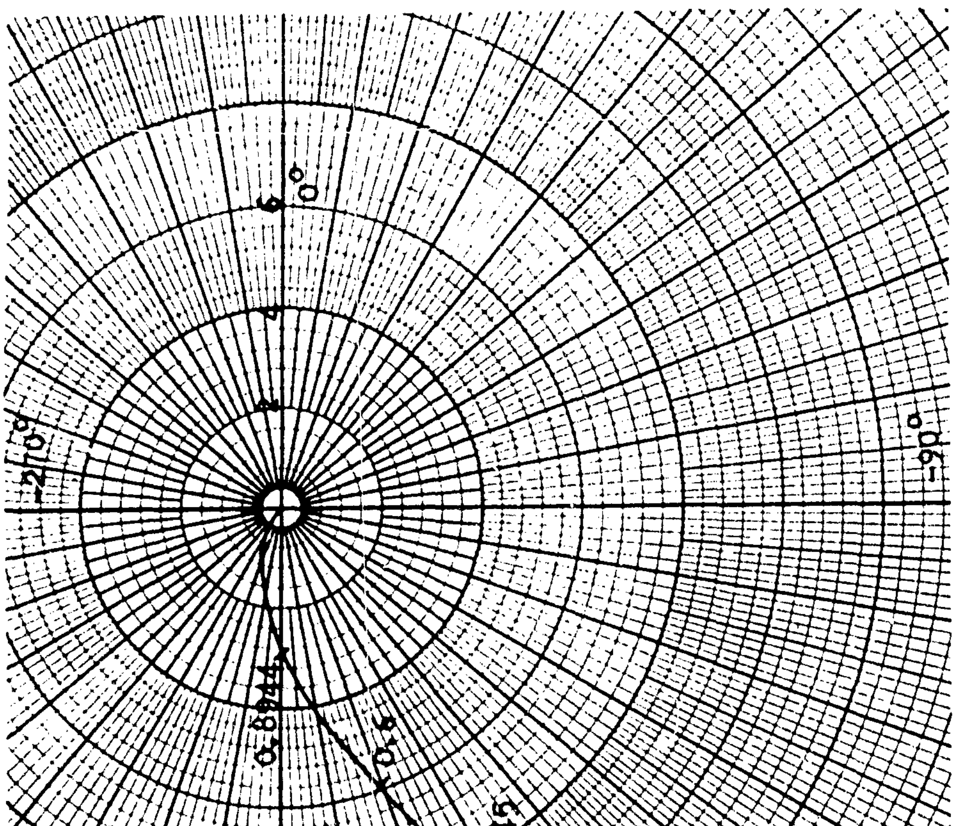

Figure 4

Direct polar plot of Eq (4): $G_3(j\omega) = \dfrac{0.476(1+j10\omega)}{(j\omega)^2(1+j\omega)^2}$

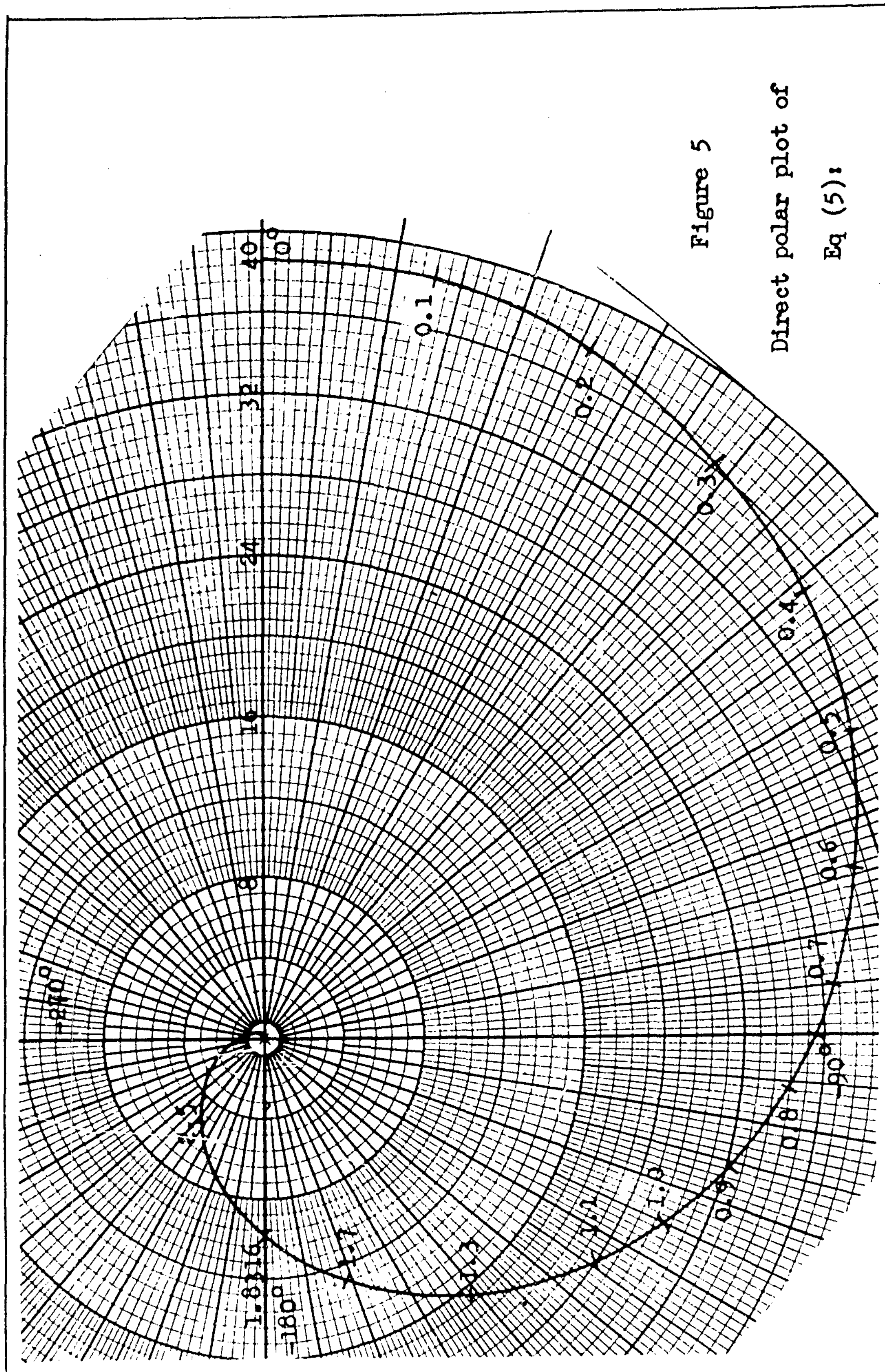

Figure 5

Direct polar plot of

Eq (5):

$$G_4(j\omega) = \frac{38.75}{(1+j\omega)(1+j0.5\omega)(1+j0.333\omega)(1+j0.25\omega)(1+j0.2\omega)}$$

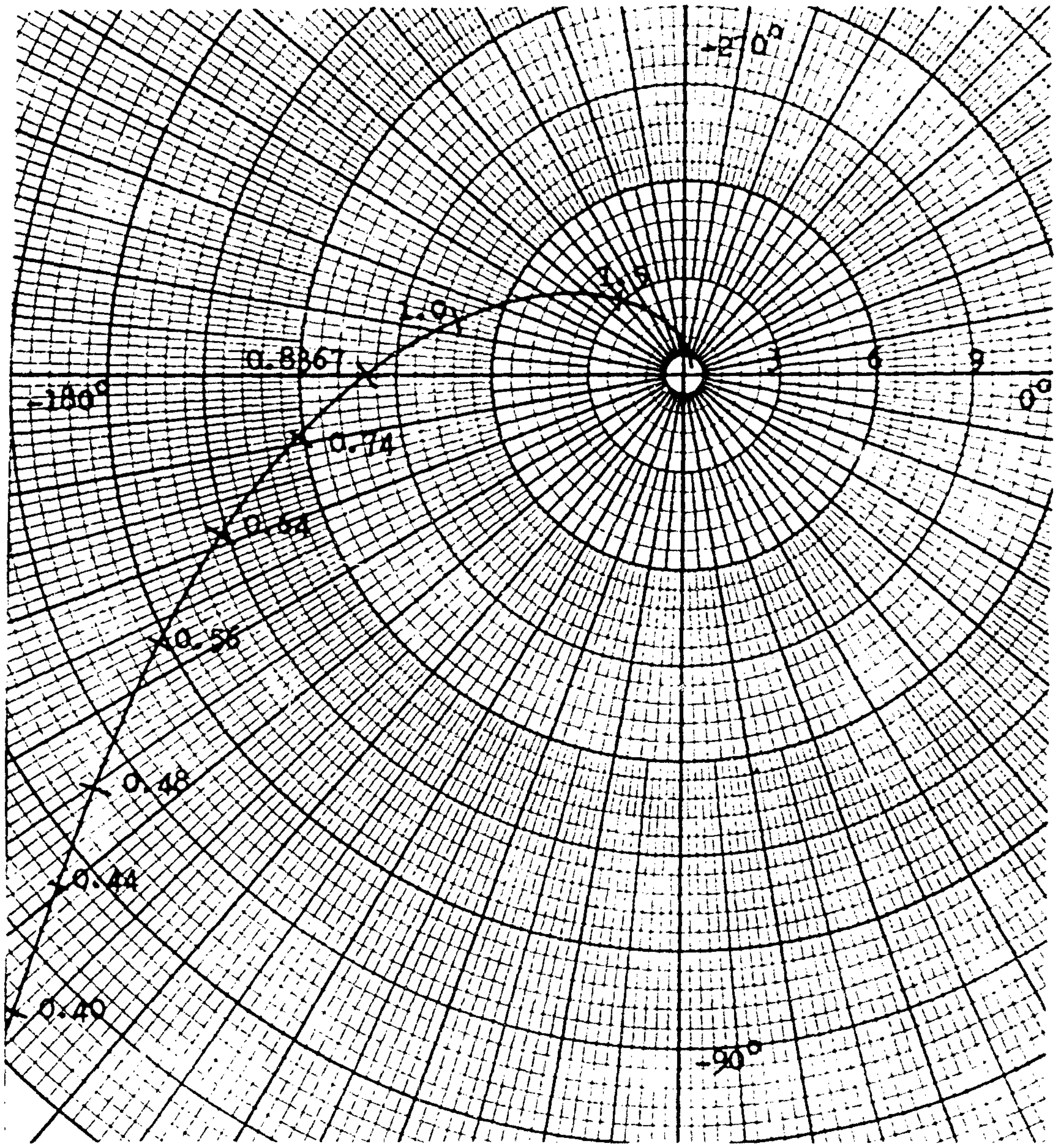

Figure 6

Direct polar plot of Eq (6):

$$G_5(j\omega) = \frac{12.54}{j\omega(1+j\omega)(1+j0.5\omega)(1+j0.333\omega)(1+j0.25\omega)}$$

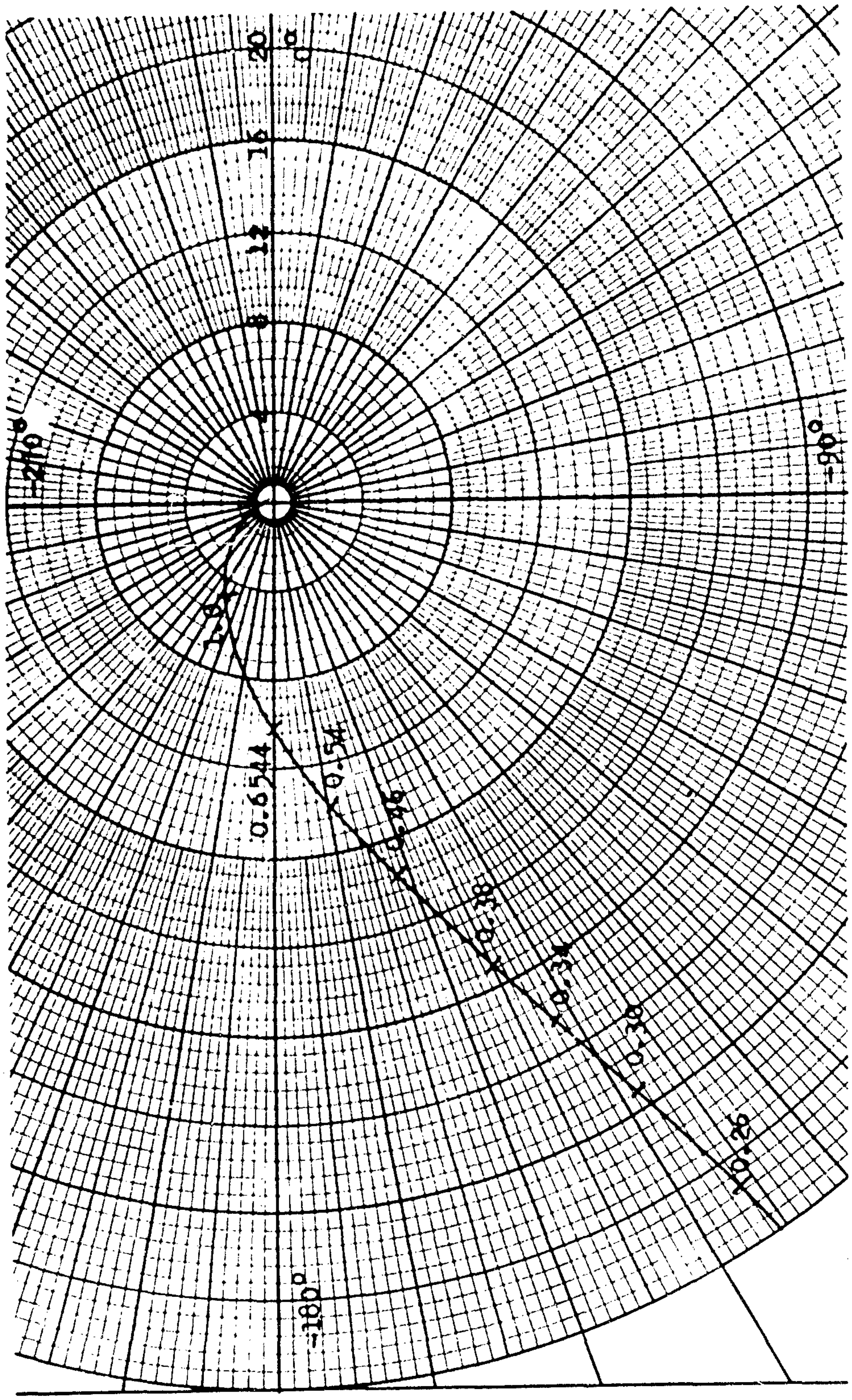

Figure 7

Direct polar plot of Eq (7): $G_6(j\omega) = \dfrac{0.9717(1+j10\omega)}{(j\omega)^2(1+j\omega)^2(1+j0.2\omega)^2}$

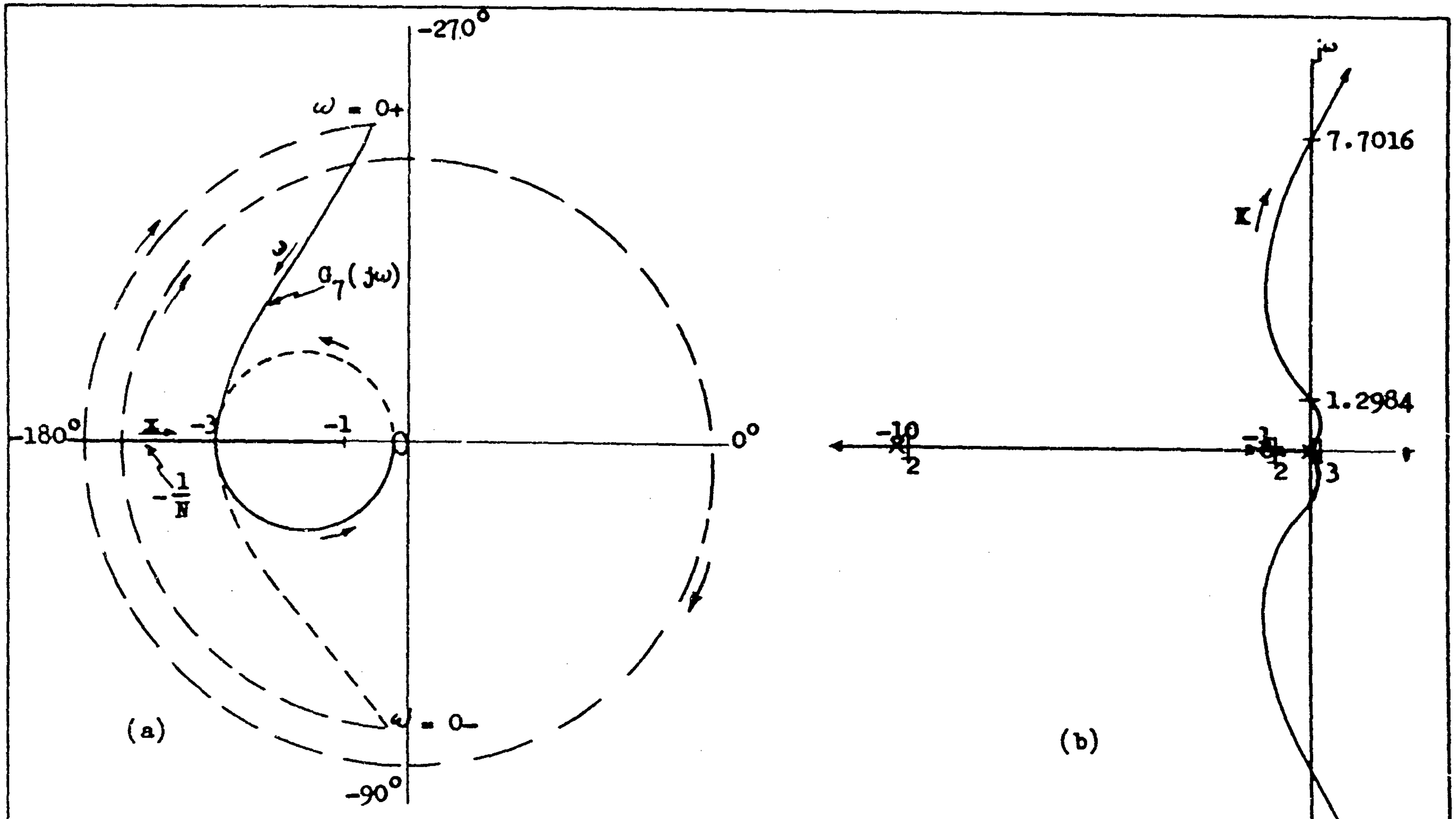

Figure 8

Sketches of the transfer function $G_7(s) = \frac{K(s+1)^2}{s^3(s+10)^2}$: (a) Direct Polar Plot (K = 248.626) and negative inverse dead zone describing function, (b) Root Locus.

III. Describing Functions

The general definition of a describing function is given on page one in the introduction of this paper. In this chapter that definition is expanded in order to define each of the specific describing-function generating schemes included in the study: conventional, minimum average error, equivalent gain, new rms, and corrected-conventional. Then the describing function that each scheme produces is listed for each of the nonlinearities included in the study: dead zone, saturation, saturation with dead zone, ideal relay, relay with hysteresis, relay with dead zone, and relay with both dead zone and hysteresis.

Definitions

Since the describing-function generating schemes differ only in the way the equivalent output sine wave from the nonlinearity is chosen, the definition of each scheme can be placed in a more or less standardized format based on the general definition of the describing function. This procedure will facilitate comparison of the methods. In each of the following definitions

$x(t) = X \sin \omega t$ = the input to the nonlinearity;

$y(t)$ = the actual nonsinusoidal output from the nonlinearity.

The Conventional Describing Function. The conventional describing function is equal to the amplitude and phase of an equivalent output sine wave, chosen as the fundamental frequency term in the Fourier series expansion of the actual nonsinusoidal output of the

nonlinearity, divided by the amplitude and phase of the input sine wave. In equation form (Ref 12:146)

$$N = \frac{(A_1^2 + B_1^2)^{\frac{1}{2}} \angle \tan^{-1}\left(\frac{A_1}{B_1}\right)}{X \angle 0^\circ} \tag{11}$$

where
$$A_1 = \frac{2}{\pi} \int_0^{\pi} y(t) \cos \omega t \, d\omega t$$

$$B_1 = \frac{2}{\pi} \int_0^{\pi} y(t) \sin \omega t \, d\omega t$$

<u>The Minimum Average Error Describing Function</u>. The minimum average error describing function is equal to the amplitude and phase of an equivalent output sine wave, so chosen as to minimize the average error between itself and the actual nonsinusoidal output of the nonlinearity, divided by the amplitude and phase of the input sine wave (Ref 2:381). Let ϕ be the phase difference between the input sine wave and the output periodic waveform. (The phase of the output is taken as the shift in axes necessary to make the output wave odd periodic.) The average error can be minimized by setting the difference of the area under a half cycle of the actual output and a half cycle of the equivalent sinusoidal output equal to zero. In equation form:

$$\begin{aligned} \text{average error} = 0 &= \int_{\phi}^{\pi+\phi} y(t) \quad d\omega t - \int_{\phi}^{\pi+\phi} Y_1 \sin(\omega t - \phi) \, d\omega t \\ &= \int_{\phi}^{\pi+\phi} y(t) \quad d\omega t - 2Y_1 \end{aligned} \tag{12}$$

where $Y_1 \sin(\omega t - \phi)$ is the equivalent output sinusoid. From Eqs (12) and (1) the describing function is, therefore,

$$N = \frac{\frac{1}{2} \int_{\phi}^{\pi+\phi} y(t) \quad d\omega t \quad \angle -\phi}{X \angle 0^\circ} \tag{13}$$

The Equivalent Gain Describing Function. The equivalent gain describing function is equal to the amplitude and phase of an equivalent output sine wave, chosen to have an amplitude equal to the peak value of the actual nonsinusoidal output of the nonlinearity, divided by the amplitude and phase of the input sine wave (Ref 10:217). In equation form

$$N = \frac{y(t)_{peak} \angle -\phi}{X \angle 0^{\circ}} \tag{14}$$

where ϕ is the phase difference between the input sine wave and the output periodic waveform. (The phase of the output is taken as the shift in axes necessary to make the output wave odd periodic.)

The New RMS Describing Function. The new rms describing function is equal to the amplitude and phase of an equivalent output sine wave, so chosen as to have the same rms value as the rms value of the actual nonsinusoidal output of the nonlinearity, divided by the amplitude and phase of the input sine wave. In equation form (Ref 2:382)

$$N = \frac{\sqrt{2}\left\{\frac{1}{2\pi}\int_0^{2}\left[y(t)\right]^2 d\,\omega t\right\}^{\frac{1}{2}} \angle -\phi}{X \angle 0^{\circ}}$$

$$= \frac{\left\{\frac{1}{\pi}\int_0^{2\pi}\left[y(t)\right]^2 d\,\omega t\right\}^{\frac{1}{2}} \angle -\phi}{X \angle 0^{\circ}} \tag{15}$$

where ϕ is the phase difference between the input sine wave and the output periodic waveform. (The phase of the output is taken as the shift in axes necessary to make the output wave odd periodic.)

The Corrected-Conventional Describing Function. The corrected-conventional describing function is equal to the amplitude and phase of an equivalent output sine wave, chosen to have an amplitude equal to the square root of the sum of the squares of the coefficients of the fundamental and third harmonic in the Fourier series expansion of the actual nonsinusoidal output of the nonlinearity[7] and a phase equal to the phase of the fundamental frequency term in the expansion, divided by the amplitude and phase of the input sine wave. In equation form

$$N = \frac{(A_1^2 + B_1^2 + A_3^2 + B_3^2)^{\frac{1}{2}} \underline{/\tan^{-1}\left(\frac{A_1}{B_1}\right)}}{X \underline{/0^\circ}} \tag{16}$$

where
$$A_1 = \frac{2}{\pi}\int_0^{\pi} y(t) \cos \omega t \; d\,\omega t$$

$$B_1 = \frac{2}{\pi}\int_0^{\pi} y(t) \sin \omega t \; d\,\omega t$$

$$A_3 = \frac{2}{\pi}\int_0^{\pi} y(t) \cos 3\,\omega t \; d\,\omega t$$

$$B_3 = \frac{2}{\pi}\int_0^{\pi} y(t) \sin 3\,\omega t \; d\,\omega t$$

[7]Only nonlinearities which produce odd-harmonic outputs are considered thus far in the definition; therefore, the third harmonic is the first harmonic above the fundamental.

The application of the 5 foregoing definitions to the 7 nonlinearities to be considered yields the 35 describing functions to be studied.

Derivations

The 35 describing functions are listed in Tables II through VIII on the following pages, with one table for each nonlinearity to be considered. The various describing functions listed are nondimensionalized to the extent necessary to enable graphic presentation of describing function by a single curve or family of curves. These describing functions were derived by applying Eqs (11), (13), (14), (15), and (16) to each nonlinearity. A list of where some of these derivations can be found is given in Appendix E. The derivations of the corrected-conventional describing functions, which are new, can be found in Appendix A, and plots of these can be found in Appendix D. Appendix B contains the derivations of the new rms describing functions for a relay with hysteresis and a relay with both dead zone and hysteresis. These describing functions had not heretofore been derived since Gibson had not yet extended the new rms describing function to nonlinearities which are not single-valued (Ref 2:384).

With the linear systems of Chapter II and the describing functions of this chapter thus established, it is now possible to proceed to the amplitude and frequency predictions and the comparison of those predictions with experimental results.

Table II

Describing Functions for Dead Zone as Derived by Various Describing-Function Generating Schemes.

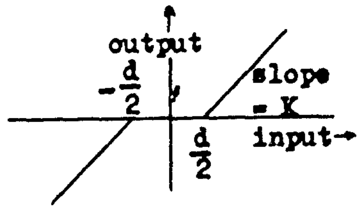

For each describing function in the table:

Definition of nonlinearity and parameters:

Definition of variable: $\alpha_d = \sin^{-1}\frac{d}{2X}$

Conditions:* $0 \leq \alpha_d \leq \pi/2$ Input: $x = X \sin\omega t$

Describing-Function Generating Scheme	Nondimensionalized Describing Function
Conventional	$\frac{N}{K} = \frac{1}{\pi}(\pi - 2\alpha_d - \sin 2\alpha_d)$
Minimum Average Error	$\frac{N}{K} = (\alpha_d - \frac{\pi}{2})\sin\alpha_d + \cos\alpha_d$
Equivalent Gain	$\frac{N}{K} = 1 - \sin\alpha_d$
New RMS	$\frac{N}{K} = \left[1 - \frac{2\alpha_d}{\pi} - \frac{3\sin 2\alpha_d}{\pi} + (2 - \frac{4\alpha_d}{\pi})\sin^2\alpha_d\right]^{\frac{1}{2}}$
Corrected-Conventional	$\frac{N}{K} = \frac{1}{\pi}\left[(\pi - 2\alpha_d - \sin 2\alpha_d)^2 + (\frac{1}{2}\sin 4\alpha_d + \frac{8}{3}\sin 2\alpha_d \sin^2\alpha_d - \frac{5}{3}\sin 2\alpha_d)^2\right]^{\frac{1}{2}}$

*This condition implies that $d/2 \leq X < \infty$. Also, if $X \leq d/2$, there is no output and $N/K = 0$.

Table III

Describing Functions for Saturation as Derived by Various Describing-Function Generating Schemes.

For each describing function in the table:

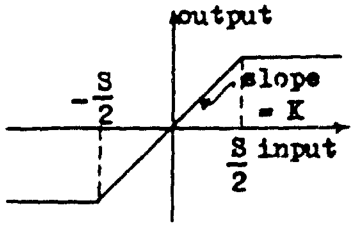

Definition of nonlinearity and parameters:

Definition of Variable: $\alpha_s = \sin^{-1}\frac{S}{2X}$

Conditions:* $0 \leq \alpha_s \leq \pi/2$ Input: $x = X \sin \omega t$

Describing-Function Generating Scheme	Nondimensionalized Describing Function
Conventional	$\frac{N}{K} = \frac{1}{\pi}(2\alpha_s + \sin 2\alpha_s)$
Minimum Average Error	$\frac{N}{K} = 1 + (\frac{\pi}{2} - \alpha_s)\sin\alpha_s - \cos\alpha_s$
Equivalent Gain	$\frac{N}{K} = \sin\alpha_s$
New RMS	$\frac{N}{K} = \left[\frac{2\alpha_s}{\pi} - \frac{\sin 2\alpha_s}{\pi} + (2 - \frac{4\alpha_s}{\pi})\sin^2\alpha_s\right]^{\frac{1}{2}}$
Corrected-Conventional	$\frac{N}{K} = \frac{1}{\pi}\left[(2\alpha_s + \sin 2\alpha_s)^2 + (\frac{5}{3}\sin 2\alpha_s - \frac{1}{2}\sin 4\alpha_s - \frac{8}{3}\sin 2\alpha_s \sin^2\alpha_s)^2\right]^{\frac{1}{2}}$

*This condition implies that $S/2 \leq X < \infty$. Also, if $X \leq S/2$, there is a linear output and $N/K = 1$.

Table IV

Describing Functions for Saturation with Dead Zone as Derived through the Application of Various Describing-Function Generating Schemes.

For each describing function in the table:

Definition of nonlinearity and parameters:

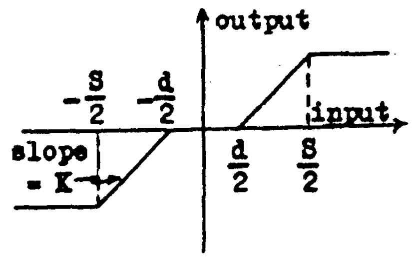

Definition of variables: $\alpha_d = \sin^{-1}\frac{d}{2X}$

$\alpha_s = \sin^{-1}\frac{S}{2X}$

Conditions:* $0 \leq \alpha_d < \alpha_s \leq \pi/2$ Input: $x = X \sin \omega t$

Describing-Function Generating Scheme	Nondimensionalized Describing Function
Conventional	$\frac{N}{K} = \frac{1}{\pi}(2\alpha_s - 2\alpha_d + \sin 2\alpha_s - \sin 2\alpha_d)$
Minimum Average Error	$\frac{N}{K} = (\alpha_d - \alpha_s)\sin\alpha_d + (\frac{\pi}{2} - \alpha_s)(\sin\alpha_s - \sin\alpha_d) + \cos\alpha_d - \cos\alpha_s$
Equivalent Gain	$\frac{N}{K} = \sin\alpha_s - \sin\alpha_d$
New RMS	$\frac{N}{K} = \left(\frac{1}{\pi}\left\{2(\alpha_s - \alpha_d) - \sin 2\alpha_s - 3\sin 2\alpha_d + 8\left[\cos\alpha_s + (\alpha_s - \frac{\pi}{2})\sin\alpha_s\right]\sin\alpha_d + 4(\frac{\pi}{2} - \alpha_d)\sin^2\alpha_d + 4(\frac{\pi}{2} - \alpha_s)\sin^2\alpha_s\right\}\right)^{\frac{1}{2}}$
Corrected-Conventional	$\frac{N}{K} = \frac{1}{\pi}\left[(2\alpha_s - 2\alpha_d + \sin 2\alpha_s - \sin 2\alpha_d)^2 + (\frac{5}{3}\sin 2\alpha_s - \frac{5}{3}\sin 2\alpha_d - \frac{1}{2}\sin 4\alpha_s + \frac{1}{2}\sin 4\alpha_d - \frac{16}{3}\sin^3\alpha_s\cos\alpha_s + \frac{16}{3}\sin^3\alpha_d\cos\alpha_d)^2\right]^{\frac{1}{2}}$

*These conditions imply that $S/2 \leq X < \infty$ and $S > d$. If $X < S/2$, Table II applies.

Table V

Describing Functions for an Ideal Relay as Derived through the Application of Various Describing-Function Generating Schemes.

For each describing function in the table:

Definition of nonlinearity and parameters:

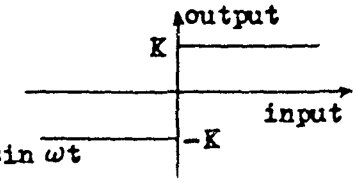

Conditions: $0 \angle X \angle \infty$ Input: $x = X \sin \omega t$

Describing-Function Generating Scheme	Nondimensionalized Describing Function
Conventional	$\frac{N}{K} = \frac{4}{\pi X} = \frac{1.273}{X}$
Minimum Average Error	$\frac{N}{K} = \frac{\pi}{2X} = \frac{1.571}{X}$
Equivalent Gain	$\frac{N}{K} = \frac{1}{X}$
New RMS	$\frac{N}{K} = \frac{\sqrt{2}}{X} = \frac{1.414}{X}$
Corrected-Conventional	$\frac{N}{K} = \frac{4}{\pi X}\sqrt{\frac{10}{9}} = \frac{1.342}{X}$

Table VI

Describing Functions for a Relay with Hysteresis as Derived through the Application of Various Describing-Function Generating Schemes.

For each describing function in the table:

Definition of nonlinearity and parameters:

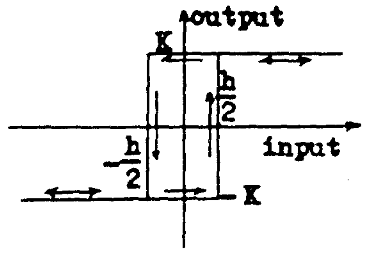

Definition of variable: $\alpha_h = \sin^{-1} \frac{h}{2X}$

Conditions: $h/2 \leq X < \infty$ Input: $x = X \sin \omega t$

Describing-Function Generating Scheme	Nondimensionalized Describing Function*
Conventional	$\frac{N}{K} = \frac{1.273}{X} e^{-j\alpha_h}$
Minimum Average Error	$\frac{N}{K} = \frac{1.571}{X} e^{-j\alpha_h}$
Equivalent Gain	$\frac{N}{K} = \frac{1}{X} e^{-j\alpha_h}$
New RMS	$\frac{N}{K} = \frac{1.414}{X} e^{-j\alpha_h}$
Corrected-Conventional	$\frac{N}{K} = \frac{1.342}{X} e^{-j\alpha_h}$

* $e^{-j\alpha_h}$ is complex number notation for $1 \angle -\alpha_h$.

Table VII

Describing Functions for a Relay with Dead Zone as Derived through the Application of Various Describing-Function Generating Schemes.

For each describing function in the table:

Definition of nonlinearity and parameters:

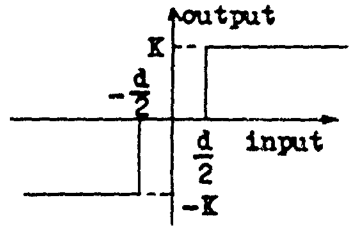

Definition of variable: $\alpha_d = \sin^{-1} \frac{d}{2X}$

Conditions:* $0 \leq \alpha_d \leq \pi/2$ Input: $x = X \sin \omega t$

Describing-Function Generating Scheme	Nondimensionalized Describing Function
Conventional	$\frac{Nd}{K} = \frac{4}{\pi} \sin 2\alpha_d$
Minimum Average Error	$\frac{Nd}{K} = (\pi - 2\alpha_d) \sin \alpha_d$
Equivalent Gain	$\frac{Nd}{K} = 2 \sin \alpha_d$
New RMS	$\frac{Nd}{K} = 2 \left[(2 - \frac{4\alpha_d}{\pi}) \sin^2 \alpha_d \right]^{\frac{1}{2}}$
Corrected-Conventional	$\frac{Nd}{K} = \frac{4}{\pi} \sin 2\alpha_d \left[1 + \frac{1}{9}(1 - 4 \sin^2 \alpha_d)^2 \right]^{\frac{1}{2}}$

*This condition implies that $d/2 \leq X < \infty$. Also, if $X \leq d/2$, there is no output and $Nd/K = 0$.

Table VIII

Describing Functions for a Relay with Dead Zone and Hysteresis as Derived through the Application of Various Describing-Function Generating Schemes.

For each describing function in the table:

Definition of nonlinearity and parameters:

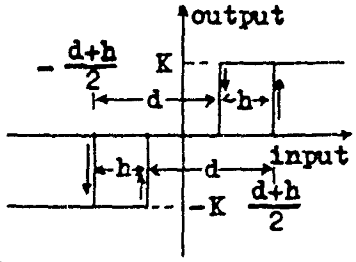

Definition of Variables: $\alpha = \sin^{-1}\left(\frac{d+h}{2X}\right)$

$$\beta = \pi - \sin^{-1}\left(\frac{d-h}{2X}\right)$$

Conditions:* $0 \leq \alpha \leq \pi/2$ Input: $x = X \sin \omega t$

Describing-Function Generating Scheme	Nondimensionalized Describing Function
Conventional	$\frac{N(d+h)}{K} = \frac{8}{\pi} \sin\alpha \; \sin\left(\frac{\beta-\alpha}{2}\right) \; e^{j\left(\frac{\pi}{2} - \frac{\alpha+\beta}{2}\right)}$
Minimum Average Error	$\frac{N(d+h)}{K} = (\beta-\alpha)\sin\alpha \; e^{j\left(\frac{\pi}{2} - \frac{\alpha+\beta}{2}\right)}$
Equivalent Gain	$\frac{N(d+h)}{K} = 2 \sin\alpha \; e^{j\left(\frac{\pi}{2} - \frac{\alpha+\beta}{2}\right)}$
New RMS	$\frac{N(d+h)}{K} = 2\left[\frac{2}{\pi}(\beta-\alpha)\sin^2\alpha\right]^{\frac{1}{2}} e^{j\left(\frac{\pi}{2} - \frac{\alpha+\beta}{2}\right)}$
Corrected-Conventional	$\frac{N(d+h)}{K} = \frac{8}{\pi} \sin\alpha \; \sin\left(\frac{\beta-\alpha}{2}\right)\left\{1 + \frac{1}{9}\left[1 - 4\cos^2\left(\frac{\beta-\alpha}{2}\right)\right]^2\right\}^{\frac{1}{2}} e^{j\left(\frac{\pi}{2} - \frac{\alpha+\beta}{2}\right)}$

*This condition implies that $(d+h)/2 \leq X < \infty$. Also, if $X \leq (d+h)/2$, there is no output and $\frac{N(d+h)}{K} = 0$.

IV. Amplitude and Frequency Predictions

In order to preserve continuity in the discussion to follow, only one nonlinearity will be discussed at a time. That is, for each nonlinearity the technique used to predict the amplitude and frequency of the self-sustained oscillations will be presented, followed by a comparison with the experimental results and a discussion of a few conclusions which may be drawn from the comparison, before moving on to another nonlinearity. Thus this chapter represents several small studies within a larger study, but this is a necessary consequence of the nature of the problem. The answer to the question "Which describing function is best?" may depend on the particular nonlinearity under consideration.

In the analysis to follow, the "gain," K, of the nonlinearity is sometimes other than unity. However, this does not defeat the purpose of having two separate axis crossings for the linear portion of the system (See Figure 2 through 8 in Chapter II) by changing the loop gain, as one might think. The main reason for having two separate axis crossings for the linear transfer functions was to provide an adequate separation of the systems into two groups, so that the "gain," K, of each nonlinearity could then be adjusted to provide a "small" amplitude limit-cycle group and a "large" amplitude limit-cycle group. That is, exactly where the "large" signal and "small" signal portions of the describing function curve occur depend on the nature of each individual nonlinearity. Therefore, the value of K must be selected individually for each nonlinearity, so

that the separation will actually provide what may be considered "large" and "small" limit-cycle amplitudes for that nonlinearity.

Saturation

If a saturation nonlinearity is introduced into one of the linear systems, $G_1(s)$ through $G_6(s)$, or $G_{3A}(s)$, in the manner shown in Figure 1(b) on page 11, a stability analysis will reveal that stable, self-sustained oscillations will result. A normalized plot of each of the five saturation describing functions listed in Table III on page 29 is shown in Figure 9 on page 38. The values of the parameters of the saturation nonlinearity were chosen as S = 3 and K = 0.5. The amplitude and frequency predictions by each of the five describing functions for each of the seven systems were calculated in the following manner:

(1) Use Eqs (2) through (8) or Figures 2 through 7 in Chapter II to calculate the negative real axis crossing point of $G_n(j\omega)$ on the direct polar plot. The value of $G_n(j\omega)$ at the negative real axis crossing is equal to $-1/N$, and the value of ω at the negative real axis crossing is the predicted frequency of the self-sustained oscillations.

(2) Calculate the value of $-K/N$ and use Figure 9 to determine the value of $2X/S$ for each system and each describing function.

(3) Calculate the value of X from the known values of $2X/S$ and S. X is then the predicted amplitude of the self-sustained oscillations for that particular describing function and system.

The results of the application of the foregoing procedure are tabulated in Table IX on page 39. In order to determine the accu-

racy of the predictions, each of the seven nonlinear systems was simulated on an analog computer. (The circuits used in the simulation are shown in Appendix C.) The analog computer experimental results are also shown in Table IX, along with the percentage of error of each prediction based on the experimental results.

Table X on page 40 is a comparison, based on the error figures in Table IX, of the various saturation describing functions. It shows that the saturation nonlinearity seems to favor the conventional describing function, although it can be seen from an analysis of Table IX that the accuracy of the corrected-conventional describing function becomes generally better as the amplitude of the limit cycle is increased. The situation is somewhat different, however, when dead zone is added to the saturation, which is the next nonlinearity to be discussed.

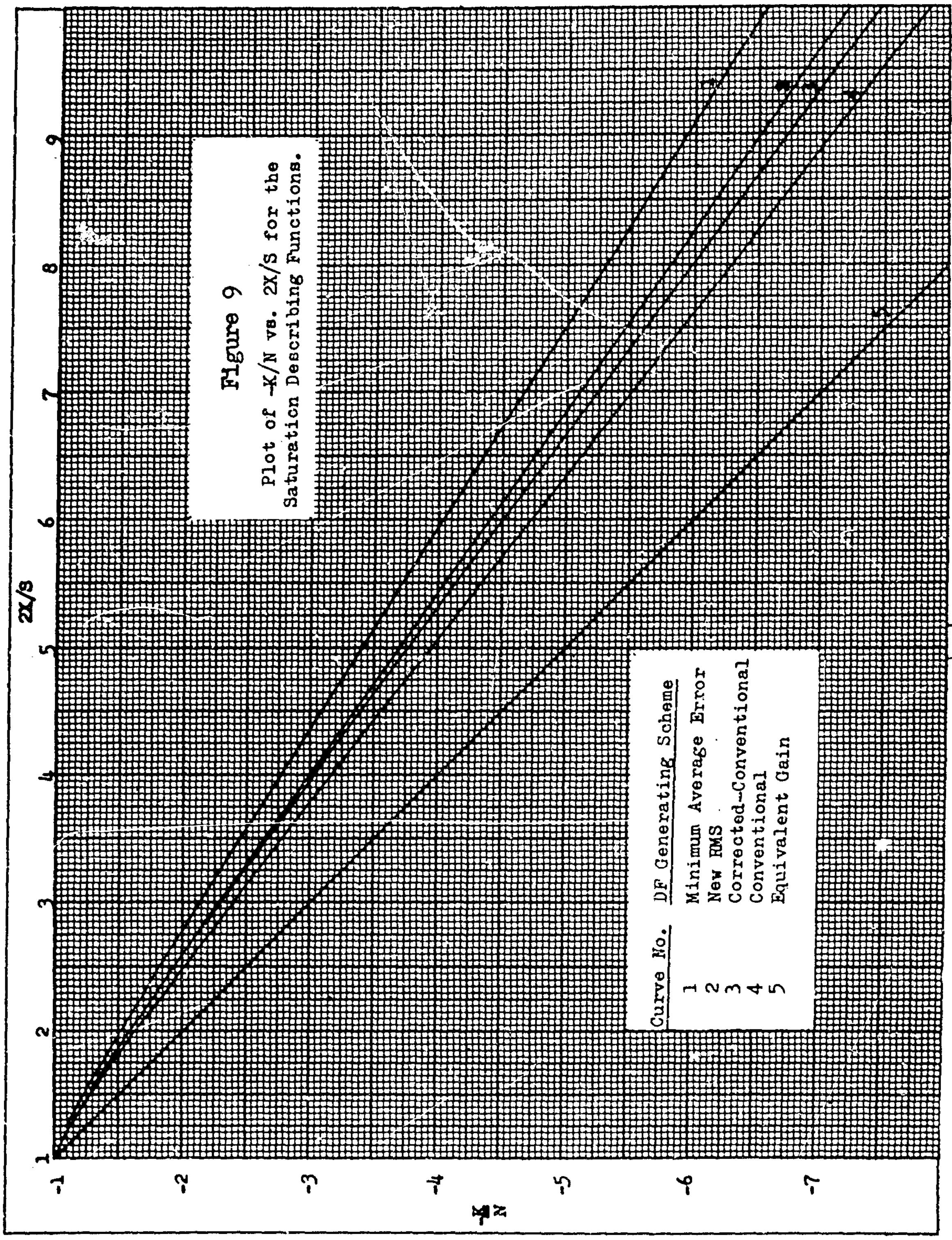

Figure 9

Plot of -K/N vs. 2X/S for the Saturation Describing Functions.

Table IX

Prediction of the Amplitude and Frequency of Self-Sustained Oscillations in Seven Different Feedback Systems with Saturation by Various Describing Functions.**

Linear Function	Experimental Amplitude	Describing Function Amplitude Predictions and Errors										Experimental Frequency (rad/sec)	Predicted* Frequency (rad/sec)	% Error in Frequency Prediction
		Conventional		Minimum Average Error		Equivalent Gain		New RMS		Corrected-Conventional				
		Amplitude	% Error	Amplitude	% Error	Amplitude	% Error	Amplitude	% Error	Amplitude	% Error			
$G_1(j\omega)$	2.723	2.715	-0.2938	2.955	+ 8.520	2.25	-17.37	2.805	+3.011	2.805	+3.011	3.279	3.3166	+1.134
$G_2(j\omega)$	2.741	2.715	-0.9486	2.955	+ 7.807	2.25	-17.91	2.805	+2.282	2.805	+2.282	1.404	1.4142	+0.7265
$G_3(j\omega)$	2.722	2.70	-0.8082	2.925	+ 7.458	2.23	-18.08	2.775	+1.947	2.775	+1.947	0.8875	0.8944	+0.7775
$G_4(j\omega)$	9.575	9.525	-0.5222	11.295	+17.96	7.50	-21.67	10.275	+7.311	10.00	+4.439	1.821	1.8316	+0.5821
$G_5(j\omega)$	9.816	9.525	-2.965	11.295	+15.07	7.70	-23.59	10.275	+4.676	10.00	+1.875	0.8192	0.83666	+2.131
$G_6(j\omega)$	10.235	9.825	-4.006	11.715	+14.46	7.75	-24.28	10.65	+4.055	10.365	+1.270	0.6334	0.6544	+3.209
$G_{3A}(j\omega)$	10.232	9.825	-3.978	11.715	+14.49	7.75	-24.26	10.65	+4.085	10.365	+1.300	0.8711	0.8944	+2.675

*All of the describing functions listed predict the same frequency.

**S = 3, K = 0.5 (See Table III, page 29).

(Original data)

Table X

Comparison of the Prediction Errors of the Various Saturation Describing Functions.

From the preceding table of predictions and errors, the arithmetic mean error, median error, etc., for each of the saturation describing functions can be calculated in order to give an overall indication of the accuracy with which a particular type of describing function (i.e., conventional, minimum average error, etc.) can predict the amplitude and frequency of self-sustained oscillations in the presence of saturation.

Error Criterion	Describing Function Amplitude Errors (%)					Describing Function Frequency Errors *
	Conventional	Minimum Average Error	Equivalent Gain	New RMS	Corrected-Conventional	
Arithmetical Mean Error	-1.9317 #	+12.252	-21.02	+3.909	+2.303	+1.6050
Median Error	-0.9486 #	+14.46	-21.67	+4.055	+1.947	+1.134
Maximum Magnitude of Error	-4.006 #	+17.96	-24.28	+7.311	+4.439	+3.209
Arithmetical Mean of Absolute Error	1.9317 #	12.252	21.02	3.909	2.303	1.6050

* All of the saturation describing functions listed predict the same frequency for an individual problem, and therefore the frequency error analysis applies equally to each type.

# Indicates the minimum magnitude of amplitude error in that row; therefore, the column with the most #'s is the column of what is possibly the best describing function for saturation.

Saturation Combined with Dead Zone

If a nonlinearity consisting of saturation combined with dead zone is introduced into one of the linear systems, $G_1(s)$ through $G_6(s)$, or $G_{3A}(s)$, in the manner shown in Figure 1(b) on page 11, a stability analysis will reveal that stable, self-sustained oscillations can exist. A normalized plot of each of the five saturation describing functions listed in Table IV on page 30 is shown in Figure 10 on page 43 for the case of S/d = 2. The values of the parmeters of the nonlinearity were chosen as S = 4, d = 2, and K = 1 for the purpose of analysis. The predictions of the amplitude and frequency of the self-sustained oscillations by each of the five describing functions for each of the seven systems mentioned were calculated in a manner similar to that used for saturation:

(1) Use Eqs (2) through (8) or Figures 2 through 7 in Chapter II to calculate the negative real axis crossing point of $G_n(j\omega)$ on the direct polar plot. The value of $G_n(j\omega)$ at the negative real axis crossing is equal to $-1/N$, and the value of ω at the negative real axis crossing is the predicted frequency of the self-sustained oscillations.

(2) Calculate the value of $-K/N$ and use Figure 10 to determine the value of $2X/d$ for each system and each describing function.

(3) Calculate the value of X from the known values of $2X/d$ and d. X is then the predicted amplitude of the self-sustained oscillations for that particular describing function and system.

The results of the application of the foregoing procedure are tabulated in Table XI on page 44. In order to determine the accuracy of the predictions, each of the seven nonlinear systems was

simulated on an analog computer. (The circuits used for the simulation are shown in Appendix C.) The analog computer experimental results are also shown in Table XI, along with the percentage of error of each prediction based on the experimental results.

Table XII on page 45 is a comparison, based on the error figures in Table XI, of the various saturation-plus-dead-zone describing functions. It shows that the saturation + dead zone nonlinearity seems to favor the corrected-conventional describing function; furthermore, analysis of Table XI shows that this is true for both large and small limit-cycle amplitude. Thus, the addition of dead zone to the saturation must have increased the harmonic content of the output of the nonlinearity to the point that a correction was needed for all amplitudes instead of just for high amplitudes. A similar thing happens when the ideal relay is analyzed.

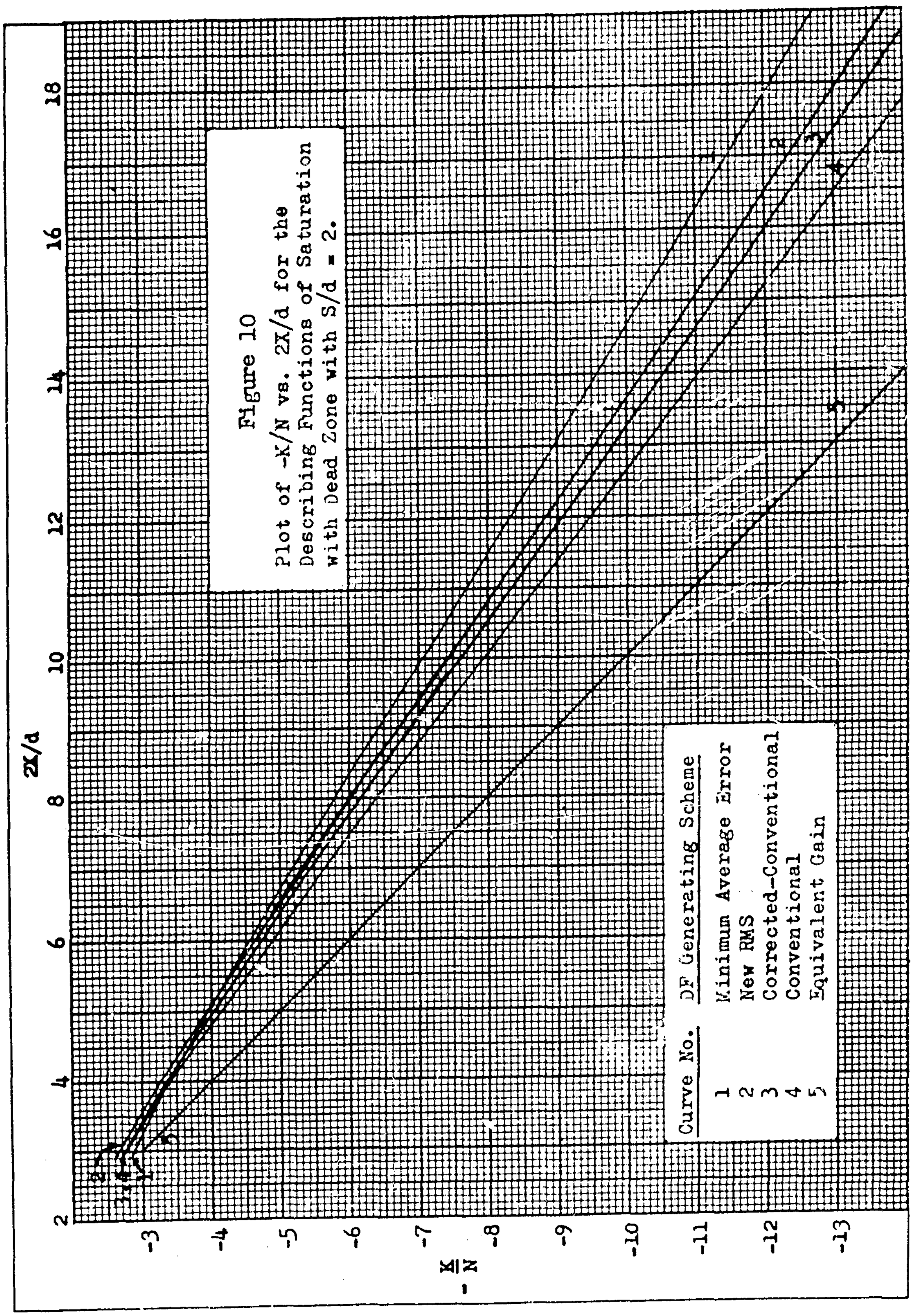

Figure 10
Plot of -K/N vs. 2X/d for the Describing Functions of Saturation with Dead Zone with S/d = 2.

Table XI

Prediction of the Amplitude and Frequency of Self-Sustained Oscillations in Seven Different Feedback Systems with Saturation Combined with Dead Zone by Various Describing Functions.**

Linear Function	Experimental Amplitude	Describing Function Amplitude Predictions and Errors										Experimental Frequency (rad/sec)	Predicted Frequency* (rad/sec)	% Error in Frequency Prediction
		Conventional		Minimum Average Error		Equivalent Gain		New RMS		Corrected-Conventional				
		Amplitude	% Error	Amplitude	% Error	Amplitude	% Error	Amplitude	% Error	Amplitude	% Error			
$G_1(j\omega)$	3.404	3.41	+0.1763	3.29	- 3.349	3.000	-11.87	3.57	+4.877	3.42	+0.4700	3.297	3.3166	+0.5945
$G_2(j\omega)$	3.428	3.41	-0.5251	3.29	- 4.026	3.000	-12.49	3.57	+4.142	3.42	-0.2334	1.404	1.4142	+0.7265
$G_3(j\omega)$	3.367	3.38	+0.3861	3.20	- 4.960	2.975	-11.64	3.51	+4.247	3.39	+0.6831	0.8909	0.8944	+0.3929
$G_4(j\omega)$	12.88	12.65	-1.786	14.66	+13.82	10.000	-22.36	13.67	+6.134	13.27	+3.028	1.816	1.8316	+0.8590
$G_5(j\omega)$	13.18	12.65	-4.021	14.66	+11.23	10.000	-24.13	13.67	+3.718	13.27	+0.6828	0.8160	0.83666	+2.532
$G_6(j\omega)$	13.53	13.08	-3.326	15.20	+12.34	10.339	-23.58	14.14	+4.509	13.74	+1.552	0.6353	0.6544	+3.006
$G_{3A}(j\omega)$	13.62	13.08	-3.965	15.20	+11.60	10.339	-24.09	14.14	+3.818	13.74	+0.8810	0.8733	0.8944	+2.416

(Original data)

*All of the describing functions listed predict the same frequency.
**S = 4, d = 2, K = 1 (See Table IV, page 30).

Table XII

Comparison of the Prediction Errors of the Various Saturation + Dead Zone Describing Functions.

From the preceding table of predictions and errors, the arithmetical mean error, median error, etc., for each of the saturation-combined-with-dead-zone describing functions can be calculated in order to give an overall indication of the accuracy with which a particular type of describing function (i.e., conventional, minimum average error, etc.) can predict the amplitude and frequency of self-sustained oscillations in the presence of both saturation and dead zone.

Error Criterion	Describing Function Amplitude Errors (%)					Describing Function Frequency Errors *
	Conventional	Minimum Average Error	Equivalent Gain	New RMS	Corrected-Conventional	
Arithmetical Mean Error	-1.8915	+ 5.236	-18.59	+4.492	+1.0091 #	+1.5038
Median Error	-1.786	+11.23	-22.36	+4.247	+0.6831 #	+0.8590
Maximum Magnitude of Error	-4.021	+13.82	-24.13	+6.134	+3.028 #	+3.006
Arithmetical Mean of Absolute Error	2.0522	8.761	18.59	4.492	1.0758 #	1.5038

* All of the saturation + dead zone describing function listed predict the same frequency for an individual problem, and therefore the frequency error analysis applies equally to each type.

# Indicates the minimum magnitude of amplitude error in that row; therefore, the column with the most #'s is the column of what is possibly the best describing function for saturation combined with dead zone.

Ideal Relay

If an ideal relay nonlinearity is introduced into one of the linear systems, $G_1(s)$ through $G_6(s)$, or $G_{3A}(s)$, in the manner shown in Figure 1(b) on page 11, a stability analysis will reveal that stable, self-sustained oscillations will result. A plot of each of the five ideal relay describing functions listed in Table V on page 31 is shown in Figure 11 on page 48. The value of K was chosen to be unity for the analysis. The predictions of the amplitude and frequency of the self-sustained oscillations by each of the five describing functions for each of the seven systems mentioned above were calculated in the following manner:

(1) Use Eqs (2) through (8) or Figures 2 through 7 in Chapter II to calculate the negative real axis crossing point of $G_n(j\omega)$ on the direct polar plot. The value of $G_n(j\omega)$ at the negative real axis crossing is equal to $-1/N$, and the value of ω at the negative real axis crossing is the predicted frequency of the self-sustained oscillations.

(2) Calculate the value of $-K/N$ and use Figure 11 or the describing function equations in Table V to determine the value of X, the predicted amplitude of the self-sustained oscillations for that particular describing function and system.

The results of the application of the foregoing procedure are tabulated in Table XIII on page 49. In order to determine the accuracy of the predictions, each of the seven nonlinear systems was simulated on an analog computer. (The circuits used for the simulation are shown in Appendix C.) The analog computer experimental

results are also shown in Table XIII, along with the percentage of error of each prediction based on the experimental results.

Table XIV on page 50 is a comparison, based on the error figures in Table XIII, of the various ideal relay describing functions. It shows that the ideal relay nonlinearity strongly favors the corrected-conventional describing function for the systems considered. The same thing seems to be true of all the various relay nonlinearities, insofar as amplitude accuracy is concerned, as will be seen in the next three sections.

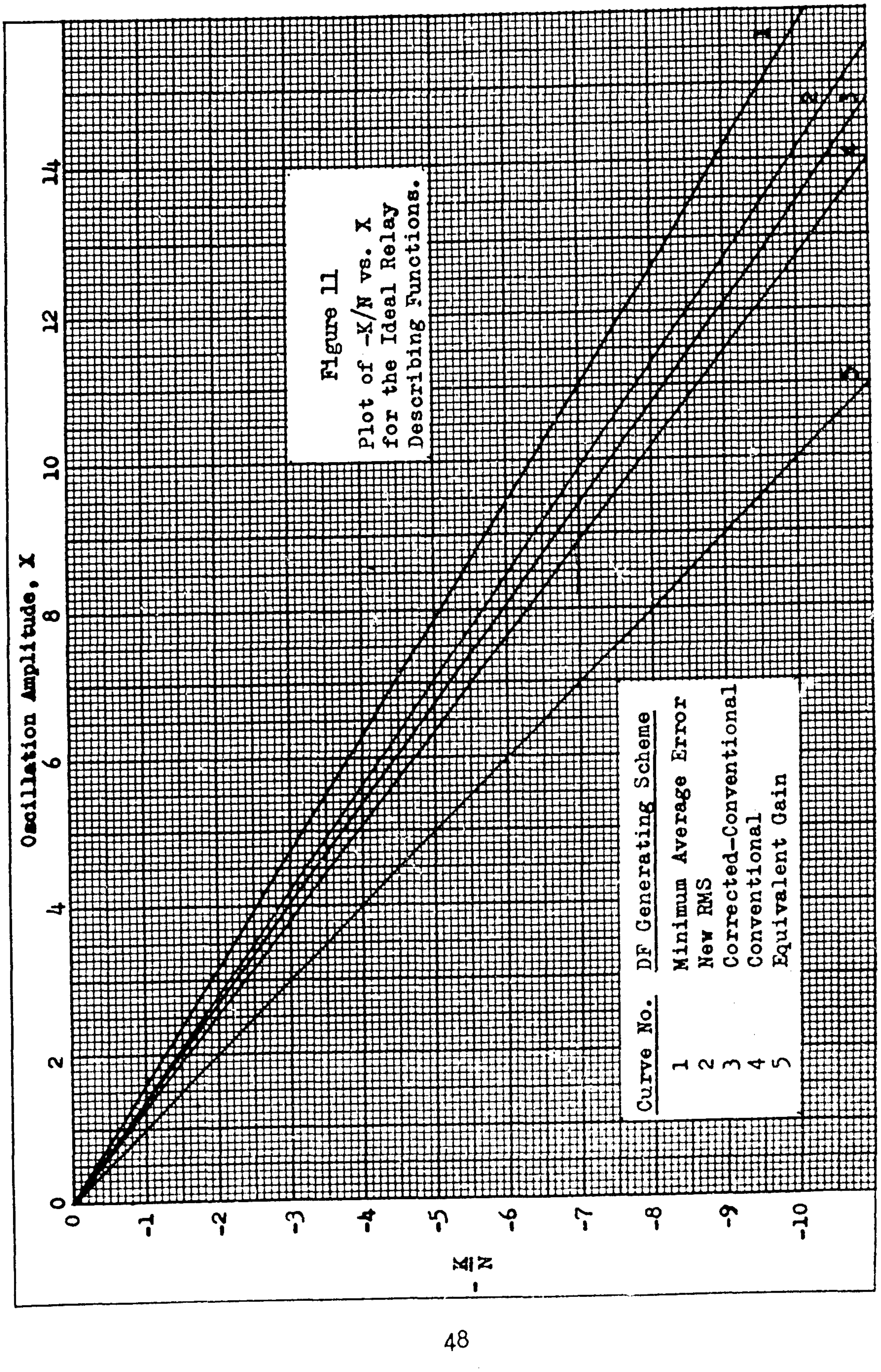

Figure 11
Plot of -K/N vs. X
for the Ideal Relay
Describing Functions.

Table XIII

Prediction of the Amplitude and Frequency of Self-Sustained Oscillations in Seven Different Feedback Systems with an Ideal Relay by Various Describing Functions **

Linear Function	Experimental Amplitude	Describing Function Amplitude Predictions and Errors										Experimental Frequency (rad/sec)	Predicted Frequency* (rad/sec)	% Error in Frequency Prediction
		Conventional		Minimum Average Error		Equivalent Gain		New RMS		Corrected-Conventional				
		Amplitude	% Error	Amplitude	% Error	Amplitude	% Error	Amplitude	% Error	Amplitude	% Error			
$G_1(j\omega)$	4.032	3.82	-5.258	4.71	+16.82	3.000	-25.60	4.24	+5.159	4.03	-0.0496	3.216	3.3166	+3.128
$G_2(j\omega)$	4.020	3.82	-4.975	4.71	+17.16	3.000	-25.37	4.24	+5.473	4.03	+0.2488	1.368	1.4142	+3.377
$G_3(j\omega)$	3.959	3.79	-4.269	4.67	+17.96	2.975	-24.85	4.21	+6.340	3.99	+0.7830	0.8684	0.8944	+2.994
$G_4(j\omega)$	13.04	12.73	-2.377	15.71	+20.48	10.000	-23.31	14.14	+8.435	13.42	+2.914	1.808	1.8316	+1.305
$G_5(j\omega)$	13.35	12.73	-4.644	15.71	+17.68	10.000	-25.09	14.14	+5.918	13.42	+0.5244	0.8147	0.83666	+2.695
$G_6(j\omega)$	13.92	13.19	-5.244	16.24	+16.67	10.339	-25.73	14.62	+5.029	13.87	-0.3592	0.6293	0.6544	+3.989
$G_{3A}(j\omega)$	13.75	13.19	-4.073	16.24	+18.11	10.339	-24.81	14.62	+6.327	13.87	+0.8727	0.8681	0.8944	+3.030

*All of the describing functions listed predict the same frequency.

(Original data)

**K = 1 (See Table V, page 31).

Table XIV

Comparison of the Prediction Errors of the Various Ideal Relay Describing Functions.

From the preceding table of predictions and errors, the arithmetical mean error, median error, etc., for each of the ideal relay describing functions can be calculated in order to give an overall indication of the accuracy with which a particular type of describing function (i.e., conventional, minimum average error, etc.) can predict the amplitude and frequency of self-sustained oscillations in the presence of an ideal relay.

Error Criterion	Describing Function Amplitude Errors (%)					Describing Function Frequency Errors *
	Conventional	Minimum Average Error	Equivalent Gain	New RMS	Corrected-Conventional	
Arithmetical Mean Error	-4.406	+17.84	-24.97	+6.097	+0.7049 #	+2.931
Median Error	-4.644	+17.68	-25.09	+5.918	+0.5244 #	+3.030
Maximum Magnitude of Error	-5.258	+20.48	-25.73	+8.435	+2.914 #	+3.989
Arithmetical Mean of Absolute Error	4.406	17.84	24.97	6.097	0.8217 #	2.931

* All of the ideal relay describing functions listed predict the same frequency for an individual problem, and therefore the frequency error analysis applies equally to each type.

# Indicates the minimum magnitude of amplitude error in that row; therefore, the column with the most #'s is the column of what is possibly the best describing function for an ideal relay.

Relay with Hysteresis

If a nonlinearity such as a relay with hysteresis is introduced into one of the linear systems, $G_1(s)$ through $G_6(s)$, or $G_{3A}(s)$, in the manner shown in Figure 1(b) on page 11, a stability analysis will reveal that stable, self-sustained oscillations will occur. A comparison of Tables V and VI (pages 31 and 32) shows that the magnitude variations of the relay-with-hysteresis describing functions are the same as those of their ideal relay counterparts; however, the hysteresis introduces an amplitude-dependent phase shift. Figure 11 on page 48 is therefore a valid plot of $-\left|\frac{K}{N}\right|$ versus X for the relay with hysteresis. In order to analyze the relay-with-hysteresis describing functions, values of h = 6 and K = 1 were chosen, and the five describing functions of Table VI were plotted in a psuedo magnitude-angle diagram fashion as shown in Figure 12 on page 54. (A magnitude rather than log-magnitude scale was used in order to preserve accuracy.) On the same graph, the magnitude versus angle relationship of each of the seven previously mentioned linear forward transfer functions was plotted. The intersection of a $G_n(j\omega)$ curve with a negative inverse describing function curve is the operating point at which that particular type of describing function predicts a stable limit cycle. One can use Figure 12, therefore, to make the amplitude and frequency predictions in the following manner:

(1) Use the magnitude-angle condition at the intersection to solve the appropriate $G_n(j\omega)$ equation (Eqs (2) through (8) in Chapter II) for ω. This value of ω is the predicted frequency of

the self-sustained oscillations.

(2) The magnitude value at each intersection is equal to $\left|\frac{1}{N}\right|$ for that particular system and describing function. Therefore Figure 11, or the magnitude portion of the describing function defining equation, can be used to determine X, the predicted amplitude of the self-sustained oscillations.

The results of the application of the foregoing procedure are tabulated in Tables XV and XVII on pages 55 and 57. In order to determine the accuracy of the predictions, each of the seven nonlinear systems was simulated on an analog computer. (The circuits used for the simulation are shown in Appendix C.) The analog computer experimental results are also shown in Tables XV and XVII, along with the percentage of error of each prediction based on the experimental results.

Table XVI on page 56 is a comparison based on the amplitude prediction error figures in Table XV, of the various relay + hysteresis describing functions. It shows that the relay-plus-hysteresis nonlinearity seems to favor the corrected-conventional describing function insofar as amplitude accuracy is concerned. However, Table XVIII on page 58, which is a comparison based on the frequency prediction error figures in Table XVII, shows that the relay-with-hysteresis nonlinearity favors the equivalent gain describing function for frequency prediction accuracy. And, from an analysis of Table XVII, the frequency prediction accuracy of the equivalent gain method apparently increases as the limit-cycle amplitude is increased. This problem of a variation in the frequency prediction

does not arise in the next section, since a relay with dead zone will not cause a phase shift.

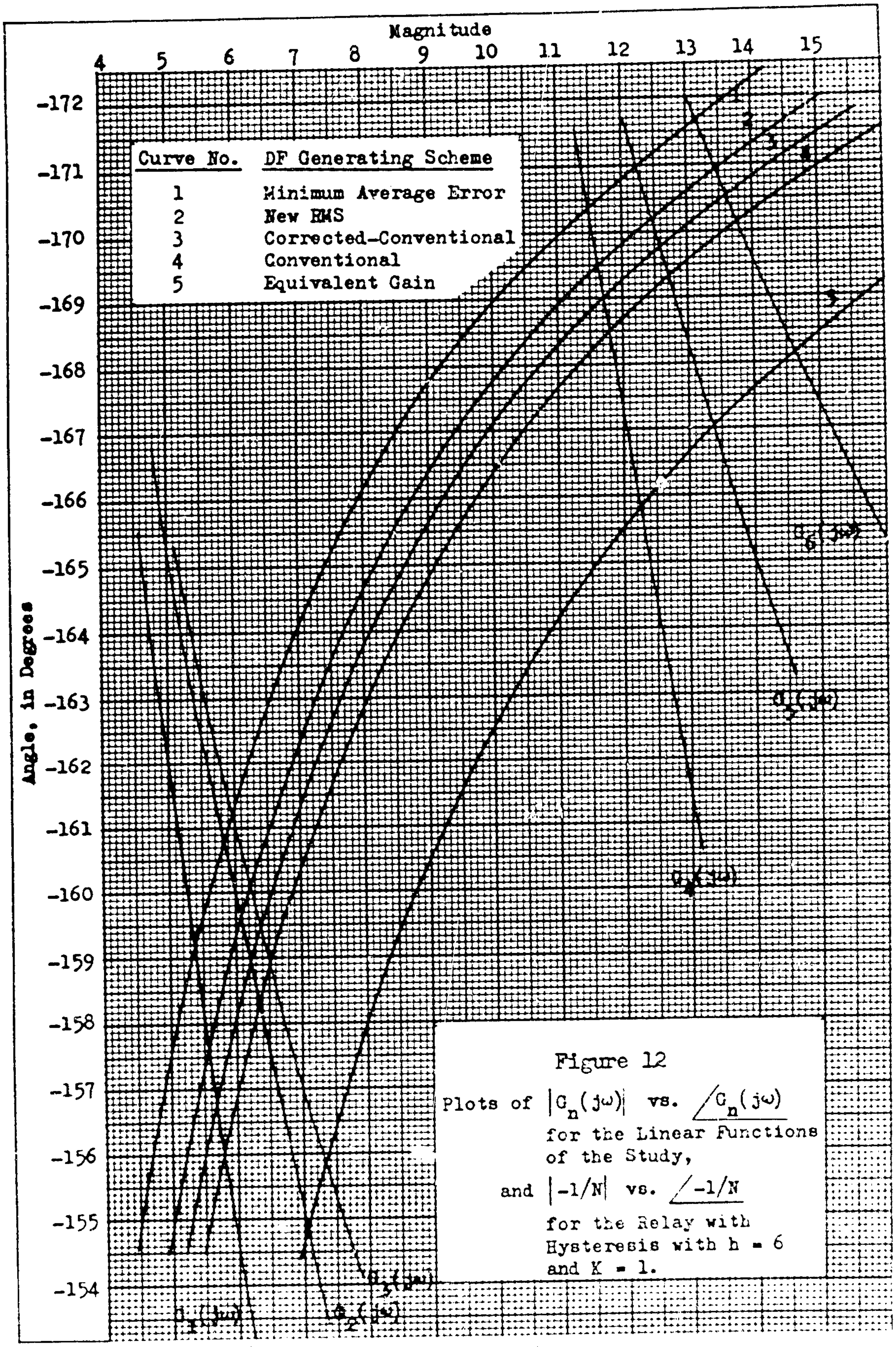

Figure 12

Plots of $|G_n(j\omega)|$ vs. $\angle G_n(j\omega)$ for the Linear Functions of the Study, and $|-1/N|$ vs. $\angle -1/N$ for the Relay with Hysteresis with h = 6 and K = 1.

Table XV

Prediction of the Amplitude of Self-Sustained Oscillations in Seven Different Feedback Systems with a Relay with Hysteresis by Various Describing Functions.*

Linear Function	Experimental Amplitude	Describing Function Amplitude Predictions and Errors									
		Conventional		Minimum Average Error		Equivalent Gain		New HMS		Corrected-Conventional	
		Amplitude	% Error	Amplitude	% Error	Amplitude	% Error	Amplitude	% Error	Amplitude	% Error
$G_1(j\omega)$	7.686	7.40	-3.721	8.45	+ 9.940	6.42	-16.47	7.88	+2.524	7.64	-0.5985
$G_2(j\omega)$	8.431	8.06	-4.400	9.15	+ 8.528	7.06	-16.26	8.60	+2.005	8.35	-0.9608
$G_3(j\omega)$	8.644	8.28	-4.211	9.37	+ 8.399	7.33	-15.20	8.81	+1.920	8.57	-0.8561
$G_4(j\omega)$	15.52	15.02	-3.222	18.01	+16.04	12.24	-21.13	16.46	+6.057	15.77	+1.611
$G_5(j\omega)$	17.16	16.20	-5.594	19.21	+11.95	13.38	-22.03	17.61	+2.622	16.91	-1.457
$G_6(j\omega)$	18.68	17.52	-6.210	20.65	+10.55	14.62	-21.73	19.00	+1.713	18.27	-2.195
$G_{3A}(j\omega)$	19.12	18.58	-2.824	21.69	+13.44	15.59	-18.46	20.07	+4.969	19.30	+0.9414

*$h = 6$, $K = 1$, (See Table VI, page 32).

(Original data)

Table XVI

Comparison of the Amplitude Prediction Errors of the Various Relay + Hysteresis Describing Functions.

From the preceding table of predictions and errors, the arithmetical mean error, median error, etc., for each of the relay-with-hysteresis describing functions can be calculated in order to give an overall indication of the accuracy with which a particular type of describing function (i.e., conventional, minimum average error, etc.) can predict the amplitude of self-sustained oscillations in the presence of a relay with hysteresis.

Error Criterion	Describing Function Amplitude Errors (%)				
	Conventional	Minimum Average Error	Equivalent Gain	New RMS	Corrected-Conventional
Arithmetical Mean Error	-4.312	+11.264	-18.75	+3.116	-0.5021 #
Median Error	-4.211	+10.55	-18.46	+2.524	-0.8561 #
Maximum Magnitude of Error	-6.210	+16.04	-22.03	+6.057	-2.195 #
Arithmetical Mean of Absolute Error	4.312	11.264	18.75	3.116	1.2314 #

# Indicates the minimum magnitude of error in that row; therefore, the column with the most #'s is the column of what is possibly the best describing function for a relay with hysteresis, from the standpoint of amplitude accuracy.

Table XVII

Prediction of the Frequency of Self-Sustained Oscillations in Seven Different Feedback Systems with a Relay with Hysteresis by Various Describing Functions.*

Linear Function	Experimental Frequency (rad/sec)	Describing Function Frequency Predictions and Errors									
		Conventional		Minimum Average Error		Equivalent Gain		New RMS		Corrected-Conventional	
		Frequency (rad/sec)	% Error	Frequency (rad/sec)	% Error	Frequency (rad/sec)	% Error	Frequency (rad/sec)	% Error	Frequency (rad/sec)	% Error
$G_1(j\omega)$	2.336	2.391	+2.354	2.494	+6.767	2.272	−2.740	2.445	+4.666	2.416	+3.425
$G_2(j\omega)$	0.9106	0.9396	+3.185	0.9868	+8.368	0.8736	−4.063	0.9642	+5.886	0.9510	+4.437
$G_3(j\omega)$	0.5473	0.5645	+3.143	0.5971	+9.099	0.5200	−4.988	0.5812	+6.194	0.5718	+4.477
$G_4(j\omega)$	1.637	1.6603	+1.423	1.6877	+3.097	1.6224	−0.8919	1.6746	+2.297	1.6674	+1.857
$G_5(j\omega)$	0.6981	0.7215	+3.352	0.7375	+5.644	0.6969	−0.1719	0.7300	+4.570	0.7253	+3.896
$G_6(j\omega)$	0.5245	0.5465	+4.194	0.5627	+7.283	0.5243	−0.0381	0.5546	+5.739	0.5508	+4.824
$G_{3A}(j\omega)$	0.7177	0.7400	+3.107	0.7623	+6.214	0.7123	−0.7524	0.7515	+4.710	0.7454	+3.860

*h = 6, K = 1 (See Table VI, page 32).

(Original data)

Table XVIII

Comparison of the Frequency Prediction Errors of the Various Relay + Hysteresis Describing Functions.

From the preceding table of predictions and errors, the arithmetical mean error, median error, etc., for each of the relay-with-hysteresis describing functions can be calculated in order to give an overall indication of the accuracy with which a particular type of describing function (i.e., conventional, minimum average error, etc.) can predict the frequency of self-sustained oscillations in the presence of a relay with hysteresis.

Error Criterion	Describing Function Frequency Errors (%)				
	Conventional	Minimum Average Error	Equivalent Gain	New RMS	Corrected-Conventional
Arithmetical Mean Error	+2.965	+6,639	-1.9493 #	+4.866	+3.825
Median Error	+3.143	+6.767	-0.8919 #	+4.710	+3.896
Maximim Magnitude of Error	+4.194 #	+9.099	-4.988	+6.194	+4.824
Arithmetical Mean of Absolute Error	2.965	6.639	1.9493 #	4.866	3.825

# Indicates the minimum magnitude of error in that row; therefore, the column with the most #'s is the column of what is possibly the best describing function for a relay with hysteresis, from the standpoint of frequency accuracy.

Relay with Dead Zone

If a nonlinearity such as a relay with dead zone is introduced into one of the linear systems, $G_1(s)$ through $G_6(s)$, or $G_{3A}(s)$, in the manner shown in Figure 1(b) on page 11, a stability analysis will reveal that stable, self-sustained oscillations can exist. A normalized plot of each of the five relay-with-dead-zone describing functions listed in Table VII on page 33 is shown in Figure 13 on page 61. For the analysis, the values of the parameters of the nonlinearity were chosen to be d = 3 and K = 1. The predictions of the amplitude and frequency of the self-sustained oscillations by each of the five describing functions for each of the seven systems mentioned were calculated as follows:

(1) Use Eqs (2) through (8) or Figures 2 through 7 in Chapter II to calculate the negative real axis crossing point of $G_n(j\omega)$ on the direct polar plot. The value of $G_n(j\omega)$ at the negative real axis crossing is equal to $-1/N$, and the value of ω at the negative real axis crossing is the predicted frequency of the self-sustained oscillations.

(2) Calculate the value of $-K/Nd$ and use Figure 13 to determine the value of $2X/d$ for each system and each describing function.

(3) Calculate the value of X from the known values of $2X/d$ and d. X is then the predicted amplitude of the self-sustained oscillations for that particular describing function and system.

The results of the application of the foregoing procedure are tabulated in Table XIX on page 62. In order to determine the accuracy of the predictions, each of the seven nonlinear systems was

simulated on an analog computer. (The circuits used for the simulation are shown in Appendix C.) The analog computer experimental results are also shown in Table XIX, along with the percentage of error of each prediction based on the experimental results.

Table XX on page 63 is a comparison, based on the error figures in Table XIX, of the various relay-plus-dead-zone describing functions. It shows that the relay + dead zone nonlinearity seems to favor the corrected-conventional describing function. This is true because, as Table XIX shows, for small amplitude limit-cycles when the harmonic content is apparently smaller, the conventional and the corrected-conventional describing functions are (nearly) the same; whereas, when the limit-cycle amplitude is increased, the corrected-conventional describing function automatically compensates for the increase in harmonic content of the output of the nonlinearity.

When hysteresis is added to the relay with dead zone, the problem of frequency variation between the predictions again arises.

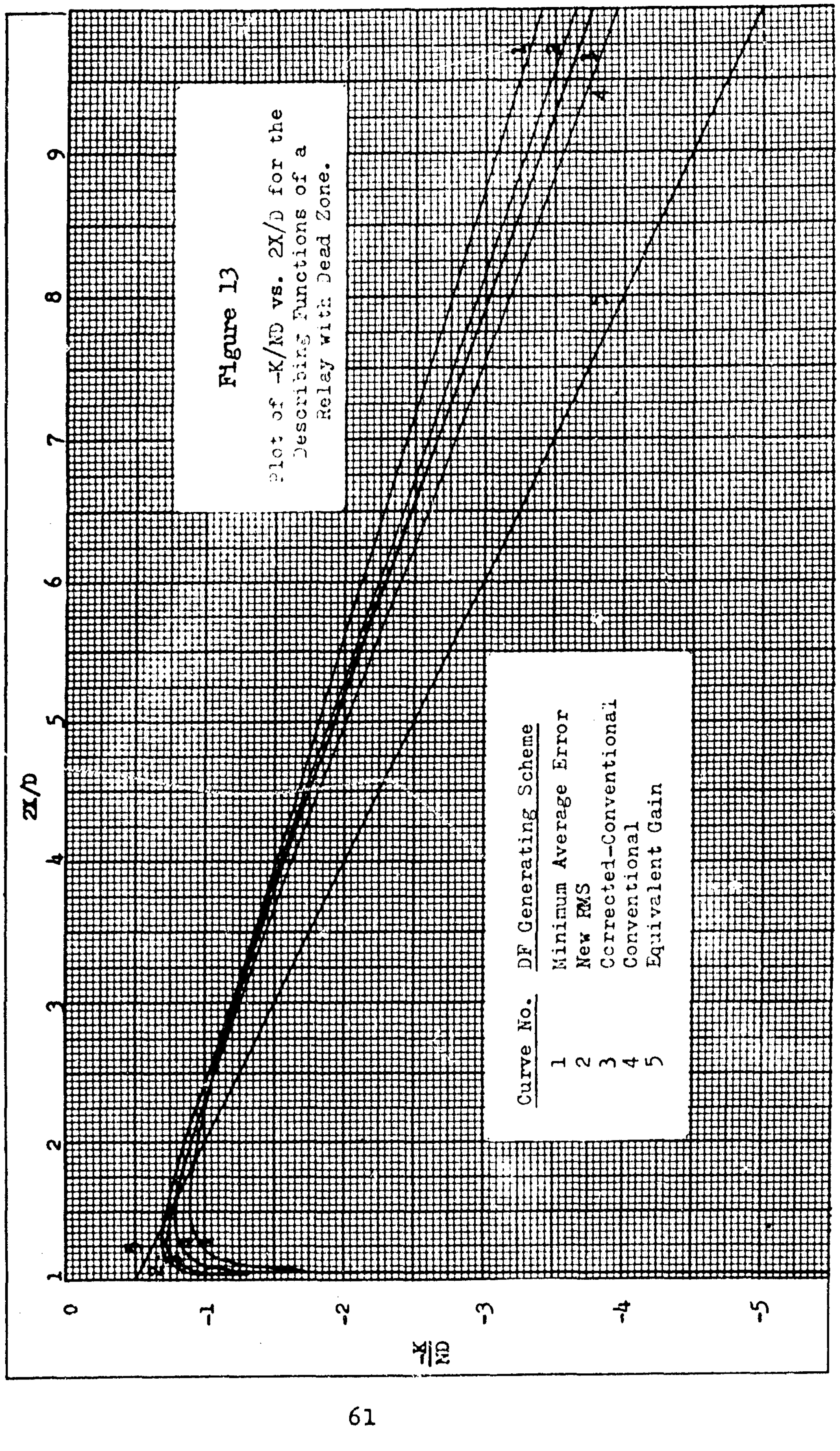

Figure 13

Plot of -K/ND vs. 2X/D for the Describing Functions of a Relay with Dead Zone.

Table XIX

Prediction of the Amplitude and Frequency of Self-Sustained Oscillations in Seven Different Feedback Systems with a Relay with Dead Zone by Various Describing Functions.**

Linear Function	Experimental Amplitude	Describing Function Amplitude Predictions and Errors										Experimental Frequency (rad/sec)	Predicted Frequency* (rad/sec)	% Error in Predicted Frequency
		Conventional		Minimum Average Error		Equivalent Gain		New RMS		Corrected-Conventional				
		Amplitude	% Error	Amplitude	% Error	Amplitude	% Error	Amplitude	% Error	Amplitude	% Error			
$G_1(j\omega)$	3.591	3.45	-3.926	3.333	- 7.185	3.000	-16.46	3.615	+0.6683	3.45	-3.926	3.251	3.3166	+2.018
$G_2(j\omega)$	3.537	3.45	-2.460	3.333	- 5.768	3.000	-15.18	3.615	+2.205	3.45	-2.460	1.391	1.4142	+1.668
$G_3(j\omega)$	3.462	3.405	-1.646	3.27	- 5.546	2.975	-14.07	3.585	+3.553	3.405	-1.646	0.8837	0.8944	+1.211
$G_4(j\omega)$	12.91	12.645	-2.053	14.70	+13.87	10.000	-22.54	13.695	+6.081	13.26	+2.711	1.809	1.8316	+1.249
$G_5(j\omega)$	13.29	12.645	-4.853	14.70	+10.61	10.000	-24.76	13.695	+3.048	13.26	-0.2257	0.8165	0.83666	+2.460
$G_6(j\omega)$	13.78	13.05	-5.298	15.255	+10.70	10.339	-24.97	14.145	+2.649	13.71	-0.5080	0.6308	0.6544	+3.741
$G_{3A}(j\omega)$	13.49	13.05	-3.262	15.255	+13.08	10.339	-23.36	14.145	+4.855	13.71	+1.631	0.8678	0.8944	+3.065

*All of the describing functions listed predict the same frequency.

**$d = 3$, $K = 1$ (See Table VII, page 33).

(Original data)

Table XX

Comparison of the Prediction Errors of the Various Relay + Dead Zone Describing Functions.

From the preceding table of predictions and errors, the arithmetical mean error, median error, etc., for each of the relay-with-dead-zone describing functions can be calculated in order to give an overall indication of the accuracy with which a particular type of describing function (i.e., conventional, minimum average error, etc.) can predict the amplitude and frequency of self-sustained oscillations in the presence of a relay with dead zone.

Error Criterion	Describing Function Amplitude Errors (%)					Describing Function Frequency Errors *
	Conventional	Minimum Average Error	Equivalent Gain	New RMS	Corrected-Conventional	
Arithmetical Mean Error	-3.357	+ 4.252	-20.19	+3.2942	-0.6320 #	+2.202
Median Error	-3.926	+10.61	-22.54	+3.048	-0.5080 #	+2.018
Maximum Magnitude of Error	-5.298	+13.87	-24.97	+6.081	-3.926 #	+3.741
Arithmetical Mean of Absolute Error	3.357	9.537	20.19	3.2942	1.8725 #	2.202

* All of the relay + dead zone describing functions listed predict the same frequency for an individual problem, and therefore the frequency error analysis applies equally to each type.

# Indicates the minimum magnitude of amplitude error in that row; therefore, the column with the most #'s is the column of what is possibly the best describing function for a relay with dead zone.

Relay with Dead Zone and Hysteresis

If a nonlinearity such as a relay with both dead zone and hysteresis is introduced into one of the linear systems, $G_1(s)$ through $G_6(s)$, or $G_{3A}(s)$, in the manner shown in Figure 1(b) on page 11, a stability analysis will reveal that stable, self-sustained oscillations can occur. A normalized plot of the magnitude of each of the five relay-with-dead-zone-and-hysteresis describing functions listed in Table VIII on page 34 is shown in Figure 14 on page 67 for the case of $d/h = 1$. The negative magnitude is used as the ordinate to permit comparison with the other describing function plots in this chapter. The angle variation, which is the same for all of the describing function schemes, is shown in Figure 15 on page 68. In order to analyze the relay-with-dead-zone-and-hysteresis describing functions, values of $d = h = 2$ and $K = 0.8$ were chosen, and the five describing functions of Table VIII were plotted in another psuedo magnitude-angle diagram shown in Figure 16 on page 69. On the same graph, the magnitude-versus-angle relationship of each of the seven previously mentioned linear forward transfer functions was plotted. The intersection of a $G_n(j\omega)$ curve with a negative inverse describing function curve is the operating point at which that particular type of describing function predicts a stable limit cycle. One can use Figure 16, therefore, to make the amplitude and frequency predictions in the following manner:

(1) Use the magnitude-angle condition at the intersection to solve the appropriate $G_n(j\omega)$ equation (Eqs (2) through (8) in Chapter II) for ω. This value of ω is the predicted frequency of the self-

sustained oscillations.

(2) The magnitude at the intersection is the predicted operating value of $\left|\frac{1}{N}\right|$ for that particular system and describing function. Therefore, Figure 14 can be used to determine the value of $2X/d$ by calculating $-\left|K/N(d+h)\right|$ and then picking $2X/d$ off of the proper curve. Alternately, the angle value at the intersection is the predicted operating value of $\angle -1/N$, so Figure 15 can be used to find $2X/d$ directly from $\angle -1/N$.

(3) Calculate the value of X from the known values of $2X/d$ and d. X is then the predicted amplitude of the self-sustained oscillations for that particular describing function and system.

The results of the application of the foregoing procedure are tabulated in Tables XXI and XXIII on pages 70 and 72, respectively. In order to determine the accuracy of these predictions, each of the seven nonlinear systems was simulated on an analog computer. (The circuits used in the simulation are shown in Appendix C.) The analog computer experimental results are also shown in Tables XXI and XXIII, along with the percentage of error of each prediction based on the experimental results.

Table XXII on page 71 is a comparison, based on the amplitude prediction error figures in Table XXI, of the various relay-with-dead-zone-and-hysteresis describing functions. It shows that the relay + dead zone + hysteresis nonlinearity favors the corrected-conventional describing function insofar as amplitude accuracy is concerned. However, Table XXIV on page 73, which is a comparison based on the frequency prediction error figures in Table XXIII,

shows that the relay + dead zone + hysteresis nonlinearity favors the equivalent gain describing function for frequency prediction accuracy. Again, as in the case of a relay with hysteresis, the accuracy of the equivalent gain frequency prediction seems to increase with limit-cycle amplitude as Table XXIII illustrates.

The last nonlinearity to be appraised by the various describing function schemes is dead zone. Since it does not provide a stable limit cycle when coupled with systems $G_1(s)$ through $G_6(s)$, or $G_{3A}(s)$, as pointed out in Chapter II, it was only analyzed with two conditionally stable systems, or rather, the same system at two gains. Therefore, the comparisons are less conclusive than for the other nonlinearities, but they are still interesting and necessary for completeness.

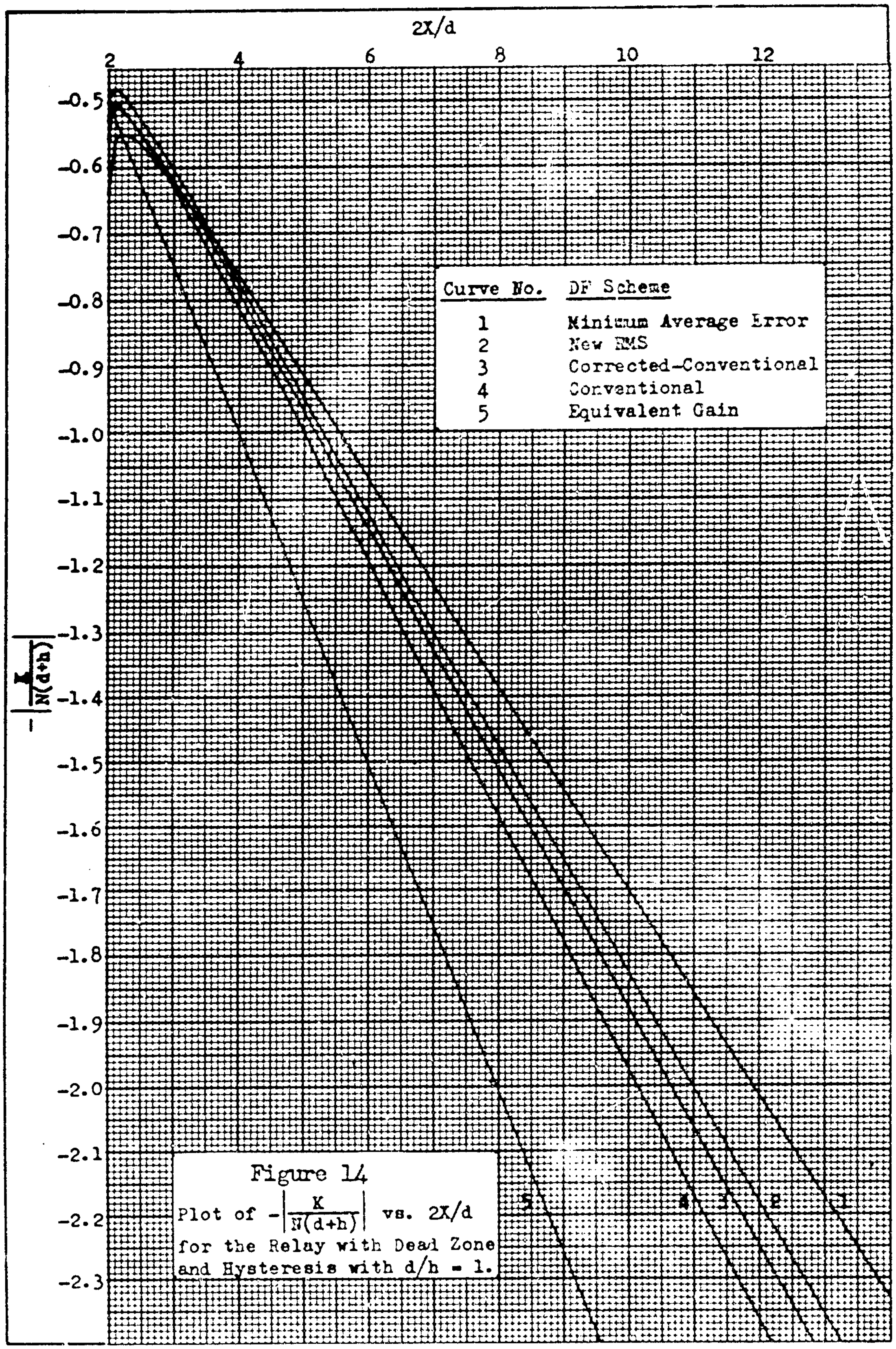

Figure 14

Plot of $-\left|\frac{K}{N(d+h)}\right|$ vs. 2X/d for the Relay with Dead Zone and Hysteresis with d/h = 1.

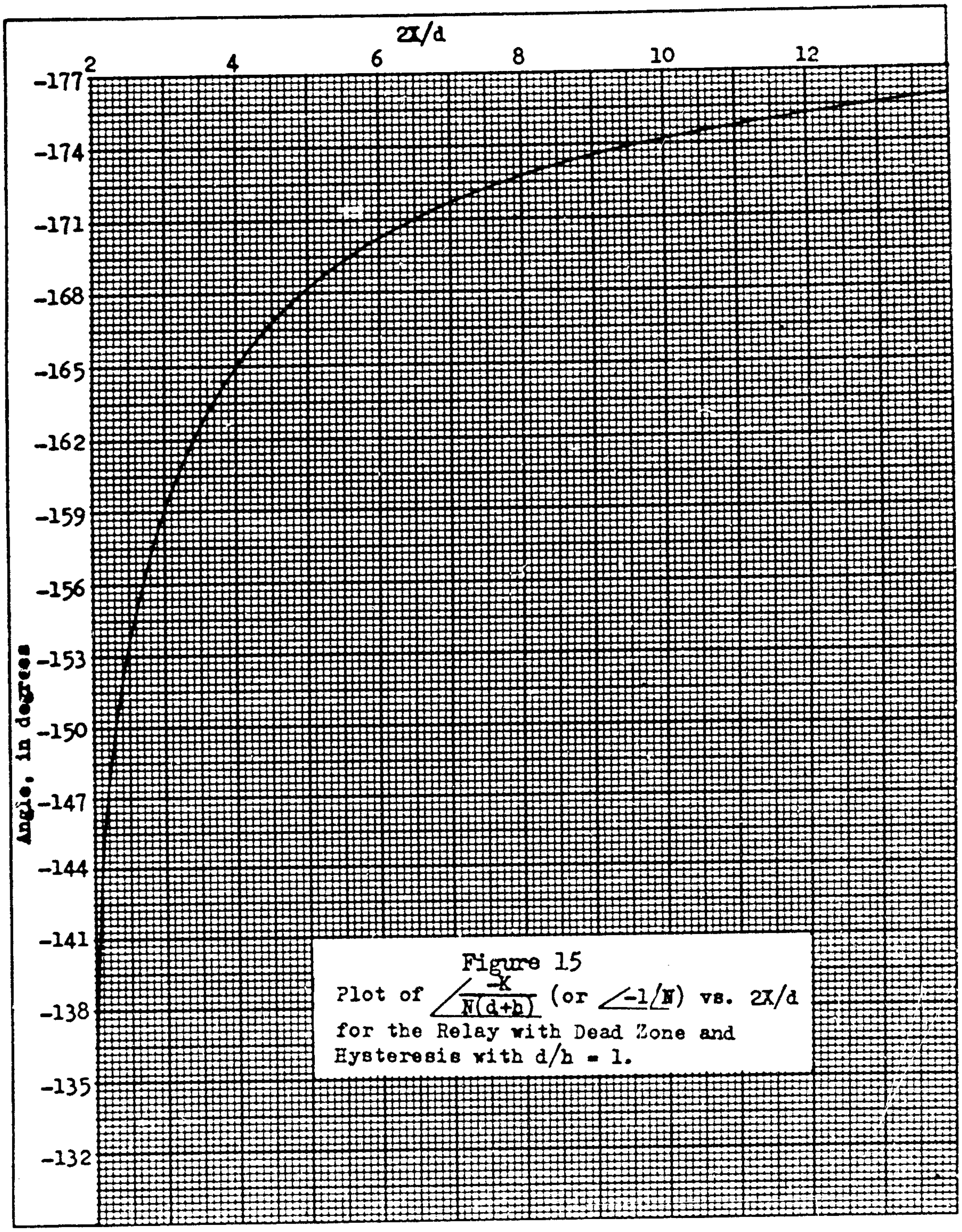

Figure 15

Plot of $\angle \frac{-K}{N(d+h)}$ (or $\angle -1/N$) vs. $2X/d$ for the Relay with Dead Zone and Hysteresis with $d/h = 1$.

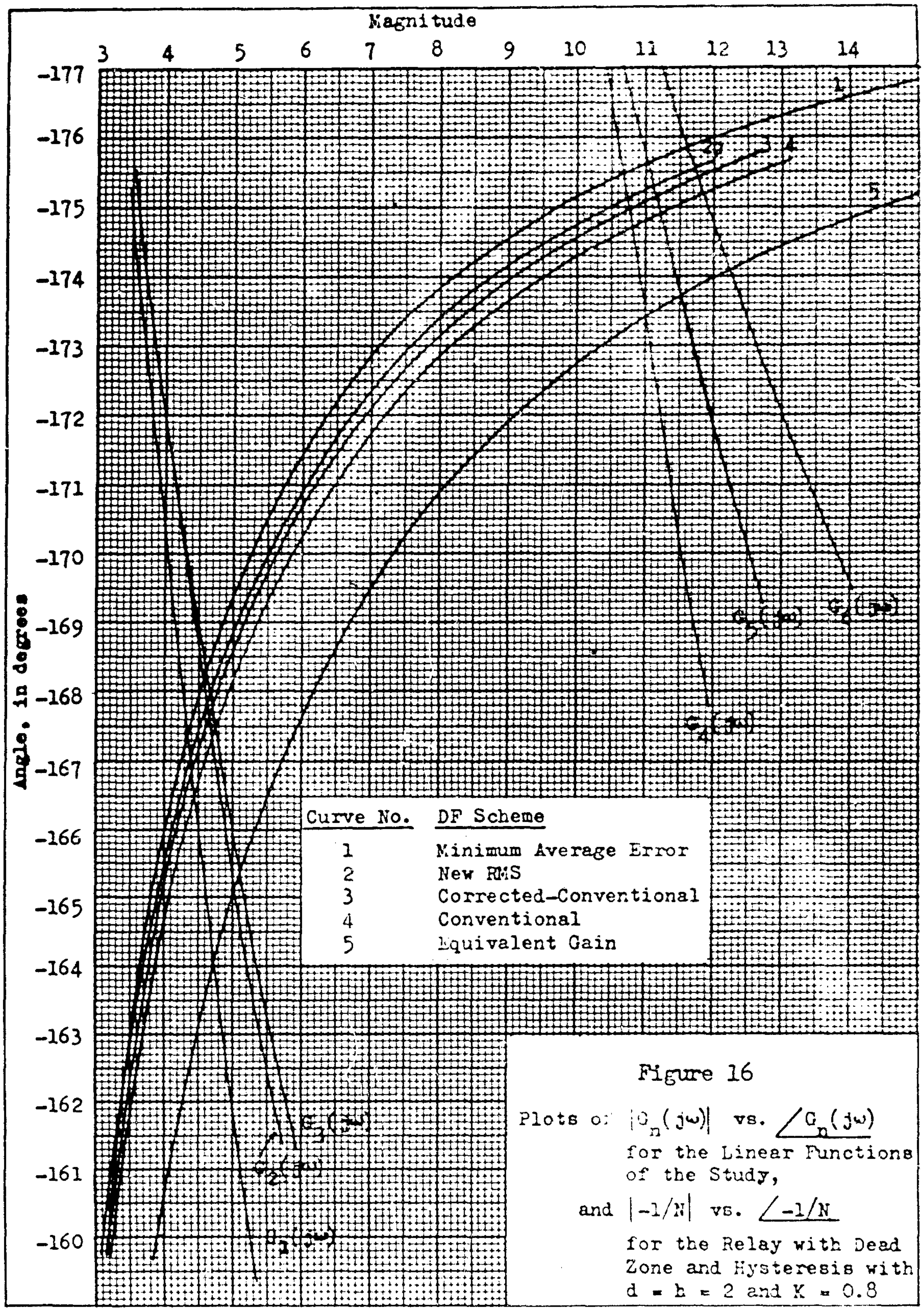

Figure 16

Plots of $|G_n(j\omega)|$ vs. $\angle G_n(j\omega)$ for the Linear Functions of the Study, and $|-1/N|$ vs. $\angle -1/N$ for the Relay with Dead Zone and Hysteresis with d = h = 2 and K = 0.8

Table XXI

Prediction of the Amplitude of Self-Sustained Oscillations in Seven Different Feedback Systems with a Relay with Dead Zone and Hysteresis by Various Describing Functions.*

Linear Function	Experimental Amplitude	Describing Function Amplitude Predictions and Errors									
		Conventional		Minimum Average Error		Equivalent Gain		New RMS		Corrected-Conventional	
		Amplitude	% Error	Amplitude	% Error	Amplitude	% Error	Amplitude	% Error	Amplitude	% Error
$G_1(j\omega)$	4.521	4.41	-2.455	4.69	+ 3.738	3.79	-16.17	4.60	+1.747	4.51	-0.2433
$G_2(j\omega)$	4.793	4.68	-2.358	5.00	+ 4.319	4.04	-15.71	4.87	+1.606	4.79	-0.0626
$G_3(j\omega)$	4.796	4.72	-1.585	5.03	+ 4.879	4.09	-14.72	4.89	+1.960	4.82	+0.5004
$G_4(j\omega)$	11.20	10.99	-1.875	12.74	+13.75	8.77	-21.70	11.85	+5.804	11.52	+2.857
$G_5(j\omega)$	11.93	11.39	-4.526	13.20	+10.65	9.19	-22.97	12.26	+2.776	11.93	0.0000
$G_6(j\omega)$	12.71	12.03	-5.350	13.95	+ 9.756	9.79	-22.97	12.92	+1.652	12.57	-1.101
$G_{3A}(j\omega)$	12.82	12.48	-2.652	14.38	+12.17	10.21	-20.36	13.39	+4.446	13.05	+1.794

*d = h = 2, K = 0.8 (See Table VIII, page 34). (Original data)

Table XXII

Comparison of the Amplitude Prediction Errors of the Various Relay + Dead Zone + Hysteresis Describing Functions.

From the preceding table of predictions and errors, the arithmetical mean error, median error, etc., for each of the relay-with-dead-zone-and-hysteresis describing functions can be calculated in order to give an overall indication of the accuracy with which a particular type of describing function (i.e., conventional, minimum average error, etc.) can predict the amplitude of self-sustained oscillations in the presence of a relay with both dead zone and hysteresis.

Error Criterion	Describing Function Amplitude Errors (%)				
	Conventional	Minimum Average Error	Equivalent Gain	New RMS	Corrected-Conventional
Arithmetical Mean Error	-2.972	+ 8.466	-19.23	+2.854	+0.5349 #
Median Error	-2.455	+ 9.756	-20.36	+1.960	0.0000 #
Maximum Magnitude of Error	-5.350	+13.75	-22.97	+5.804	+2.857 #
Arithmetical Mean of Absolute Error	2.972	8.466	19.23	2.854	0.9369 #

# Indicates the minimum magnitude of error in that row; therefore, the column with the most #'s is the column of what is possibly the best describing function for a relay with both dead zone and hysteresis, from the standpoint of amplitude accuracy.

Table XXIII

Prediction of the Frequency of Self-Sustained Oscillations in Seven Different Feedback Systems with a Relay with Dead Zone and Hysteresis by Various Describing Functions.*

Linear Function	Experimental Frequency (rad/sec)	Describing Function Frequency Predictions and Errors									
		Conventional		Minimum Average Error		Equivalent Gain		New RMS		Corrected-Conventional	
		Frequency (rad/sec)	% Error	Frequency (rad/sec)	% Error	Frequency (rad/sec)	% Error	Frequency (rad/sec)	% Error	Frequency (rad/sec)	% Error
$G_1(j\omega)$	2.706	2.754	+1.774	2.788	+3.030	2.663	-1.589	2.775	+2.550	2.765	+2.180
$G_2(j\omega)$	1.096	1.117	+1.916	1.136	+3.650	1.072	-2.190	1.128	+2.920	1.124	+2.555
$G_3(j\omega)$	0.6800	0.691	+1.618	0.703	+3.382	0.658	-3.235	0.698	+2.647	0.695	+2.206
$G_4(j\omega)$	1.729	1.752	+1.330	1.764	+2.024	1.732	+0.1735	1.758	+1.677	1.756	+1.562
$G_5(j\omega)$	0.7611	0.7804	+2.536	0.7885	+3.600	0.7676	+0.8540	0.7845	+3.074	0.7830	+2.877
$G_6(j\omega)$	0.5786	0.6011	+3.889	0.6089	+5.237	0.5895	+1.884	0.6050	+4.563	0.6033	+4.269
$G_{3A}(j\omega)$	0.7894	0.8145	+3.180	0.8250	+4.510	0.7984	+1.140	0.8202	+3.902	0.8177	+3.585

*$d = h = 2$, $K = 0.8$ (See Table VIII, page 34).

(Original data)

Table XXIV

Comparison of the Frequency Prediction Errors of the Various Relay + Dead Zone + Hysteresis Describing Functions.

From the preceding table of predictions and errors, the arithmetical mean error, median error, etc., for each of the relay-with-dead-zone-and-hysteresis describing functions can be calculated in order to give an overall indication of the accuracy with which a particular type of describing function (i.e., conventional, minimum average error, etc.) can predict the frequency of self-sustained oscillations in the presence of a relay with both dead zone and hysteresis.

Error Criterion	Describing Function Frequency Errors (%)				
	Conventional	Minimum Average Error	Equivalent Gain	New RMS	Corrected-Conventional
Arithmetical Mean Error	+2.320	+3.633	-0.4232 #	+3.048	+2.748
Median Error	+1.916	+3.600	+0.1735 #	+2.920	+2.555
Maximum Magnitude of Error	+3.889	+5.237	-3.235 #	+4.563	+4.269
Arithmetical Mean of Absolute Error	2.320	3.633	1.581 #	3.048	2.748

# Indicates the minimum magnitude of error in that row; therefore, the column with the most #'s is the column of what is possibly the best describing function for a relay with both dead zone and hysteresis, from the standpoint of frequency accuracy.

Dead Zone

If a dead zone nonlinearity is introduced into one of the linear systems, $G_7(j\omega)$ or $G_{7A}(j\omega)$, in the manner illustrated in Figure 1(b) on page 11, a stability analysis will reveal that stable, self-sustained oscillations will result. (See Figure 8, page 22.) A normalized plot of each of the five dead zone describing functions listed in Table II on page 28 is shown in Figure 17 on page 77. Interestingly, the new rms describing function and the corrected-conventional describing function for dead zone differ by such a small amount that, in effect, they plot as the same curve. For the analysis, the amount dead zone was set at $d = 6$ and the gain of the nonlinearity at $K = 0.5$. The predictions of the amplitude and frequency of the self-sustained oscillations by each of the five describing functions for each of the two systems mentioned were calculated as follows:

(1) Use Eqs (9) and (10) to calculate the negative real axis crossing point of the direct polar plot of $G_7(j\omega)$ and $G_{7A}(j\omega)$, respectively. (Again, see Figure 8, page 22. The pertinent crossing of $G_7(j\omega)$ was set at -3 and $G_{7A}(j\omega)$ at -10, of course, as discussed in Chapter II.) The value of $G_n(j\omega)$ at the crossing outside of the -1 point is equal to $-1/N$, and the value of ω at this crossing is the predicted frequency of the self-sustained oscillations.

(2) Calculate the value of $-K/N$ and use Figure 17 to determine the value of $2X/d$ for each system and describing function.

(3) Calculate the value of X from the known values of $2X/d$

and d. X is then the predicted amplitude of the self-sustained oscillations for that particular describing function and system.

The results of the application of the foregoing procedure are tabulated in Table XXV on page 78. In order to determine the accuracy of the predictions, both of the nonlinear systems were simulated on an analog computer. (The circuits used for the simulation are shown in Appendix C.) The analog computer experimental results are also shown in Table XXV, along with the percentage of error of each prediction based on the experimental results. The frequency error for system $G_{7A}(j\omega)$ was far greater than any other frequency error in the entire study. This can probably be explained with Figure 18 on page 78. As can be seen in Figure 18, the basic describing function assumption that $x(t)$ is approximately sinusoidal is quite poor for system $G_{7A}(j\omega)$ with dead zone, whereas it was a good assumption in every other case. However, it is interesting to note that the amplitude predictions were not seriously affected by the failure of this assumption.

Table XXVI on page 79 is a comparison, based on the error figures of Table XXV, of the various dead zone describing functions. It shows that the dead zone nonlinearity favors both the new rms and the corrected conventional describing functions since they give essentially the same results (to three or four place accuracy).

The describing function comparison tables at the end of each section of this chapter have used four error criteria as a basis for drawing conclusions about the accuracy of each type of describing function. These criteria were chosen because, in the author's

opinion, the "best" describing function should:

(1) have an arithmetical mean error (or average error) very close to zero, indicating that the errors encountered with that describing function will be randomly distributed about zero error, rather than about some positive or negative error value, so that chances of having an error of almost zero are maximum;

(2) have a median error close to the value of the arithmetical mean error to indicate, to some extent, that the data gathered was representative and not "lopsided";

(3) have the smallest maximum magnitude of error possible in order to give an indication of its maximum "tolerance"; and

(4) have the smallest arithmetical mean of absolute error as an indication of the error magnitude that can usually be expected.

This concludes the analysis of the describing function schemes as they apply to specific nonlinearities. In the next chapter an overall, general comparison will be made.

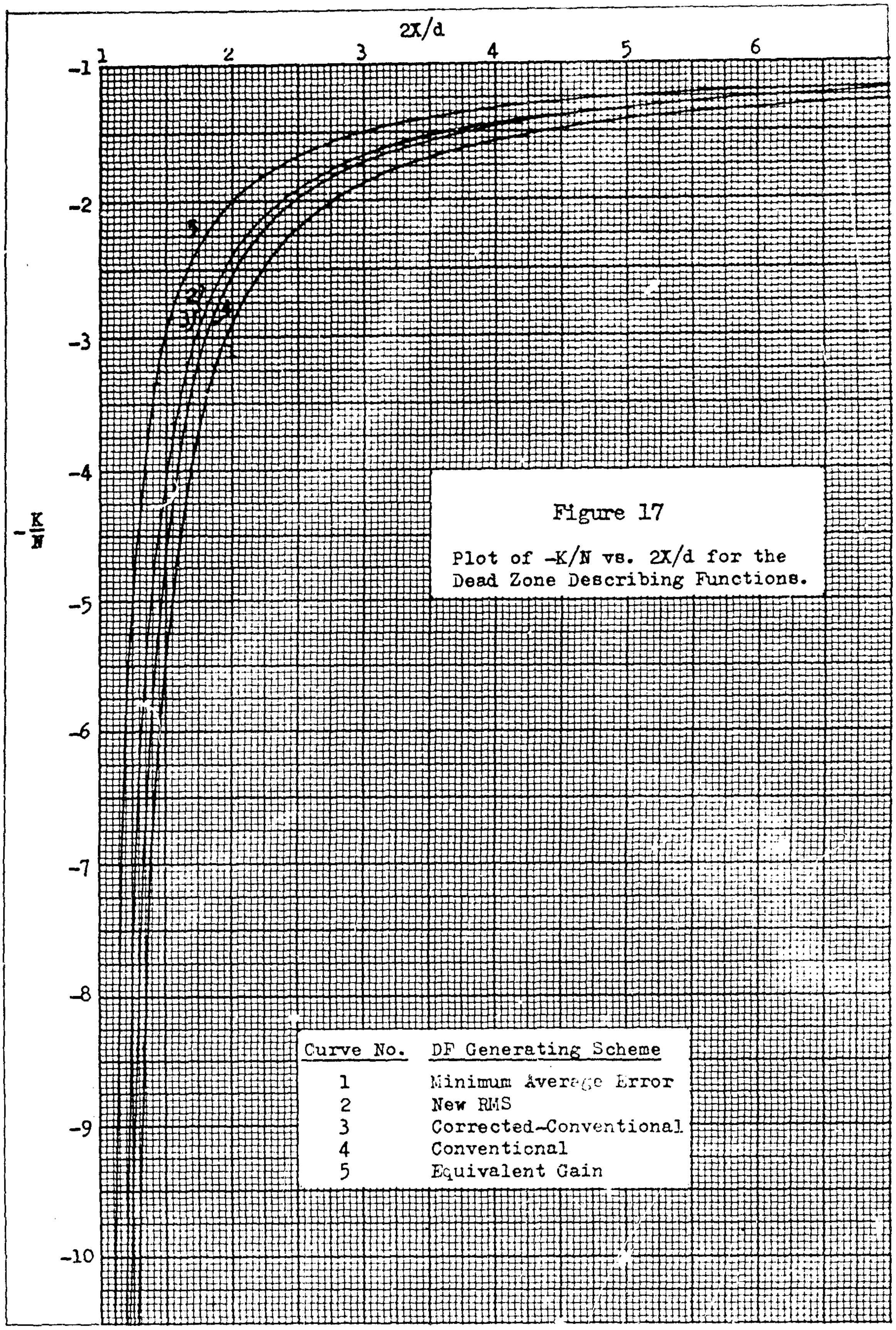
2X/d
1
2
3
4
5
6
-1
-2
-3
-4
-5
-6
-7
-8
-9
-10
$-\frac{K}{N}$
5
2
3
1
4
Figure 17
Plot of -K/N vs. 2X/d for the Dead Zone Describing Functions.
Curve No. DF Generating Scheme
1 Minimum Average Error
2 New RMS
3 Corrected-Conventional
4 Conventional
5 Equivalent Gain

Table XXV

Prediction of the Amplitude and Frequency of Self-Sustained Oscillations in Two Different Feedback Systems with Dead Zone by Various Describing Functions.
(d = 6, K = 0.5; see Table II, page 28.)

Linear Function	Experimental Amplitude	Describing Function Amplitude Predictions and Errors										Experimental Frequency (rad/sec)	Predicted Frequency* (rad/sec)	% Error in Frequency Prediction
		Conventional		Minimum Average Error		Equivalent Gain		New RMS		Corrected-Conventional				
		Amplitude	% Error	Amplitude	% Error	Amplitude	% Error	Amplitude	% Error	Amplitude	% Error			
$G_7(j\omega)$	11.16	11.43	+2.419	13.14	+17.74	9.000	-19.35	10.92	-2.151	10.92	-2.151	1.280	1.2984	+ 1.438
$G_{7A}(j\omega)$	4.273	4.41	+3.206	4.65	+ 8.823	3.750	-12.24	4.16	-2.645	4.16	-2.645	1.069	1.2984	+21.46**

(Original data)

*All of the describing functions listed predict the same frequency.
**The large error in the frequency prediction for the system containing dead zone and $G_{7A}(j\omega)$ is obviously due to the fact that the input, x, is no longer approximately sinusoidal, as (b) below indicates. In all of the other closed loop systems studied and recorded in this thesis, the input, x, was approximately sinusoidal, like the system containing dead zone and $G_7(j\omega)$ shown in (a) below.

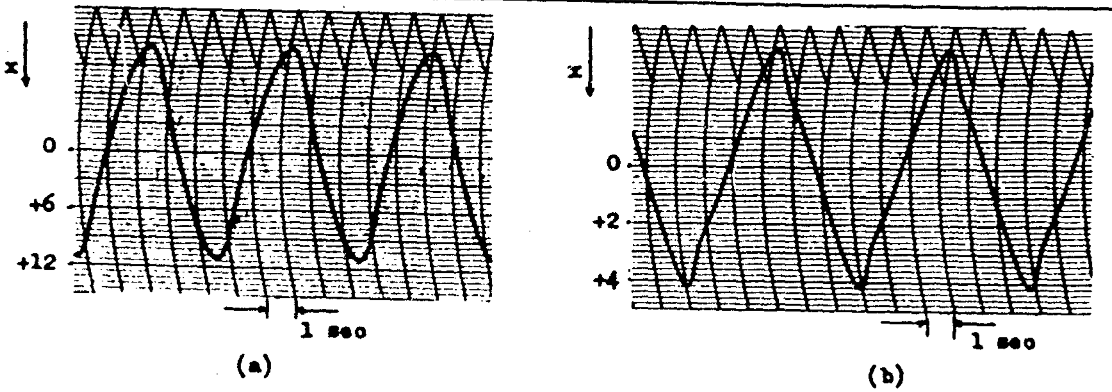

Figure 18

Self-sustained oscillations of systems (a) $G_7(j\omega)$ and (b) $G_{7A}(j\omega)$ with dead zone in a closed loop.

Table XXVI

Comparison of the Prediction Errors of the Various Dead Zone Describing Functions.

From the preceding table of predictions and errors, the arithmetical mean error, median error, etc., for each of the dead zone describing functions can be calculated in order to give an overall indication of the accuracy with which a particular type of describing function (i.e., conventional, minimum average error, etc.) can predict the amplitude and frequency of self-sustained oscillations in the presence of dead zone.

Error Criterion	Describing Function Amplitude Errors (%)					Describing Function Frequency Errors *
	Conventional	Minimum Average Error	Equivalent Gain	New RMS	Corrected-Conventional	
Arithmetical Mean Error	+2.813	+13.282	-15.80	-2.398 #	-2.398 #	+11.449
Median Error	+2.813	+13.282	-15.80	-2.398 #	-2.398 #	+11.449
Maximum Magnitude of Error	+3.206	+17.74	-19.35	-2.645 #	-2.645 #	+21.46
Arithmetical Mean of Absolute Error	2.813	13.282	15.80	2.398 #	2.398 #	11.449

* All of the dead zone describing functions listed predict the same frequency for an individual problem, so the frequency error analysis applies equally to each type.

# Indicates the minimum magnitude of amplitude error in that row; therefore, the column with the most #'s is the column of what is possibly the best describing function for dead zone.

V. Conclusions

Some readers may feel that, while attempting to find which describing function is more accurate, the author has only complicated the problem by adding still another scheme to the field. However, as this chapter attempts to show, although the corrected-conventional describing function may be more empirical than theoretical, it does remove some of the restraints and add a lot of accuracy to the analysis of a wide range of intermediate-order nonlinear feedback control systems.

Overall Comparison of the Describing-Function Generating Schemes

Table XXVII on the following page is an overall comparison of the amplitude prediction errors of the various types of describing functions included in this study. It shows quite conclusively that in general, to obtain amplitude prediction accuracy when using the describing function technique of stability analysis, one should use the corrected-conventional describing-function generating scheme to derive the describing function. Table XXVII shows that the corrected-conventional describing function is generally about two percent more accurate than the conventional describing function for intermediate-order nonlinear systems such as those included in this study. It also shows that, in general, no advantage is gained by using the new rms describing function instead of the conventional describing function. (However, the new rms describing function provided a slight improvement for the various relay nonlinearities

Table XXVII

Overall Comparison of the Amplitude Prediction Errors of the Various Describing Functions.

From the tables of predictions and errors in the preceding chapter, an overall arithmetical mean error, median error, etc., can be calculated for each type of describing function (i.e., conventional, minimum average error, etc.) in order to give an indication of the accuracy with which that particular type can predict the amplitude of self-sustained oscillations in a general nonlinear feedback system. Each error figure in the table, therefore, includes the results of 44 amplitude predictions, comprised of the 7 nonlinearities and 9 linear systems used in this study.

Error Criterion	Describing Function Amplitude Errors (%)				
	Conventional	Minimum Average Error	Equivalent Gain	New RMS	Corrected-Conventional
Arithmetical Mean Error	-2.874	+10.039	-20.25	+3.672	+0.4348 #
Median Error	-3.242	+11.415	-21.72	+3.937	+0.6830 #
Maximum Magnitude of Error	-6.210	+20.48	-25.73	+8.435	+4.439 #
Arithmetical Mean of Absolute Error	3.155	11.441	20.25	3.890	1.420 #

# Indicates the minimum magnitude of error in that row; therefore, the column with the most #'s is the column of what is possibly the best describing-function generating scheme to use, in general, in order to attain amplitude accuracy.

discussed in Chapter IV, but the improvement was not nearly as significant as that provided by the corrected-conventional describing function.) In summary, the corrected-conventional describing function provides certain advantages over the other describing function schemes for every type of nonlinearity tested and, in general, it has a mean and a median closer to zero than any other, a maximum magnitude of error less than any other, and an average absolute error less than any other describing function tested, insofar as amplitude prediction accuracy is concerned.

Trends in Describing Function Predictions

Since there are an infinite number of nonlinearities which could be introduced into an infinite number of feedback systems, the 44 varieties analyzed in this paper certainly do not constitute a conclusive proof of the corrected-conventional describing function's superior accuracy. But on the basis of this study, it certainly seems permissible to postulate that the corrected-conventional describing function can usually give the control engineer a more quantitative answer to his stability problem than he was able to previously obtain from the conventional describing function, except perhaps in a very complex system which provides almost perfect low pass filtering. The reason for this can be gleaned to some extent from the prediction tables in Chapter IV. A close analysis of the prediction tables in Chapter IV shows that the amplitude accuracy of the conventional describing function decreases as the limit-cycle amplitude, X, increases. This is so because, as Thaler and Pastel point out (Ref 12:172), the conventional describing func-

tion becomes less dependable as the signal level increases. In addition, the amplitude accuracy of the conventional describing function decreases as the order of the system decreases, since less filtering of the higher harmonics occurs. And, as the tables show, the amplitude accuracy of the conventional describing function also seems to depend on system type, decreasing as the system type is increased. The corrected-conventional describing functions, on the other hand, seem to be relatively unaffected by changes in limit-cycle amplitude, system type, or system order for the intermediate order systems of the study. This seems to come about from the inherent correction in the variation afforded by the third harmonic. Thus, by using the corrected-conventional describing function, the engineer can remove the small-signal limitation and relax somewhat the sine-wave input assumption, thus providing a more quantitative analysis tool for his real-life problems.

The amplitude accuracy of the new rms describing function is also relatively insensitive to limit-cycle amplitude and system order changes in the intermediate-order system range. However, it is not as accurate as the corrected-conventional describing function, and it seems to be quite sensitive to changes in system type.

For the purpose of attaining accurate amplitude predictions with the describing function stability analysis technique, it appears that the minimum average error and equivalent gain schemes are completely out of the question. This is to be expected, however, since Gibson introduced the minimum average error technique only as an example, and Prince's equivalent gain technique is

intended primarily for analytical-graphical, closed-loop frequency response analysis. Graphical methods for producing the closed-loop frequency response from any describing function scheme do exist, however, (Ref 12:195-210) and the corrected-conventional describing function applied in this manner might produce more accurate results than Prince's method, at least for nonlinearities which do not produce a phase shift.

All five types of describing functions presented in this paper predict the same frequency of oscillation, except when the nonlinearity produces a phase shift, as the relay + hysteresis and relay + dead zone + hysteresis nonlinearities in this study do. In those cases it seems that the equivalent gain describing function is more accurate for frequency prediction, with the accuracy increasing as the limit-cycle amplitude is increased. This increase in accuracy with amplitude may be due in part to the same sort of phenomenon explained by Johnson for the conventional describing function (Ref 6:175); that is, as the limit-cycle amplitude is increased, the intersection of the negative inverse describing function locus and the direct polar plot locus become more orthogonal (see Figures 12 and 16, pages 54 and 69), and it is the nearly tangential intersections which give misleading results.

If the corrected-conventional describing function is to be acceptable to the control system engineer, it must be shown why, in fact, this new technique should produce more accurate amplitude predictions than the conventional describing function, or any of the others.

The Case for the Corrected-Conventional Describing Function.

The only two methods of generating describing functions which have met with much success prior to this study, insofar as predicting accurate limit-cycle amplitudes is concerned, are the conventional and new rms techniques (Ref 3:1321). In order for the conventional technique to be completely accurate, it is necessary for the linear portion of the loop to act as a perfect low-pass filter. However, for intermediate order systems, the linear portion of the loop is far from being a perfect low-pass filter. Consequently, some higher harmonics, although attenuated, are fed back to the input of the nonlinearity along with the fundamental. For intermediate order systems, the conventional describing function will, therefore, underestimate the amplitude, X, of the signal returning to the nonlinearity.

The new rms describing function, on the other hand, assumes that their is no filtering of the higher harmonics by the linear portion of the loop, but rather, that the output sinusoid is just reshaped into a fundamental frequency sine wave of equal energy (Ref 2:301). Appendix F shows that the new rms describing function, in effect, takes as the amplitude of the equivalent output sine wave from the nonlinearity, the square root of the sum of the squares of all the Fourier coefficients in the Fourier expansion of the actual output of the nonlinearity. Obviously, some filtering of harmonics higher than the fundamental will result in an intermediate order system, so the new rms describing function will, therefore, overestimate the amplitude, X, of the signal returning to the non-

linearity.

What actually happens to the higher harmonics lies between what the conventional and new rms methods assume. The real case for the corrected-conventional describing function is, therefore, that it considers only the most prominent higher harmonic, in addition to the fundamental, by taking as the amplitude of the equivalent output sine wave, the square root of the sum of the squares of the first and third Fourier coefficients in the Fourier Series expansion of the actual output of the nonlinearity. The corrected-conventional method therefore assumes that the joint effect of all of the higher harmonics, each attenuated by a different amount through the linear portion of the loop, can be adequately approximated by including the unattenuated effect of the third harmonic only. Thus, the prediction afforded by the corrected-conventional describing function will lie between that of the conventional and new rms techniques and will therefore be more realistic than either. The results of the experimental portion of this study support this conclusion quite well.

Recommendations

Use of the third harmonic for amplitude prediction correction of the conventional describing function by the technique of the corrected-conventional describing function defined on page 26 has met with much success, as attested by this paper. Perhaps by applying some sort of correction to the angle, as well as to the magnitude of the conventional describing function, the loss in frequency prediction accuracy for nonlinearities which produce phase shifts could be reclaimed, or even improved. That is, a suitable describing func-

tion for future study might be defined by the relation

$$N = \frac{(A_1^2 + B_1^2 + A_3^2 + B_3^2)^{\frac{1}{2}} \Big/ \tan^{-1}\left[\frac{A_1^2 + A_3^2}{B_1^2 + B_3^2}\right]^{\frac{1}{2}}}{X \,\underline{/0^\circ}} \tag{17}$$

where A_1, A_3, B_1, and B_3 are defined as on page 26. This definition would give the same describing function as the corrected-conventional definition when the nonlinearity output is naturally odd periodic, but would modify the angle of the corrected-conventional describing function when the output of the nonlinearity is not naturally odd periodic. Although the resulting describing functions might appear very complex, they could be tabulated easily with the aid of a digital computer and plotted. Once an accurate plot is obtained, it makes little difference how complex the relationship was from which it came.

The success of the corrected-conventional describing function in improving the prediction of the amplitude of self-sustained oscillations in a nonlinear feedback system perhaps warrants further exploration. The corrected-conventional describing functions of nonlinearities not included in this paper should be derived, catalogued, and tested for accuracy. Such additional nonlinearities might include negative defficiency (Ref 12:150), backlash, nonlinearities described by algebraic equations such as $y = x \cdot |x|$ or $y = x^3$, and nonlinearities described by differential equations.

Finally, it might be interesting to see which type of describing function can most accurately predict the closed loop frequency response and jump resonance.

All of the questions posed by the preceeding recommendations must be answered before the question "Which describing function is best?" can be fully answered. However, based on the results of this paper, it seems safe to recommend the following procedure for treating the stability analysis of intermediate-order systems:

(1) For dead zone, dead zone with saturation, ideal relay, and relay with dead zone nonlinearities, use the corrected-conventional describing function for the best results in both amplitude and frequency prediction of limit cycles.

(2) For relay with hysteresis and relay with both hysteresis and dead zone, use the corrected-conventional describing function for the amplitude prediction and the equivalent gain describing function for the frequency prediction.

(3) For saturation nonlinearities, use the conventional describing function for small-signal analysis and the corrected-conventional describing function for large-signal analysis; although not much will be lost by using the corrected-conventional describing function exclusively.

Bibliography

Part A - Numbered References Cited in the Text and Appendices

1. D'Azzo, J. J., and C. H. Houpis. Feedback Control System Analysis and Synthesis. New York: McGraw-Hill Book Company, Inc., 1960.

2. Gibson, John E. Nonlinear Automatic Control. New York: McGraw-Hill Book Company, Inc., 1963.

3. Gibson, J. E., and K. S. Prasanna-Kumar. "A New RMS Describing Function for Single-Valued Nonlinearities." Proceedings of the IRE, 49:1321 (August 1961).

4. Gille, J.-C., M. J. Pelegrin, and P. Decaulne. Feedback Control Systems. New York: McGraw-Hill Book Company, Inc., 1959.

5. Johnson, Clarence L. Analog Computer Techniques (Second Edition). New York: McGraw-Hill Book Company, Inc., 1963.

6. Johnson, E. C. "Sinusoidal Analysis of Feedback-Control Systems Containing Nonlinear Elements." Transactions of the AIEE, 71, Part II, Applications and Industry: 169-181 (1952).

7. Klotter, Karl. "An Extension of the Conventional Concept of the Describing Function," in Proceedings, Symposium on Nonlinear Circuit Analysis, Volume 6. Brooklyn, New York: Polytechnic Institute of Brooklyn, 1956, pp. 151-162.

8. Kochenburger, R. J. "A Frequency Response Method for Analyzing and Synthesizing Contactor Servomechanisms." Transactions of the AIEE, 69, Part I: 270-284 (1950)

9. Kuo, Benjamin C. Automatic Control Systems. Englewood Cliffs, N. J.: Prentice-Hall, Inc., 1962.

10. Prince, Luther T., Jr. "A Generalized Method for Determining the Closed-Loop Frequency Response of Nonlinear Systems." Transactions of the AIEE, 73, Part II, Applications and Industry: 217-224 (1954).

11. Siefert, William W., and Carl W. Steeg, Jr. (editors). Control Systems Engineering. New York: McGraw-Hill Book Company, Inc., 1960.

12. Thaler, George J., and Marvin P. Pastel. Analysis and Design of Nonlinear Feedback Systems. New York: McGraw-Hill Book Company, Inc., 1962.

Part B - Supplementary References

Choksy, N. H. "A New Analytic Stability Criterion for Use with Describing Functions," in Preprints of Technical Papers, Fourth Joint Automatic Control Conference. New York: American Institute of Chemical Engineers, June 1963, pp. 481-484.

Cosgriff, Robert L. Nonlinear Control Systems. New York: McGraw-Hill Book Company, Inc., 1958.

Chestnut, H. "Approximate Frequency-Response Methods for Representing Saturation and Dead Band." Transactions, ASME, 76: 1345-1364 (1954).

Deekshatulu, B. L. "How to Evaluate Harmonic Response of Nonlinear Components." Control Engineering, 10: 53-56 (October 1963).

Ergin, E. I., V. D. Norum, and T. G. Windeknecht. Techniques for Analysis of Nonlinear Attitude Control Systems for Space Vehicles, Volumes II and IV. Wright-Patterson AFB, Ohio: Flight Control Laboratory, ASD, June 1962.

Graham, Dunstan, and Duane McRuer. Analysis of Nonlinear Control Systems. New York: John Wiley and Sons, Inc., 1961.

Grief, H. D. "Describing Function Method of Servomechanism Analysis Applied to Most Commonly Encountered Nonlinearities." Transactions of the AIEE, 72, Part II, Applications and Industry: 243-248 (1953).

Klotter, Karl. "How to Obtain Describing Functions for Nonlinear Feedback Systems." Transactions, ASME, 76, Part II: 183-190 (1957).

Kochenburger, Ralph J. "Limiting in Feedback Control Systems." Transactions, AIEE, 72, Part II, Applications and Industry: 180-194 (1953).

Ku, Yu-hsiu. Analysis and Control of Nonlinear Systems. New York: Ronald Press Company, 1958.

Ku, Y. H., and C. F. Chen. "New Method for Evaluating Describing Function of Hysteresis-Type Nonlinearities." Franklin Institute-Journal, 273: 226-241 (March 1962).

Satyendra, K. N. "Describing Functions Representing the Effect of

Inertia, Backlash, and Coulomb Friction on the Stability of an Automatic Control System." _Transactions of the AIEE_, _75_, _Part II_, _Applications and Industry_: 243-249 (1956).

Sridhar, R. "A General Method for Deriving Describing Functions for a Class of Nonlinearities." _IRE Transactions on Automatic Control_, _AC-5_: 135-141 (June 1960).

Thomas, C. H. "Stability Characteristics of Closed-Loop Systems with Dead Band." _Transactions_, _ASME_, _76_: 1365-1382 (1954).

Truxall, John G. _Automatic Feedback Control System Synthesis._ New York: McGraw-Hill Book Company, Inc., 1955.

Appendix A

Derivations of the Corrected-Conventional Describing Functions Used in this Study

The definition of the corrected-conventional describing function given in Eq (16) on page 26 is quite general, but the definition can often be simplified by taking advantage of certain symmetries in the output waveform. For odd-periodic, odd-harmonic outputs from the nonlinearity, Eq (16) becomes simply (nondimensionalized)

$$\frac{N}{K} = \frac{(Y_1^2 + Y_3^2)^{\frac{1}{2}}}{KX} \tag{18}$$

where Y_1 = Fundamental amplitude = $(A_1^2 + B_1^2)^{\frac{1}{2}} = B_1$, since $A_1 = 0$;

Y_3 = 3rd harmonic amplitude = $(A_3^2 + B_3^2)^{\frac{1}{2}} = B_3$, since $A_3 = 0$;

X = Amplitude of the sinusoidal input to the nonlinearity;

K = Gain of the nonlinearity.

Obviously, the derivation of the corrected-conventional describing function is similar to that of the conventional, except that the amplitude of the third Fourier harmonic must be determined as well as the fundamental. As a first example, consider the case of saturation combined with dead zone.

Saturation Combined with Dead Zone

As Figure 19 on the following page shows, the output of the nonlinearity is both odd periodic and odd harmonic; therefore, the coefficients of the cosine terms in the Fourier expansion of the output waveform are all zero, as are the coefficients of all the even sine

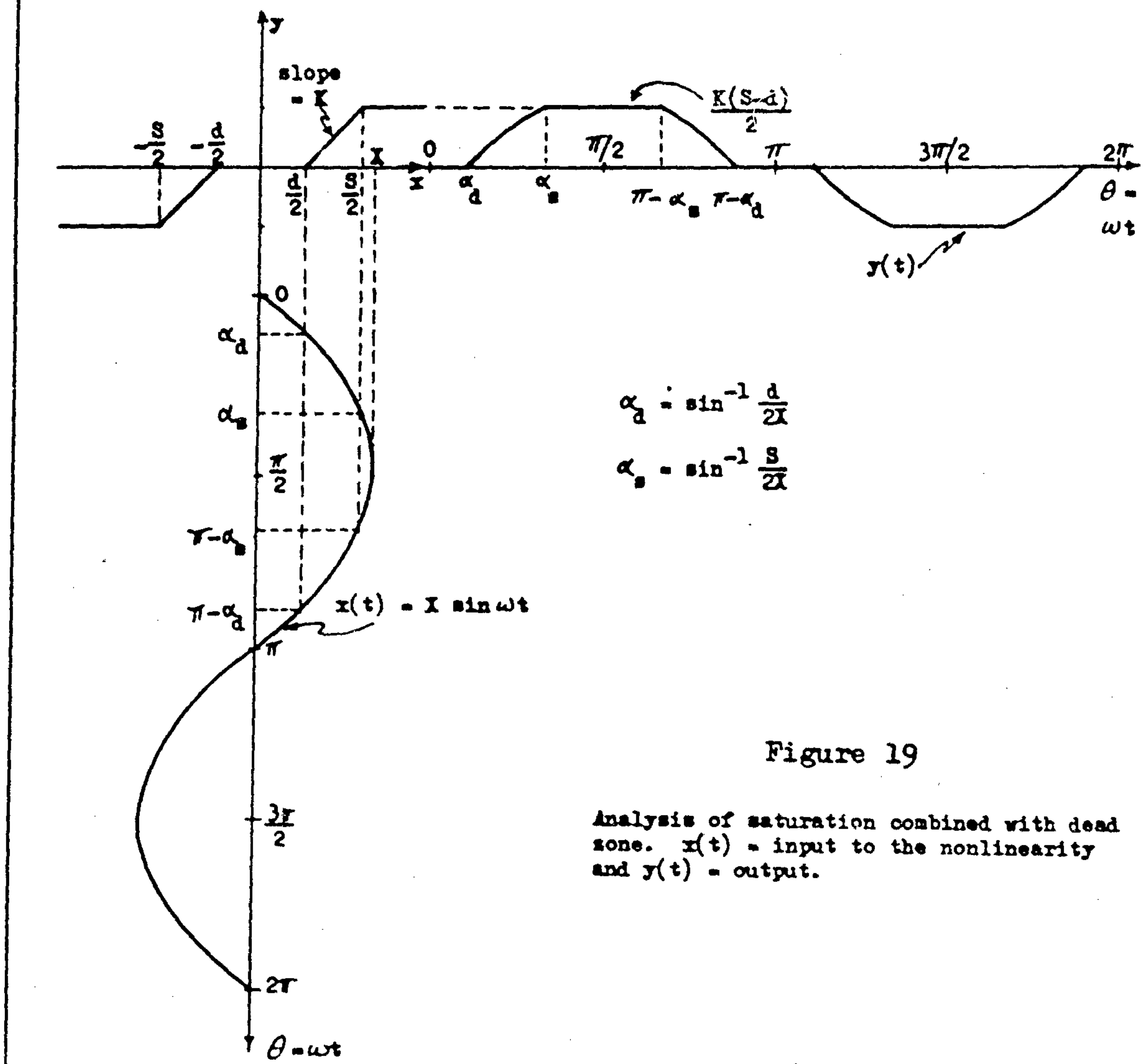

Figure 19

Analysis of saturation combined with dead zone. x(t) = input to the nonlinearity and y(t) = output.

(Adapted from Ref 1:436)

terms. Also, because of this symmetry, the expression for the coefficient of the fundamental is (Ref 1:436-7)

$$Y_1 = \frac{4}{\pi}\int_0^{\frac{\pi}{2}} y(t)\ \sin\theta\ d\theta$$

$$= \frac{4}{\pi}\int_{\alpha_d}^{\alpha_s} (KX\ \sin\theta\ - \frac{Kd}{2})\sin\theta\ d\theta + \frac{4}{\pi}\int_{\alpha_s}^{\frac{\pi}{2}} \frac{K(S-d)}{2}\ \sin\theta\ d\theta \qquad (19)$$

which, when integrated, becomes

$$Y_1 = \frac{KX}{\pi}\ (2\alpha_s - 2\alpha_d + \sin\ 2\alpha_s - \sin\ 2\alpha_d) \qquad (20)$$

Similarly, the coefficient of the third harmonic is

$$Y_3 = \frac{4}{\pi}\int_0^{\frac{\pi}{2}} y(t)\ \sin\ 3\theta\ d\theta \qquad (21)$$

$$= \frac{4}{\pi}\int_{\alpha_d}^{\alpha_s} (KX\ \sin\theta\ - \frac{Kd}{2})\sin\ 3\theta\ d\theta + \frac{4}{\pi}\int_{\alpha_s}^{\frac{\pi}{2}} \frac{K(S-d)}{2}\ \sin\ 3\theta\, d\theta$$

which, when integrated, becomes

$$Y_3 = \frac{KX}{\pi}\ (\frac{5}{3}\ \sin\ 2\alpha_s - \frac{5}{3}\ \sin\ 2\alpha_d - \frac{1}{2}\ \sin\ 4\alpha_s + \frac{1}{2}\ \sin\ 4\alpha_d\ -$$

$$\frac{16}{3}\ \sin^3\alpha_s\ \cos\alpha_s + \frac{16}{3}\ \sin^3\alpha_d\ \cos\alpha_d) \qquad (22)$$

From Eqs (18), (20), and (22) the (nondimensional) corrected-conventional describing function for saturation combined with dead

zone is therefore

$$\frac{N}{K} = \frac{1}{\pi}\Big[(2\alpha_s - 2\alpha_d + \sin 2\alpha_s - \sin 2\alpha_d)^2 + (\frac{5}{3}\sin 2\alpha_s - \frac{5}{3}\sin 2\alpha_d - \frac{1}{2}\sin 4\alpha_s + \frac{1}{2}\sin 4\alpha_d - \frac{16}{3}\sin^3\alpha_s \cos\alpha_s + \frac{16}{3}\sin^3\alpha_d \cos\alpha_d)^2\Big]^{\frac{1}{2}} \tag{23}$$

The (nondimensional) corrected-conventional describing function for saturation can be found by letting $\alpha_d = 0$ in Eq (23); that is,

$$\frac{N}{K} = \frac{1}{\pi}\Big[(2\alpha_s + \sin 2\alpha_s)^2 + (\frac{5}{3}\sin 2\alpha_s - \frac{1}{2}\sin 4\alpha_s - \frac{8}{3}\sin 2\alpha_s \sin^2\alpha_s)^2\Big]^{\frac{1}{2}} \tag{24}$$

Similarly, by letting $\alpha_s = \pi/2$ in Eq (23), one can find the (nondimensional) corrected-conventional describing function for dead zone to be

$$\frac{N}{K} = \frac{1}{\pi}\Big[(\pi - 2\alpha_d - \sin 2\alpha_d)^2 + (-\frac{5}{3}\sin 2\alpha_d + \frac{1}{2}\sin 4\alpha_d + \frac{8}{3}\sin 2\alpha_d \sin^2\alpha_d)^2\Big]^{\frac{1}{2}} \tag{25}$$

Eqs (24) and (25) can also be obtained by a Fourier analysis of the output wave of the nonlinearity as was done for saturation combined with dead zone.

Relay with Dead Zone and Hysteresis

Using the same technique as in the preceding derivation, one can derive the (nondimensional) corrected-conventional describing

function for a relay with dead zone and hysteresis, and then simplify the result for the specific cases of a relay with dead zone only, a relay with hysteresis only, and an ideal relay.

Figure 20 on the following page shows that the output of the relay-dead zone-hysteresis nonlinearity is not symmetrical about the origin. However, odd-periodic and odd-harmonic symmetry can be recovered by a phase shift of the axis by the amount $(\pi/2 - \frac{\alpha+\beta}{2})$. This angle is therefore the angle of <u>any</u> describing function which is generated by a scheme which does not introduce a phase shift when applied to an odd-periodic, odd-harmonic function. Since all of the describing-function generating schemes studied in this paper meet this requirement, the expression for the angle of the corrected-conventional describing function for a relay with dead zone and hysteresis is

$$\angle N = \angle \frac{N}{K} = \angle \frac{N\cdot(d+h)}{K} = \frac{\pi}{2} - \frac{\alpha+\beta}{2} = -\theta \qquad (26)$$

After the axis is shifted, the output waveform is odd-periodic and odd-harmonic. Therefore, all of the cosine coefficients and the even sine coefficients are zero, and the amplitude of the fundamental (integrating with the axis shifted to $-\angle N$) is

$$Y_1 = \frac{4}{\pi}\int_0^{\frac{\pi}{2}} y(t)\ \sin\theta\ d\theta$$

$$= \frac{4}{\pi}\int_{\alpha+\angle N}^{\frac{\pi}{2}} K\ \sin\theta\ d\theta \qquad (27)$$

or

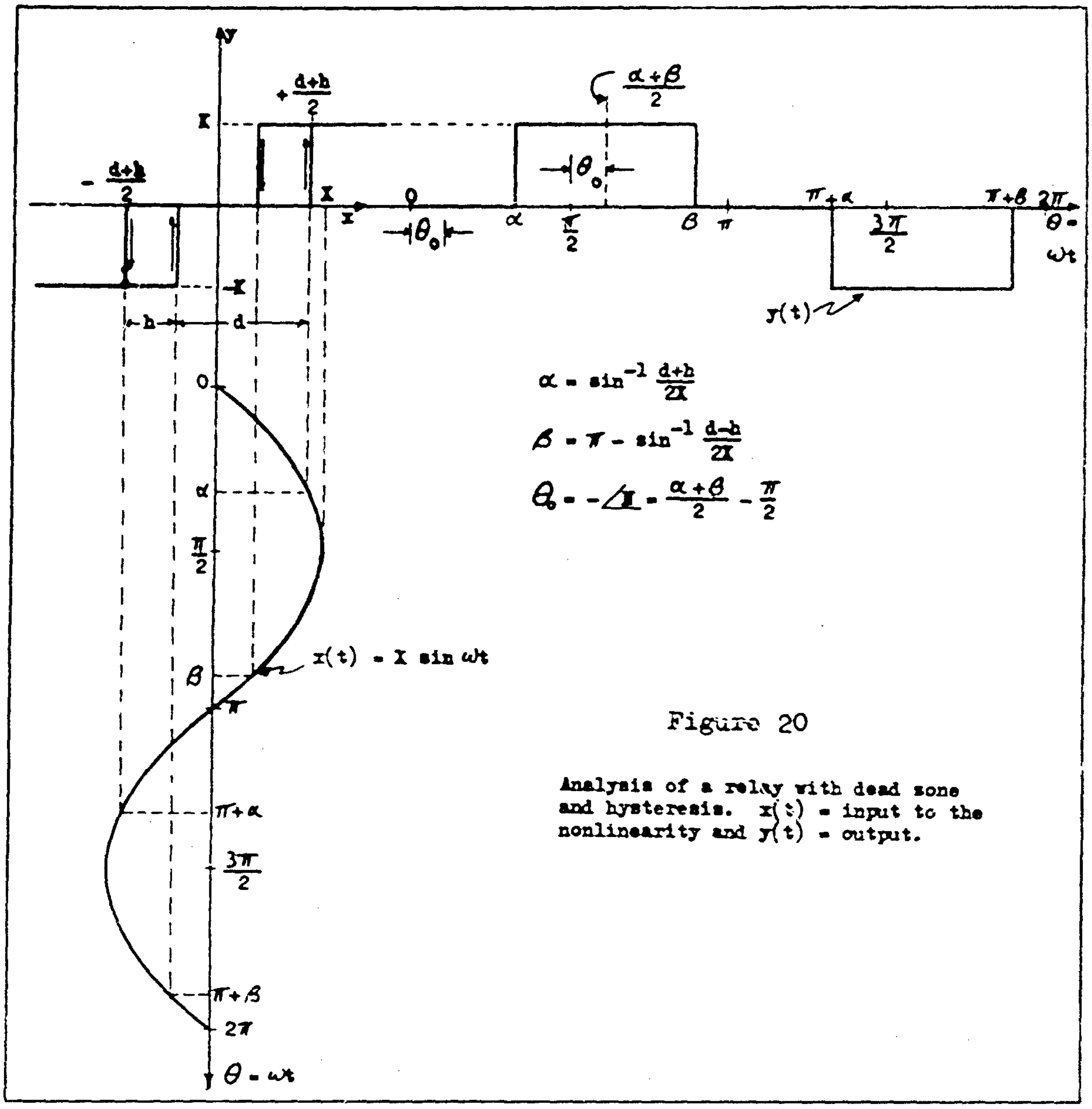

Figure 20

Analysis of a relay with dead zone and hysteresis. x(t) = input to the nonlinearity and y(t) = output.

$$Y_1 = \frac{4}{\pi}\int_{\frac{\pi}{2}+\frac{\alpha-\beta}{2}}^{\frac{\pi}{2}} K \sin\theta \, d\theta \tag{28}$$

which, when integrated, becomes

$$Y_1 = \frac{4K}{\pi} \sin\left(\frac{\beta-\alpha}{2}\right) \tag{29}$$

Similarly, the coefficient of the third harmonic is

$$Y_3 = \frac{4}{\pi}\int_0^{\frac{\pi}{2}} y(t) \sin 3\theta \, d\theta$$

$$= \frac{4}{\pi}\int_{\frac{\pi}{2}+\frac{\alpha-\beta}{2}}^{\frac{\pi}{2}} K \sin 3\theta \, d\theta \tag{30}$$

which, when integrated, becomes

$$Y_3 = \frac{4K}{3\pi} \sin\left(\frac{\beta-\alpha}{2}\right)\left[1 - 4\cos^2\left(\frac{\beta-\alpha}{2}\right)\right] \tag{31}$$

From Eqs (18), (29), and (31) the magnitude of the (nondimensional) corrected-conventional describing function for a relay with dead zone and hysteresis is

$$\left|\frac{N}{K}\right| = \frac{4}{\pi X} \sin\left(\frac{\beta-\alpha}{2}\right)\left\{1 + \frac{1}{9}\left[1 - 4\cos^2\left(\frac{\beta-\alpha}{2}\right)\right]^2\right\}^{\frac{1}{2}} \tag{32}$$

or, substituting $X = \frac{d+h}{2\sin\alpha}$,

$$\left|\frac{N\cdot(d+h)}{K}\right| = \frac{8}{\pi} \sin\alpha \, \sin\left(\frac{\beta-\alpha}{2}\right)\left\{1 + \frac{1}{9}\left[1 - 4\cos^2\left(\frac{\beta-\alpha}{2}\right)\right]^2\right\}^{\frac{1}{2}} \tag{33}$$

The (nondimensional) corrected-conventional describing function for a relay with dead zone only can be determined by letting $h = 0$ in the foregoing analysis; then,

$$\alpha = \sin^{-1}\frac{d}{2X} \equiv \alpha_d \tag{34}$$

$$\beta = \pi - \sin^{-1}\frac{d}{2X} = \pi - \alpha_d \tag{35}$$

So Eq (26) becomes

$$\angle N = \frac{\pi}{2} - \frac{\alpha_d + \pi - \alpha_d}{2} = 0 \tag{36}$$

Therefore the describing function for a relay with dead zone is determined from Eq (33) to be

$$\frac{Nd}{K} = \frac{4}{\pi}\sin 2\alpha_d\left[1 + \frac{1}{9}(1 - 4\sin^2\alpha_d)^2\right]^{\frac{1}{2}} \tag{37}$$

Similarly, by letting $d = 0$

$$\alpha = \sin^{-1}\frac{h}{2X} \equiv \alpha_h \tag{38}$$

$$\beta = \pi - \sin^{-1}\frac{-h}{2X} = \pi + \alpha_h \tag{39}$$

And, by substituting these values of α and β into Eqs (26) and (32), one can find the (nondimensional) corrected-conventional describing function for a relay with hysteresis to be

$$\angle N = \angle\frac{N}{K} = -\alpha_h \tag{40}$$

$$\left|\frac{N}{K}\right| = \frac{4}{\pi X}\left(\frac{10}{9}\right)^{\frac{1}{2}} \tag{41}$$

Furthermore, for an ideal relay $\alpha_h = 0$, and therefore

$$\frac{N}{K} = \frac{4}{\pi X} \left(\frac{10}{9}\right)^{\frac{1}{2}} \tag{42}$$

Eqs (37), (40), (41), and (42) can also be found by a Fourier analysis of the output waveform of the respective nonlinearities as was done for saturation combined with dead zone and the relay with dead zone and hysteresis.

Plots of all of the describing functions derived in this appendix can be found in Appendix D.

Appendix B

Derivations of the New RMS Describing Functions which Introduce Hysteresis

As pointed out on pages 6 and 8 of the introduction, one way of extending the new rms describing function to polar-symmetrical nonlinearities which are not single-valued is to let the angle of the describing function be the angle of phase shift necessary to make the output of the nonlinearity odd periodic. This, incidently, is the same angle that is obtained for the conventional describing function through a Fourier analysis. Again, as with the corrected-conventional describing function derivations in Appendix A, one can take advantage of the quarter-wave symmetry which occurs after the shift in axes to modify Eq (15) on page 25 for simpler integration. For example, after shifting the axes of the output of the relay + dead zone + hysteresis nonlinearity shown in Figure 20 on page 96 to θ_o, the output becomes odd periodic, and the angle of the new rms describing function is, therefore,

$$\angle N = -\theta_o = \frac{\pi}{2} - \frac{\alpha+\beta}{2} \tag{43}$$

Then, the magnitude of the new rms describing function is

$$|N| = \left[\frac{\int_{\alpha+\left(\frac{\pi}{2}-\frac{\alpha+\beta}{2}\right)}^{\frac{\pi}{2}} K^2\, d\theta}{\int_0^{\frac{\pi}{2}} X^2 \sin^2\theta\, d\theta}\right]^{\frac{1}{2}} \tag{44}$$

because of the quarter wave symmetry. Integrating, one will obtain

$$|N| = \left[\frac{K^2 \theta \Big|_{\frac{\pi}{2} + \frac{\alpha - \beta}{2}}^{\frac{\pi}{2}}}{X^2 \left(\frac{\theta}{2} - \frac{\sin 2\theta}{4} \right) \Big|_0^{\frac{\pi}{2}}} \right]^{\frac{1}{2}}$$

$$= K \left[\frac{2}{\pi X^2} (\beta - \alpha) \right]^{\frac{1}{2}} \tag{45}$$

So the (nondimensional) new rms describing function, with angle expressed in exponential form, is

$$\frac{N}{K} = \left[\frac{2}{\pi X^2} (\beta - \alpha) \right]^{\frac{1}{2}} e^{j\left(\frac{\pi}{2} - \frac{\alpha + \beta}{2}\right)} \tag{46}$$

or, substituting $X = \frac{d + h}{2 \sin \alpha}$,

$$\frac{N(d+h)}{K} = 2 \left[\frac{2}{\pi} (\beta - \alpha) \sin^2 \alpha \right]^{\frac{1}{2}} e^{j\left(\frac{\pi}{2} - \frac{\alpha + \beta}{2}\right)} \tag{47}$$

By letting d = 0 in Figure 20, one can find the (nondimensional) new rms describing function for a relay with hysteresis. Then

$$\alpha = \sin^{-1} \frac{h}{2X} = \alpha_h \tag{38}$$

$$\beta = \pi - \sin^{-1} \frac{-h}{2X} = \pi + \alpha_h \tag{39}$$

So that, from Eq (46),

$$\frac{N}{K} = \frac{\sqrt{2}}{X} e^{-j\alpha_h} \tag{48}$$

Appendix C

Experimental Procedure and Analog Computer Circuits

In order to add credibility to the experimental results, as well as to allow the reader to repeat the experiment, the experimental procedure used by the author is explained in the following discussion.

Procedure

Figure 21 on the following page shows the computer, plotter, and test equipment arrangement used in the experimental determination of the amplitude and frequency of the self-sustained oscillations in the nonlinear feedback systems of the study. Figures 23 through 29 on pages 107 through 111 show general analog computer circuits equivalent to the block diagram arrangement in Figure 22 for each of the linear forward transfer functions, $G_1(s)$ through $G_7(s)$. The general circuit for $G_{3A}(s)$ is the same as that of $G_3(s)$ in Figure 25, but with the outer loop gain increased by a factor of 3.475. Similarly, the general circuit for $G_{7A}(s)$ is the same as that of $G_7(s)$ in Figure 29, but with the outer loop gain increased by 3.333. Figures 30 through 36 on pages 111 through 115 contain the differential relay mechanizations of the various nonlinearities studied. These differential relay circuits were introduced in place of the box labled "N" in each of the general circuits for the specific tests required. The procedure for measurement of the resulting oscillations was as follows (See Figure 21):

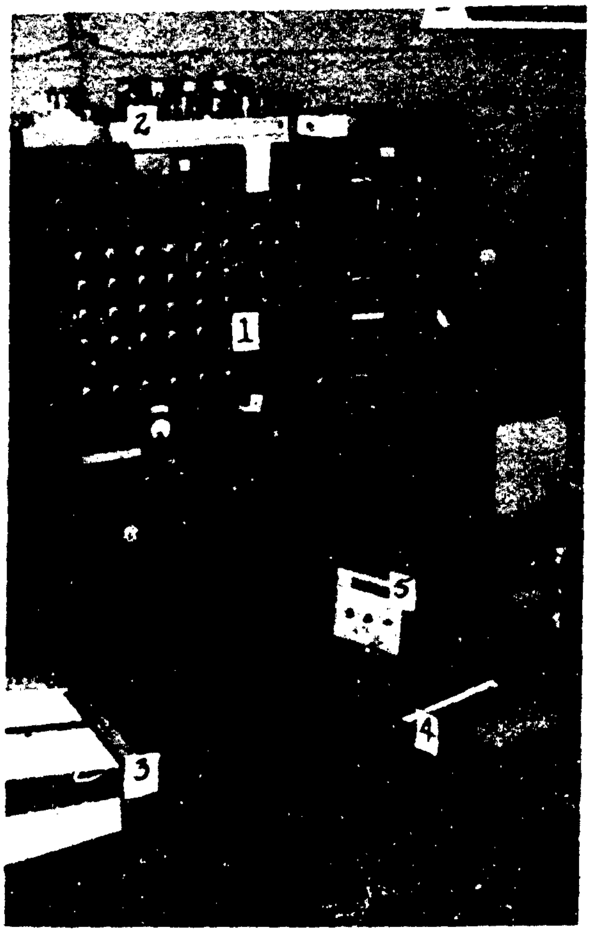

Figure 21

Analog computer test arrangement for the measurement of the amplitude and frequency of self-sustained oscillations: (1) REAC Electronic Analogue Computer, Model C-101, Reeves Instrument Corporation; (2) Differential Relay Unit; (3) Variplotter Plotting Board, Model 1100-E, Electronic Associates, Inc.; (4) Dynagraph Recorder, Type MC, Offner Electronics, Inc.; (5) Digital Voltmeter, Model 4011-4, Beckman Industries, Inc.

(1) The differential relay circuit and general circuit for a particular case to be tested were wired together on the REAC patch-panel, after proper amplitude scaling based on the predicted amplitude. (Note that the figures in this appendix have been labled in terms of k, the amplitude scale factor, in order to facilitate scaling each run.) The potentiometers on the REAC were then set to four-place accuracy with the digital voltmeter.

(2) The REAC was switched to "Operate" and the ensuing oscillations were recorded on both the Variplotter and the Dynagraph. An initial value of c which was greater than the dead zone was required to initiate oscillations in the systems that had nonlinearities with dead zone.

(3) After the oscillation had stabilized for a few cycles, the REAC was switched back to "Reset."

(4) The amplitude of the oscillation was then accurately determined by measuring the positive and negative initial condition voltage (on the integrator from which X was being recorded) necessary to move the pen of the Variplotter precisely to the level of the positive and negative peaks of the previously recorded self-sustained oscillation. This initial condition voltage was measured to four-place accuracy with the digital voltmeter. The amplitude of the oscillation was then taken as the average of the magnitude of the positive and negative peak so measured. By using this technique, one can eliminate any variation in the linearity of the Variplotter, and very accurate results can be obtained.

(5) The frequency of the oscillation was accurately determined by measuring the period of a previously recorded self-sustained oscillation from a Dynagraph recording. Since the Dynagraph was run at one of its maximum speeds during the test (100 or 250 mm/sec) and the frequency of oscillation was quite low (0.5 to 3.3 radians/sec), the measurement of the period of the oscillation was also quite precise. The frequency in radians/sec is then 2π divided by the period.

Verification

In order to verify the accuracy of this experimental procedure, one of the runs, $G_4(s)$ plus saturation and dead zone, was programmed and run on the digital computer. $G_4(s)$ was chosen as the linear function to be checked because it was the worst of all of the analog circuit designs due to the high loop gains. The dead zone and saturation nonlinearity was chosen because it was one of the more complex nonlinearities studied from a standpoint of simulation difficulty, and it was felt that the sensitivity of the differential relays might introduce a small error in the simulations, and this error would be most prominent in a nonlinearity with several relays.

A numerical integration time increment of 0.004 seconds was used for the digital computer study. The results indicated a limit cycle at the output with an amplitude of 12.832, and a frequency of 1.822 rad/sec. The analog computer run gave an amplitude of 12.88 and a frequency of 1.816 rad/sec for the same problem.

Since the difference between the digital and analog results was less than half a percent (see Table XXVIII below) in what is considered to be one of the least accurate analog runs, it is felt that the validity of the entire set of analog computer results is sufficient for a basis of comparison of the various describing functions.

Table XXVIII

Comparison of Analog and Digital Simulations

	Amplitude	Frequency
Digital Computer Result	12.832	1.822
Analog Computer Result	12.88	1.816
% Difference in Results	0.3741	0.3293

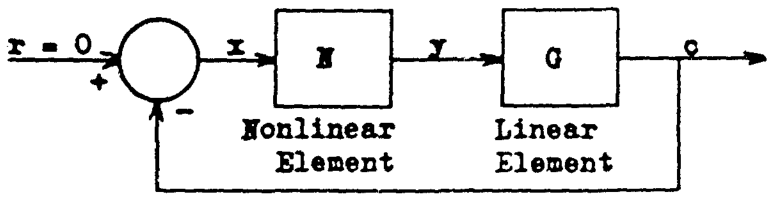

Figure 22

General block diagram of a feedback system with a nonlinearity.

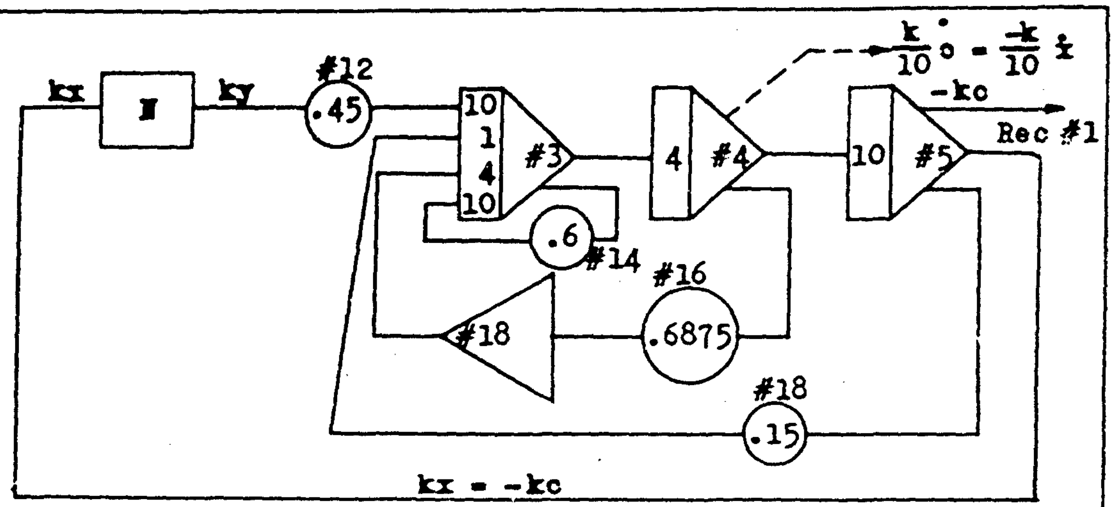

Figure 23

General analog computer circuit for the determination of the amplitude and frequency of sustained oscillations in a closed loop with linear system $G_1(s)$ and a nonlinearity.

Transfer function: $G_1(s) = \frac{180}{(s+1)(s+2)(s+3)} = \frac{C(s)}{Y(s)}$

Mechanized differential equation: $D^3c = 180y - 6D^2c - 11Dc - 6c$

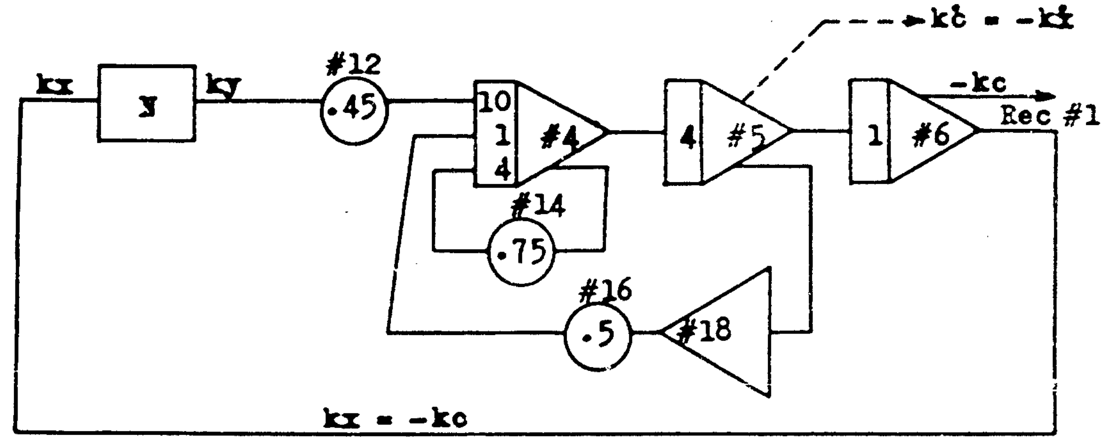

Figure 24

General analog computer circuit for the determination of the amplitude and frequency of sustained oscillations in a closed loop with linear system $G_2(s)$ and a nonlinearity.

Transfer function: $G_2(s) = \dfrac{18}{s(s+1)(s+2)} = \dfrac{C(s)}{Y(s)}$

Mechanized differential equation: $D^3c = 18y - 3D^2c - 2Dc$

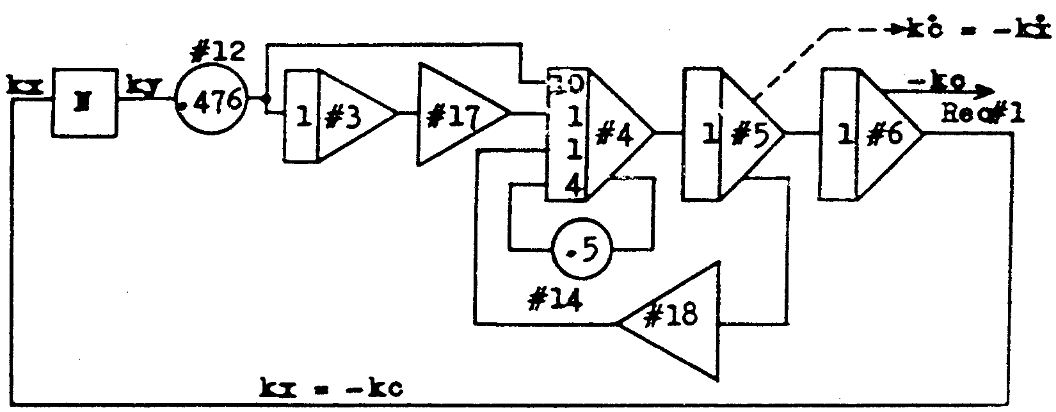

Figure 25

General analog computer circuit for the determination of the amplitude and frequency of sustained oscillations in a closed loop with linear system $G_3(s)$ and a nonlinearity.

Transfer function: $G_3(s) = \dfrac{4.76(s+0.1)}{s^2(s+1)^2}$

Mechanized differential equation: $D^3c = 4.76y + 0.476\,\dfrac{Y}{D} - 2D^2c - Dc$

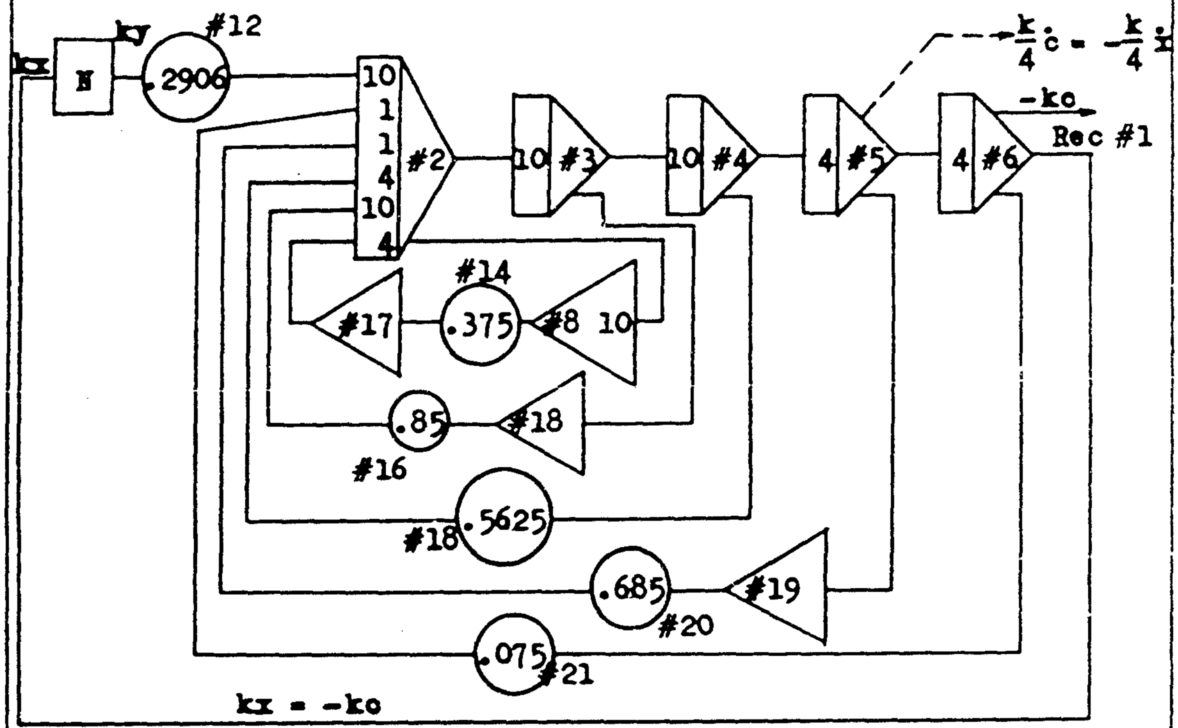

Figure 26

General analog computer circuit for the determination of the amplitude and frequency of sustained oscillations in a closed loop with linear system $G_4(s)$ and a nonlinearity.

Transfer function: $G_4(s) = \dfrac{4650.3}{(s+1)(s+2)(s+3)(s+4)(s+5)} = \dfrac{C(s)}{Y(s)}$

Mechanized differential equation:

$$D^5c = 4650.3y - 15D^4c - 85D^3c - 225D^2c - 274Dc - 120c$$

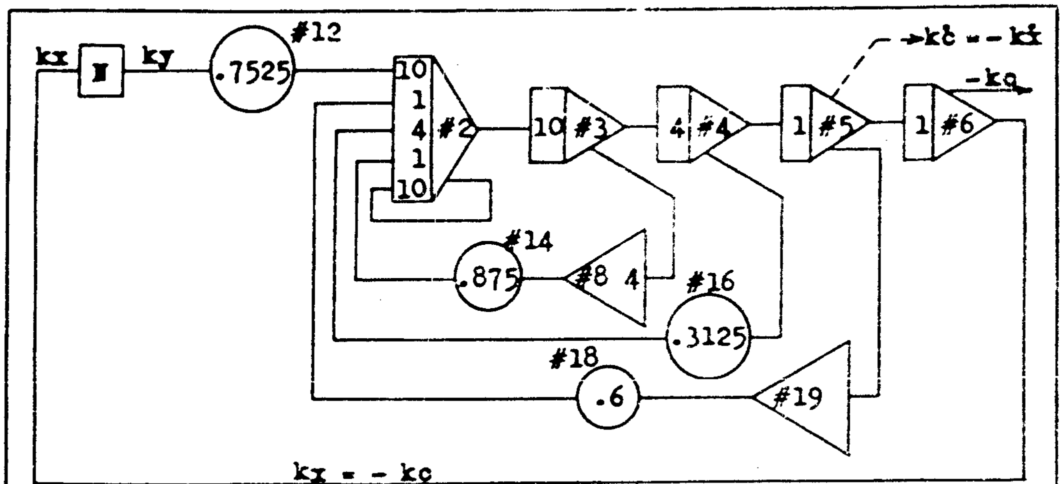

Figure 27

General analog computer circuit for the determination of the amplitude and frequency of sustained oscillations in a closed loop with linear system $G_5(s)$ and a nonlinearity.

Transfer function: $G_5(s) = \dfrac{301}{s(s+1)(s+2)(s+3)(s+4)} = \dfrac{C(s)}{Y(s)}$

Mechanized differential equation:

$$D^5c = 301y - 10D^4c - 35D^3c - 50D^2c - 24Dc$$

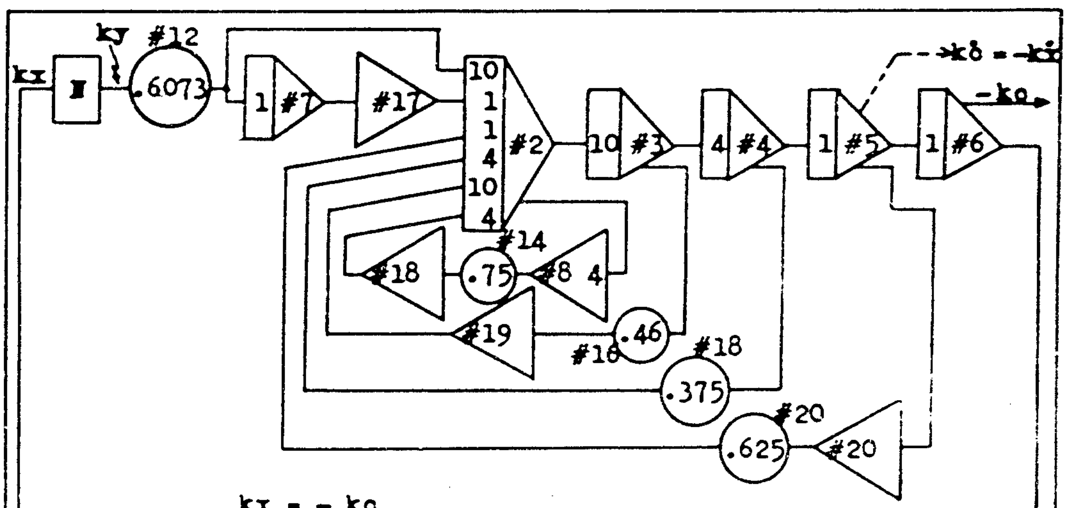

Figure 28

General analog computer circuit for the determination of the amplitude and frequency of sustained oscillations in a closed loop with linear system $G_6(s)$ and a nonlinearity.

Transfer function: $G_6(s) = \dfrac{242.9\ (s+0.1)}{s^2(s+1)^2(s+5)^2} = \dfrac{C(s)}{Y(s)}$

Mechanized differential equation:

$$D^5c = 242.9y + 24.29y/D - 12D^4c - 46D^3c - 60D^2c - 25Dc$$

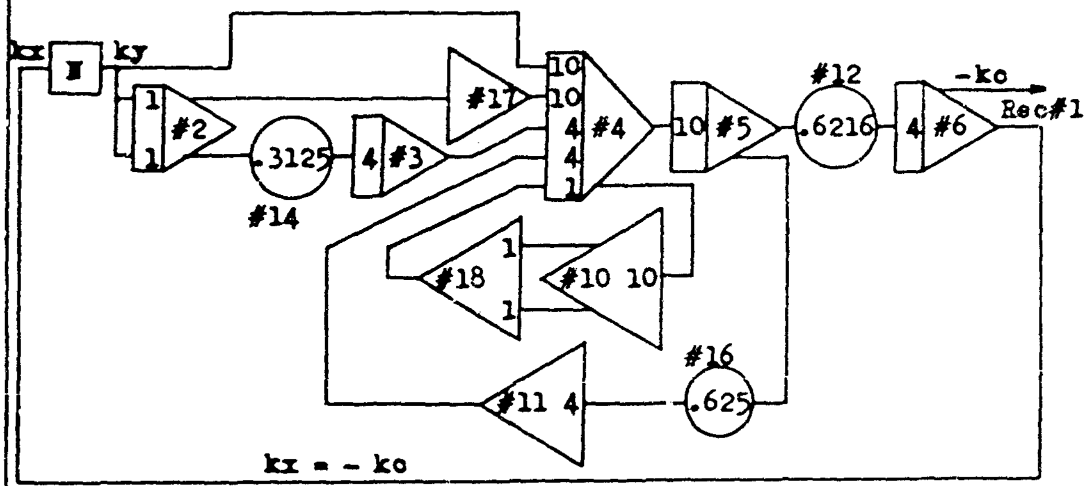

Figure 29

General analog computer circuit for the determination of the amplitude and frequency of sustained oscillations in a closed loop with linear system $G_7(s)$ and a nonlinearity.

Transfer function: $G_7(s) = \dfrac{248.626\,(s+1)^2}{s^3(s+10)^2} = \dfrac{C(s)}{Y(s)}$

Mechanized differential equation:

$$D^3c = 248.626y + 497.252\,\frac{y}{D} + 248.626\,\frac{y}{D^2} - 20D^2c - 100Dc$$

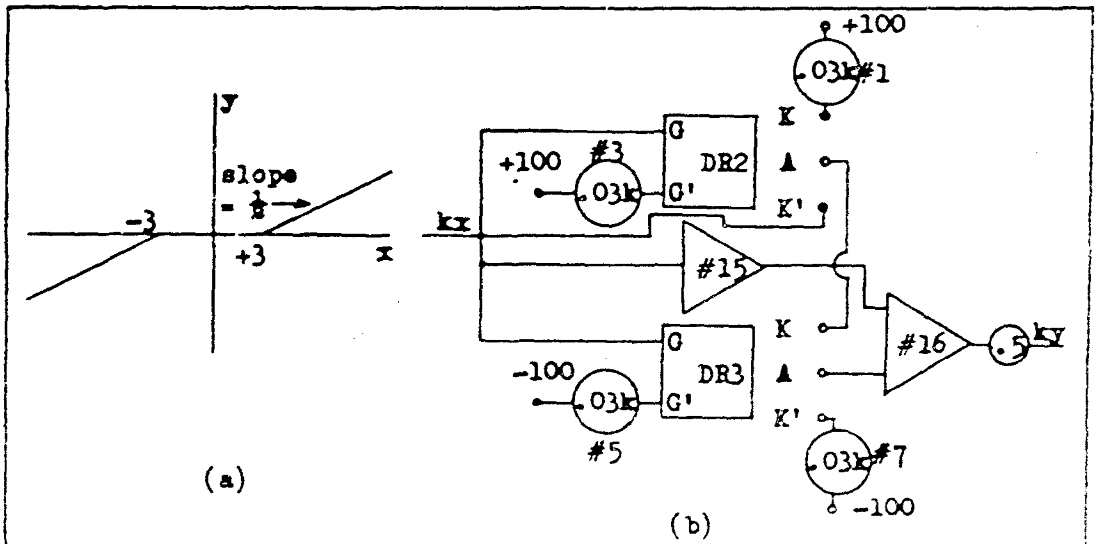

Figure 30

Mechanization of dead zone (d = 6, K = 0.5) with differential relays: (a) transfer characteristic, (b) analog computer circuit.

(From Ref 5:192)

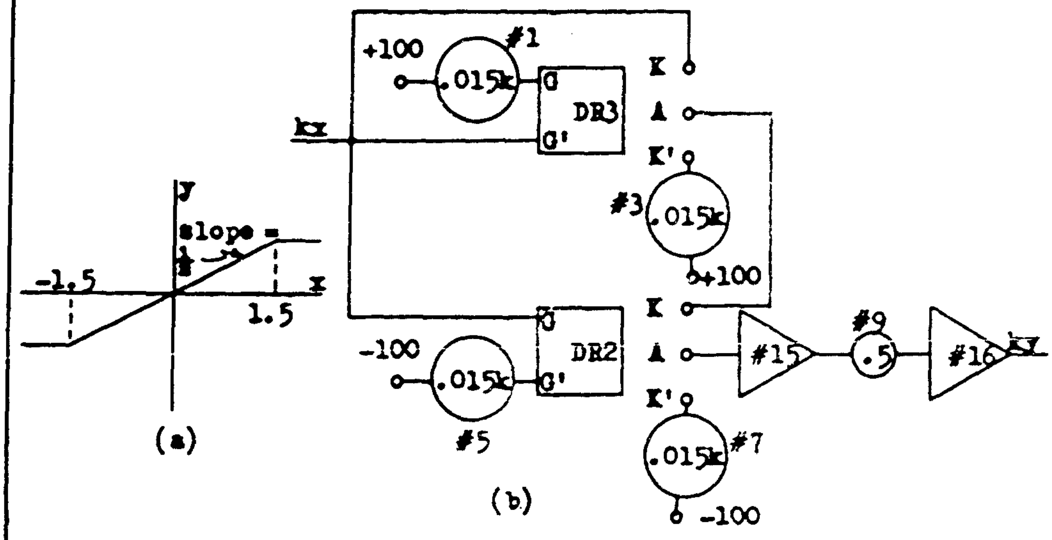

Figure 31

Mechanization of saturation (S = 3, K = 0.5) with differential relays: (a) transfer characteristic, (b) analog computer circuit.

(From Ref 5 :188)

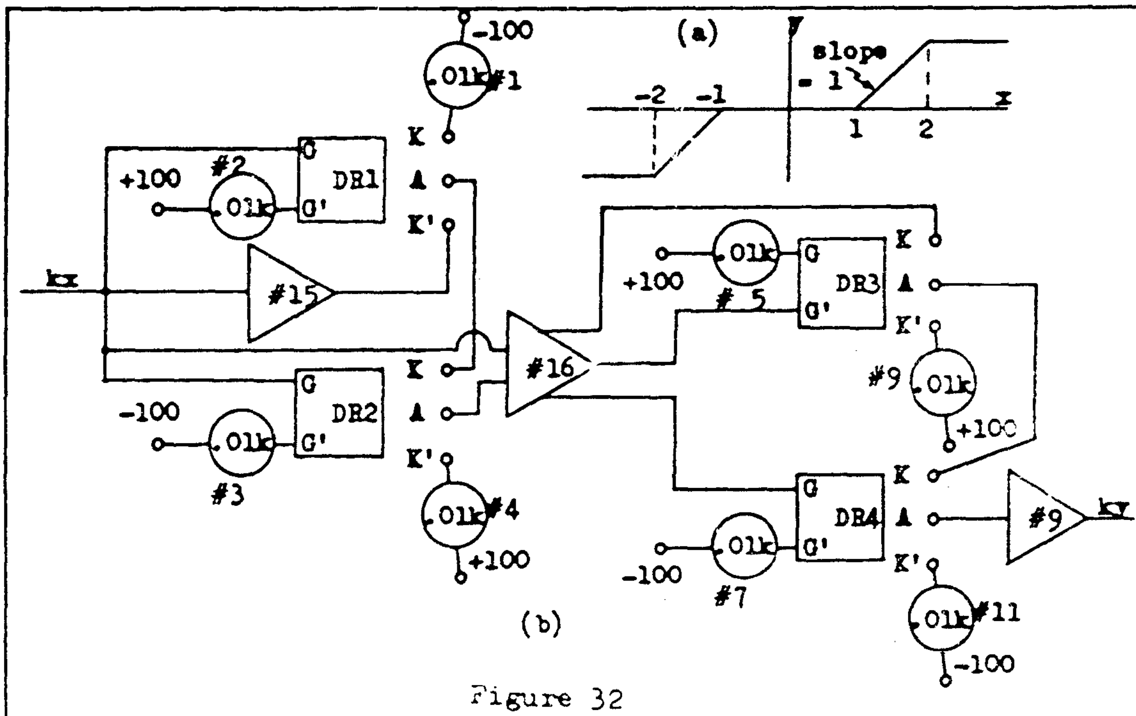

Figure 32

Mechanization of saturation with dead zone (d = 2, S = 4, K = 1) with differential relays: (a) transfer characteristic, (b) analog computer circuit.

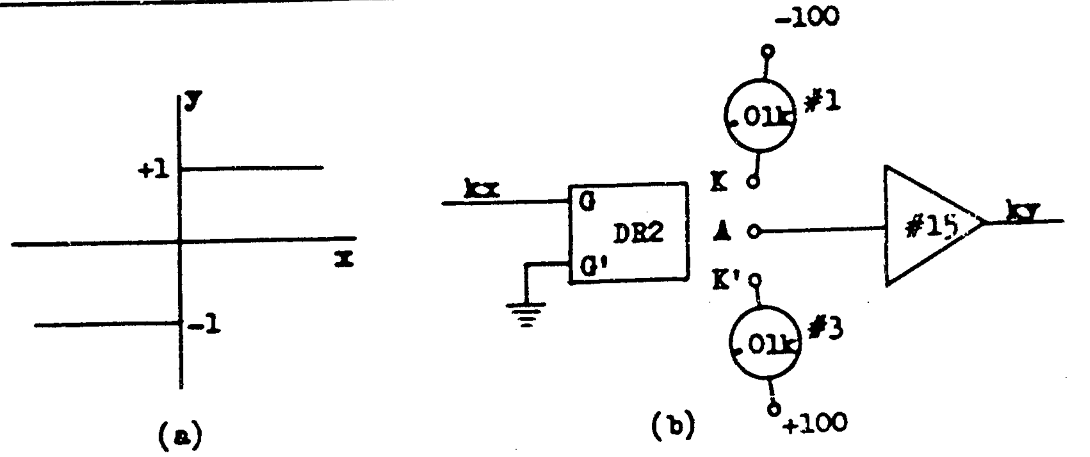

Figure 33

Mechanization of an ideal relay (K = 1) with differential relays: (a) transfer characteristic, (b) analog computer circuit.

(From Ref 5 :190)

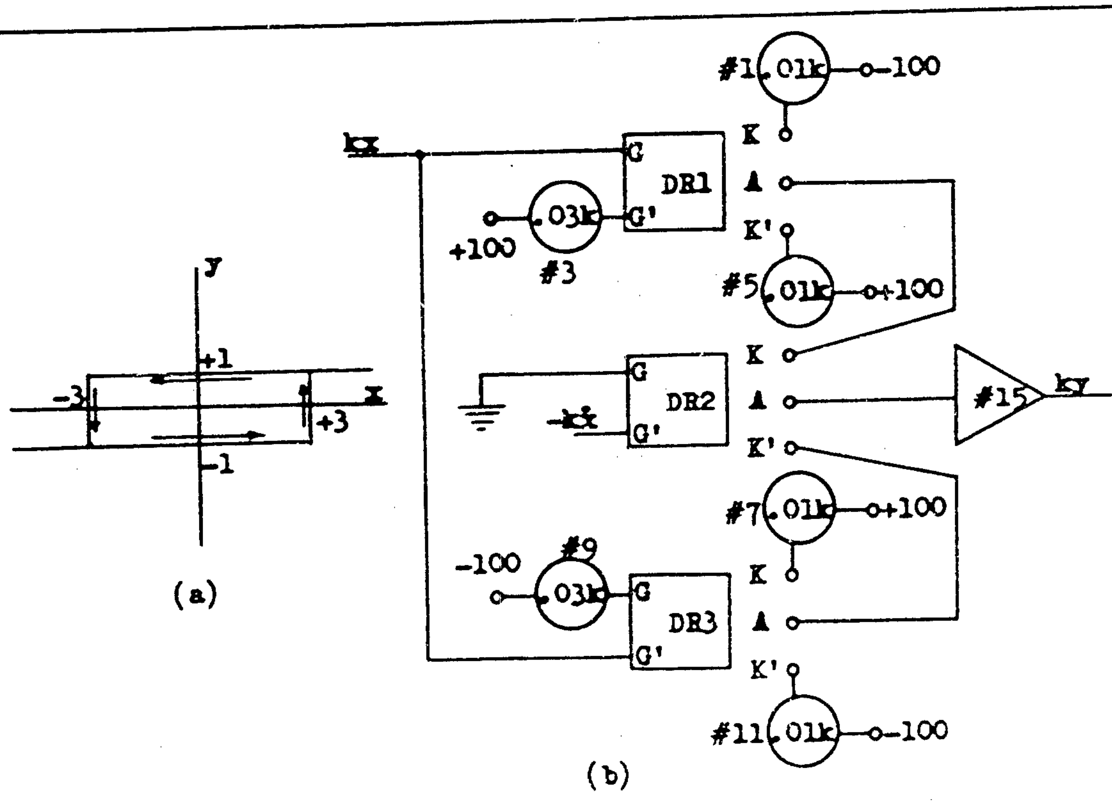

Figure 34

Mechanization of a relay with hysteresis (h = 6, K = 1) with differential relays: (a) transfer characteristic, (b) analog computer circuit.

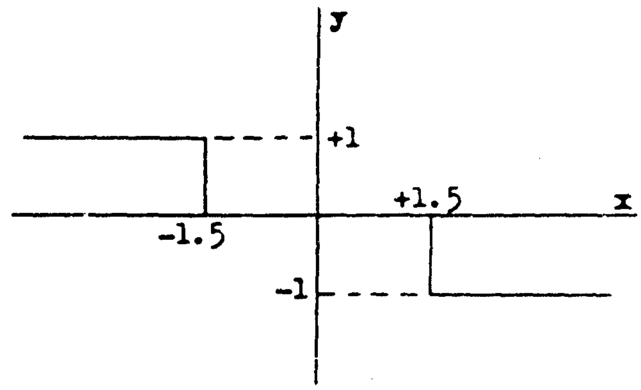

(a)

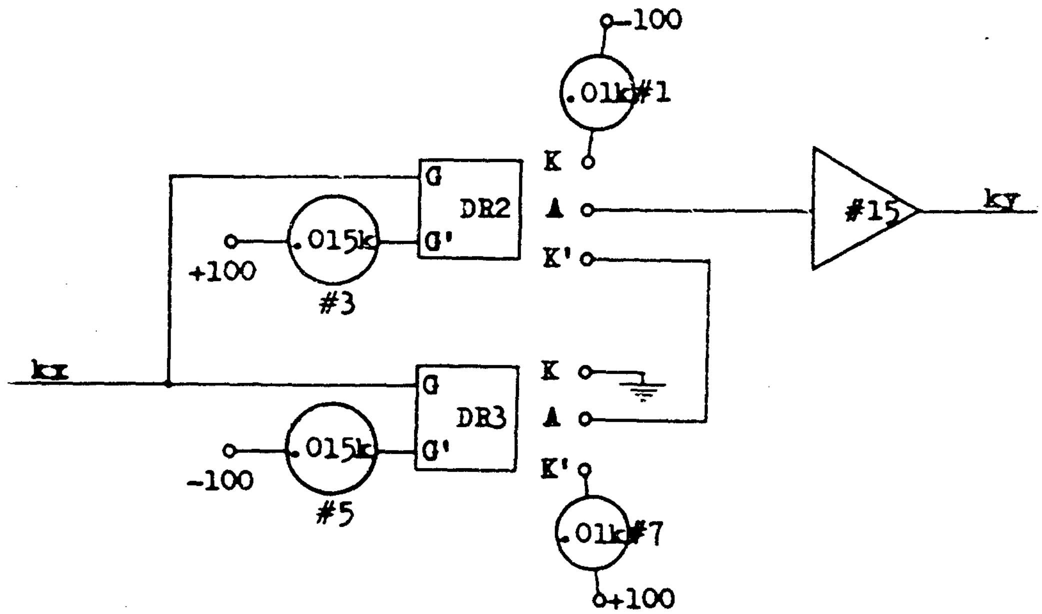

(b)

Figure 35

Mechanization of a relay with dead zone (d = 3, K = 1) with differential relays: (a) transfer characteristic, (b) analog computer circuit.

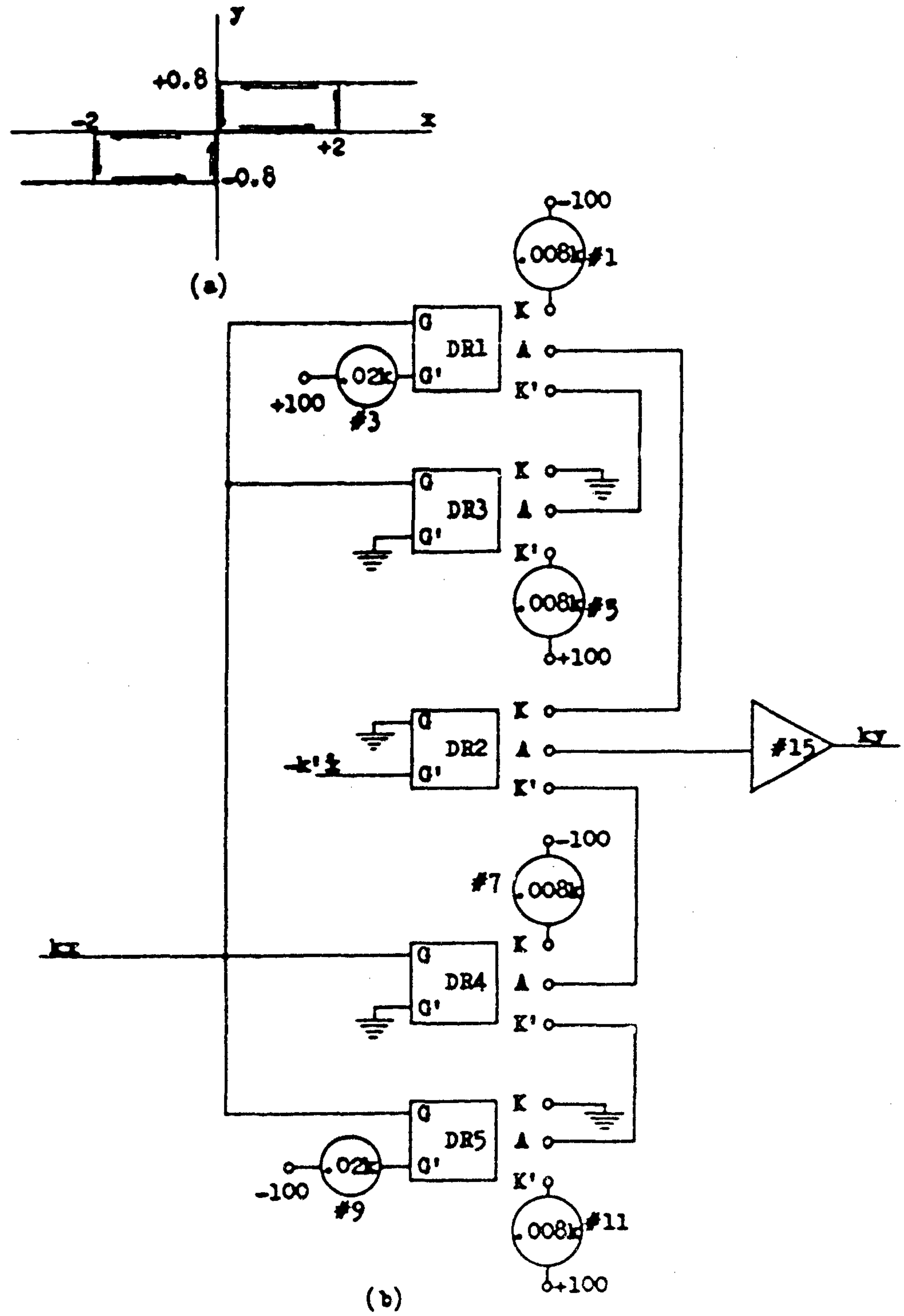

Figure 36

Mechanization of a relay with dead zone and hysteresis($d = h = 2$, $K = 0.8$) with differential relays: (a) transfer characteristic, (b) analog computer circuit.

Appendix D

Plots of the Corrected-Conventional Describing Functions

Figures 37 through 44 on the following pages are plots of the corrected-conventional describing functions derived in Appendix A and listed in Tables II through VIII in Chapter III. The plots are normalized as were those in Chapter IV, but the ordinate and the abscissa are the reciprocal of those in the graphs of Chapter IV. This is done so that the entire graph can be plotted, without having one scale or the other become infinite. (The ideal relay plot is an exception, but it is merely a straight line relationship.) Therefore each curve is a complete presentation of the corrected-conventional describing function for that nonlinearity.

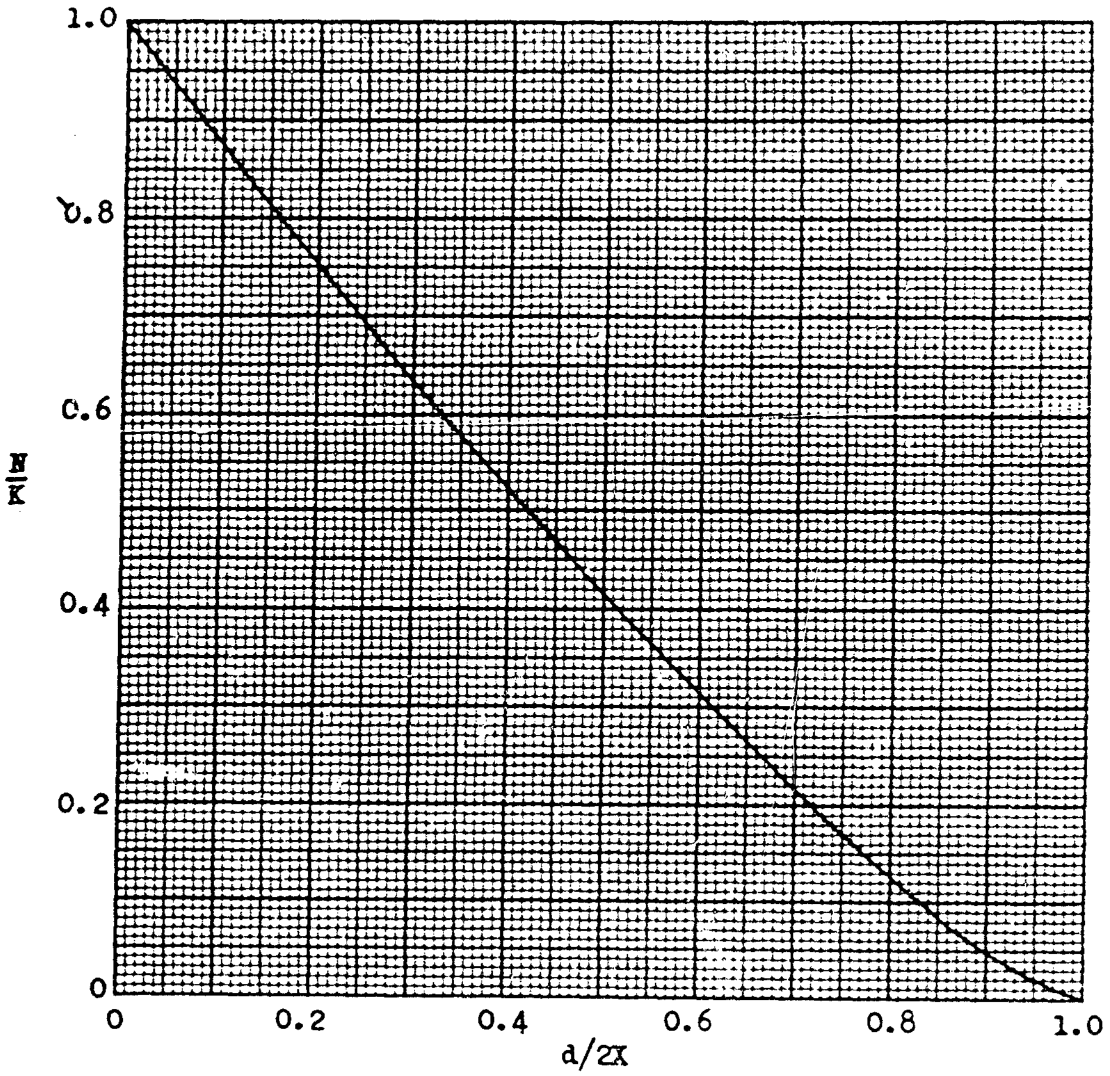

Figure 37

The non-dimensionalized corrected-conventional describing function of dead zone, where

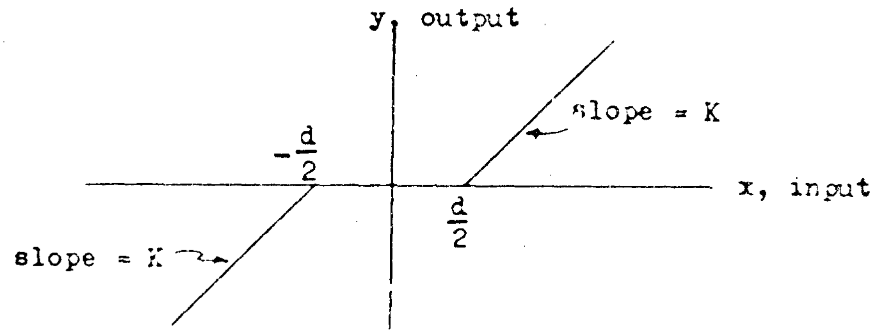

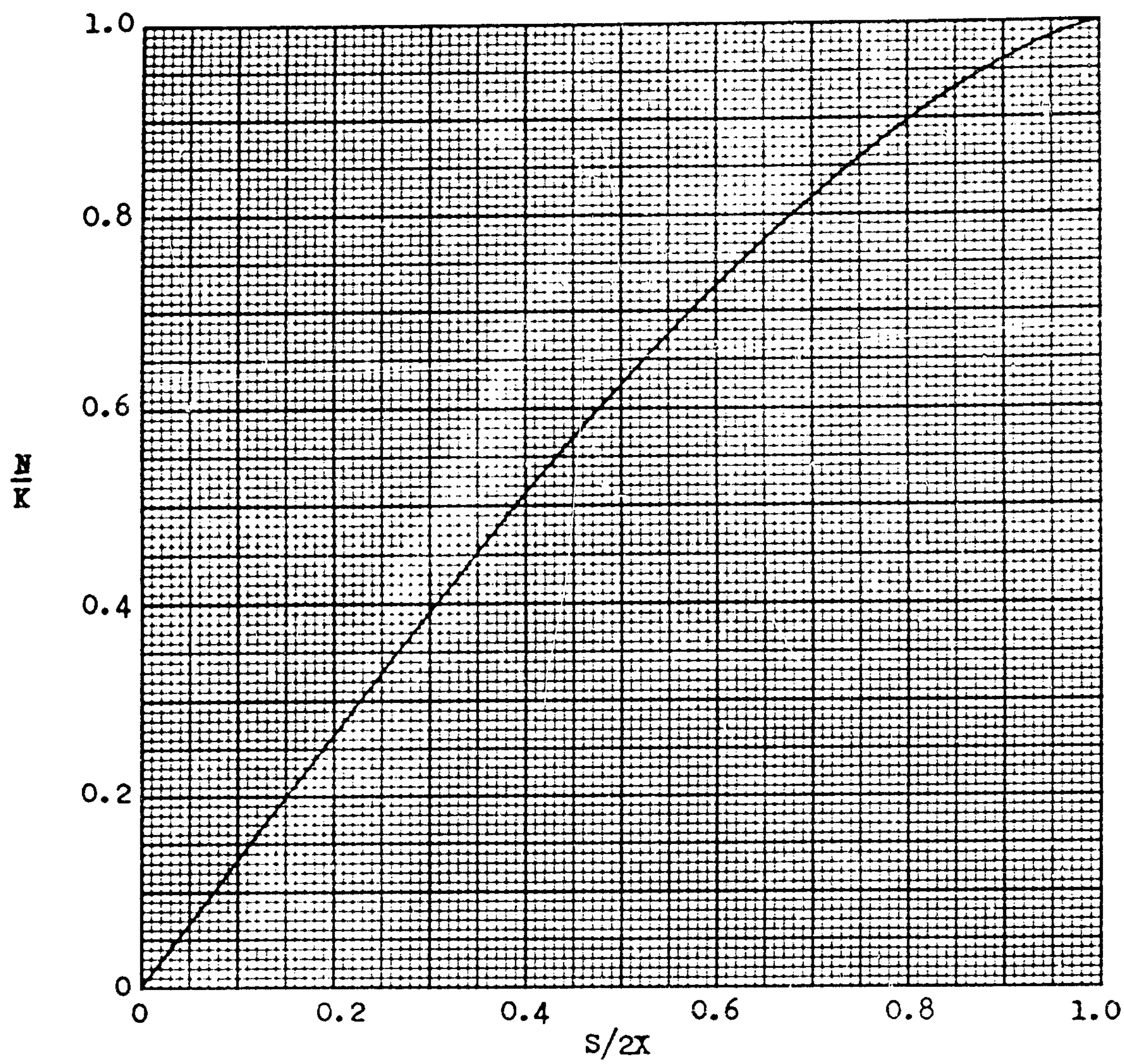

Figure 38

The non-dimensionalized corrected-conventional describing function of saturation, where

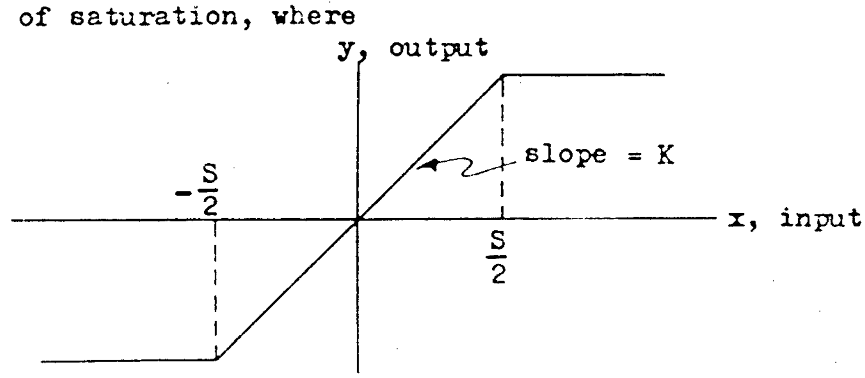

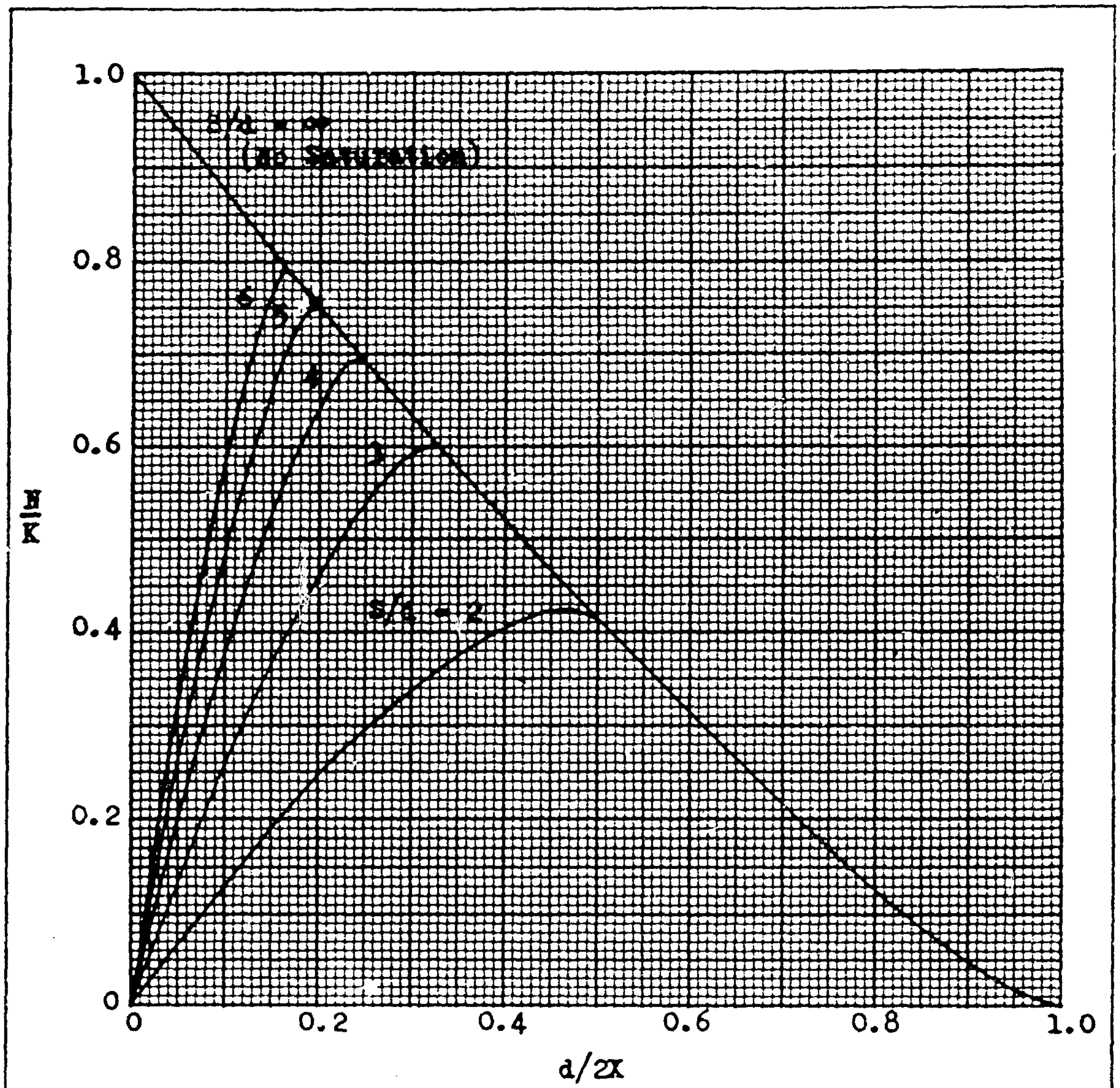

Figure 39

A family of curves for the non-dimensionalized corrected-conventional describing function of dead zone combined with saturation, where

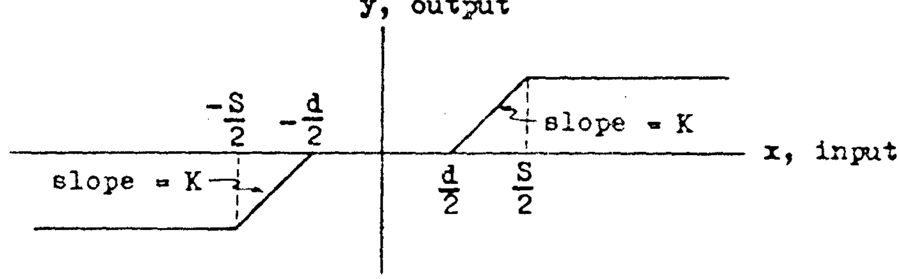

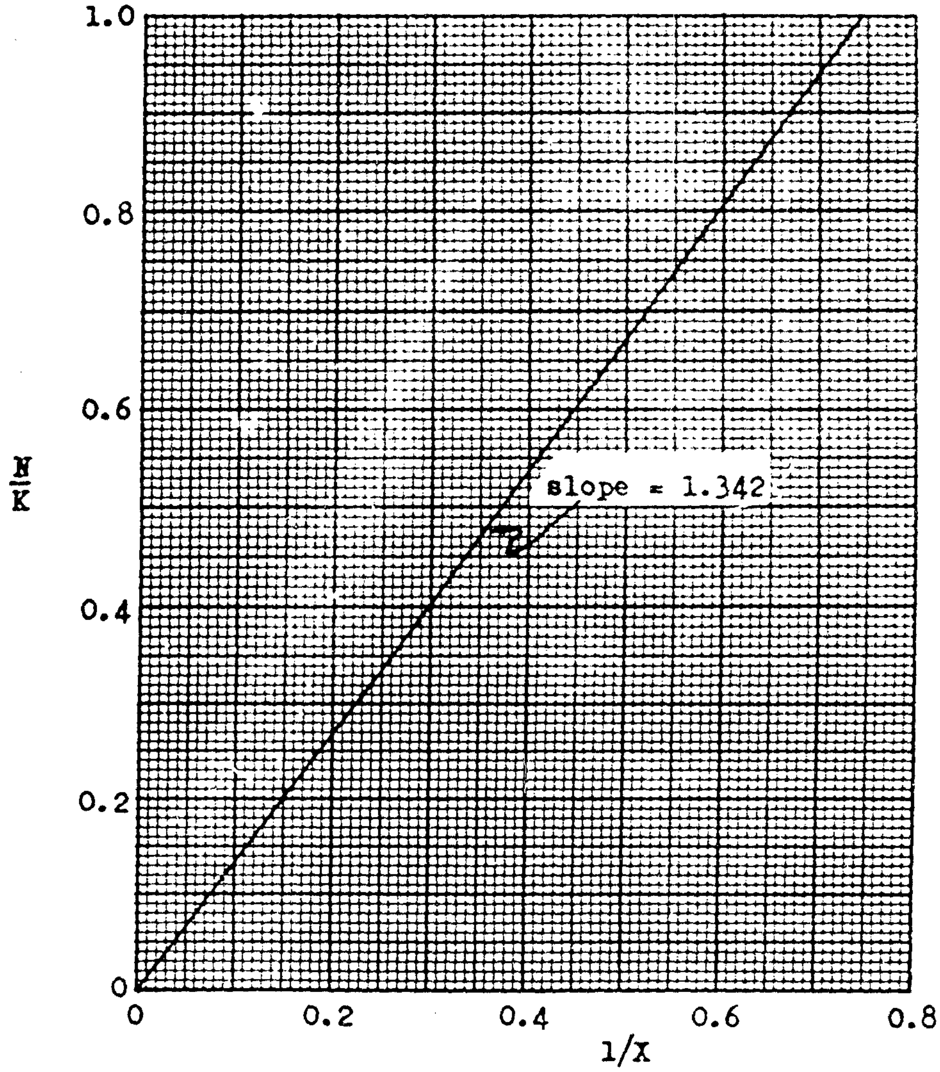

Figure 40

The non-dimensionalized corrected-conventional describing function of an ideal relay, where

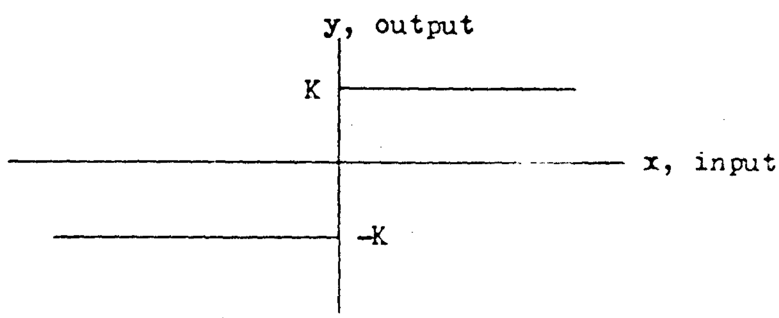

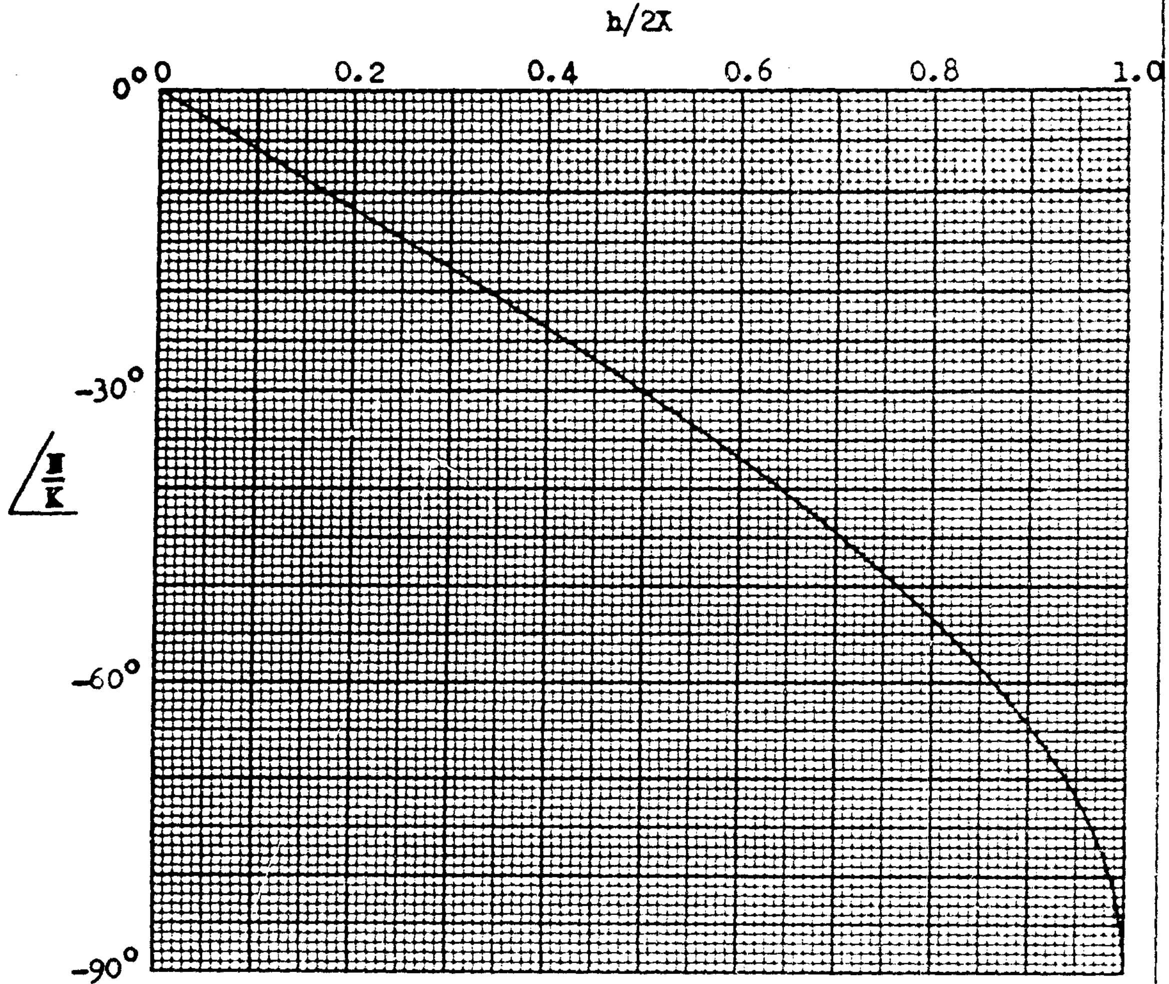

Figure 41

Angle of the corrected-conventional describing function of a relay with hysteresis, (the magnitude variation of the describing function of a relay with hysteresis is the same as for an ideal relay, and therefore the curve on the preceding page can be used) where

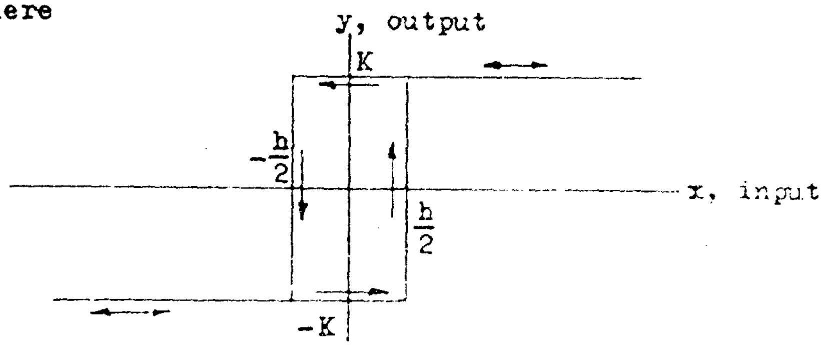

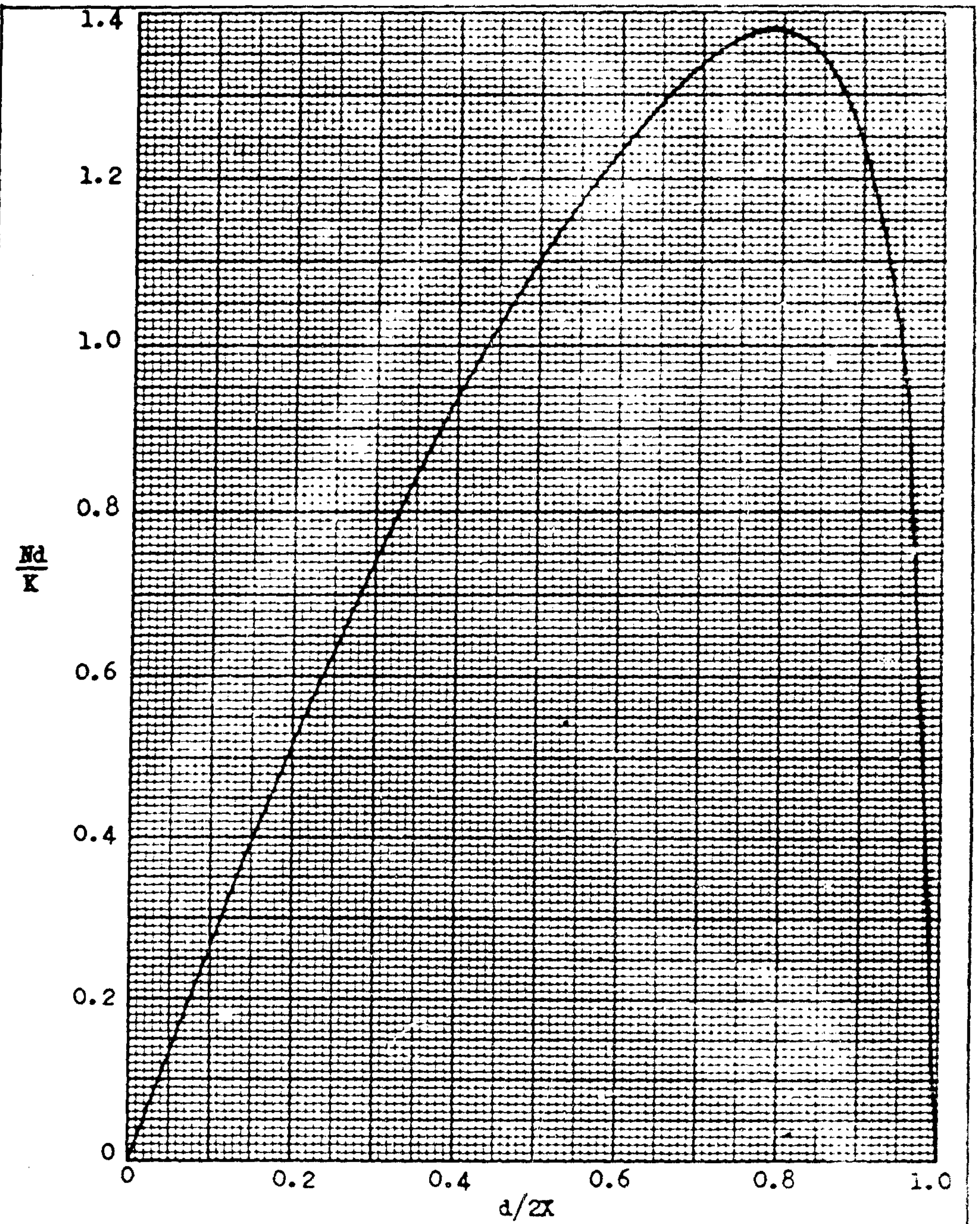

Figure 42

The non-dimensionalized corrected-conventional describing function of an ideal relay (3 position) or a relay with dead zone, where

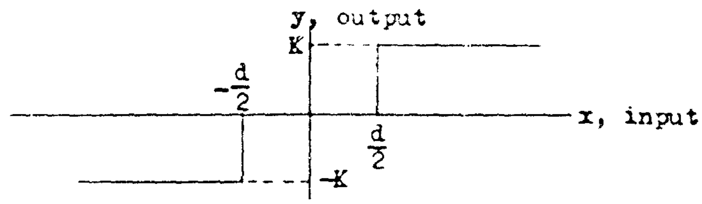

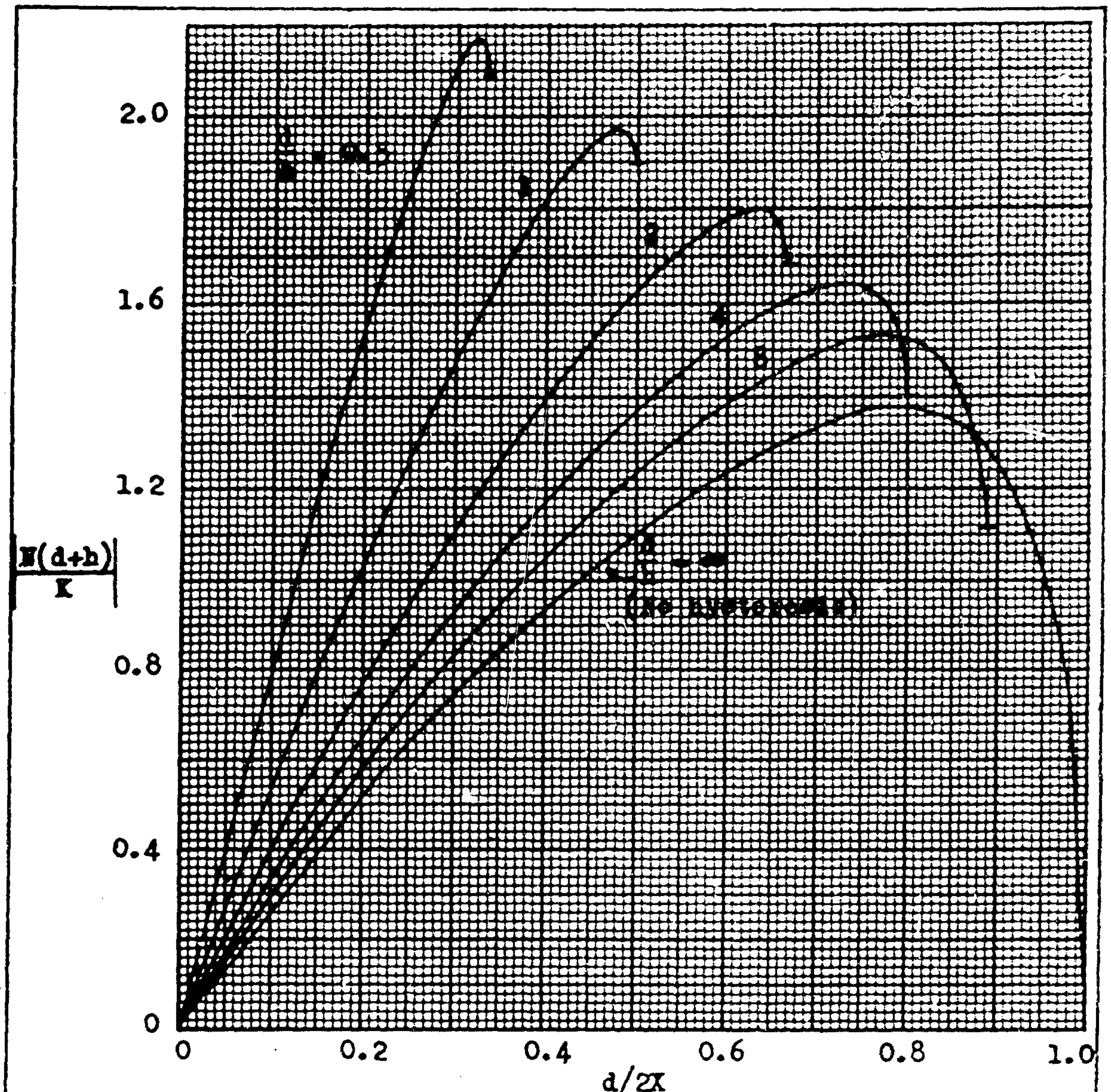

Figure 43

A family of curves for the magnitude of the non-dimensionalized corrected-conventional describing function of a relay with dead zone and hysteresis, where

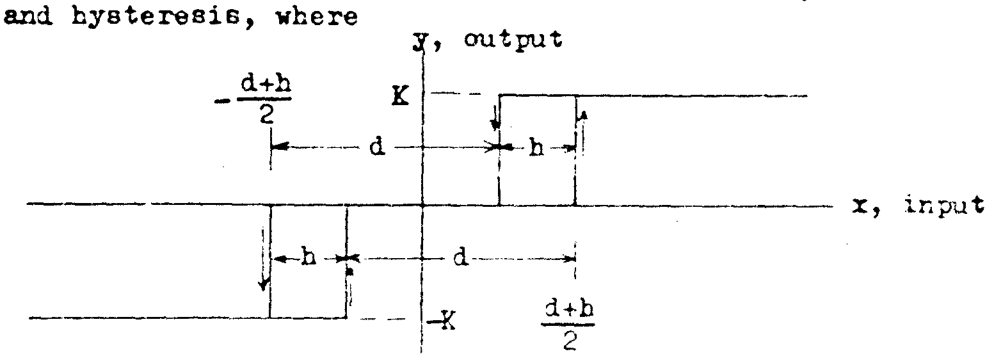

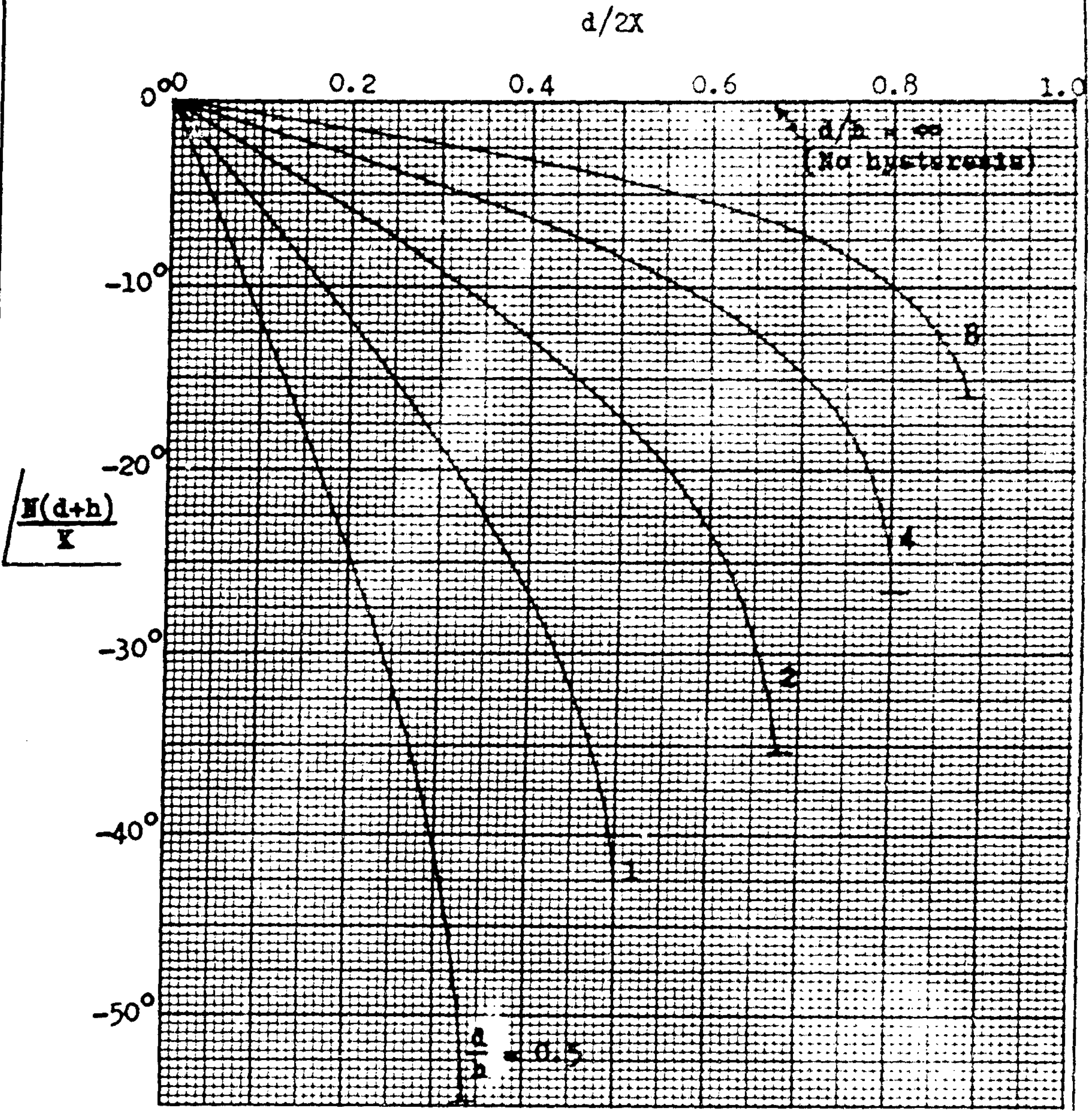

Figure 44

A family of curves for the angle of the non-dimensionalized corrected-conventional describing function of a relay with dead zone and hysteresis, where

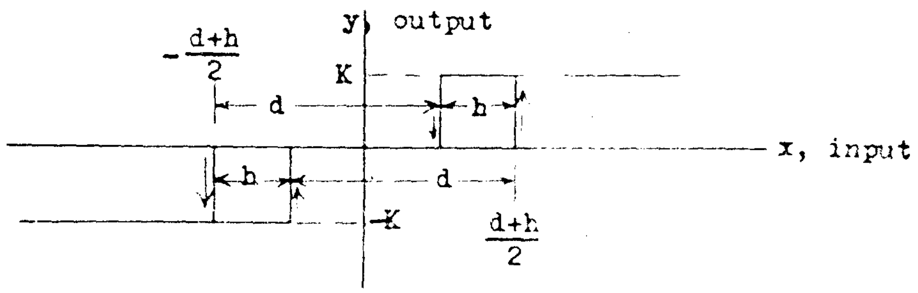

Appendix E

Other Describing Function Derivations

Although each of the 35 describing functions listed in Tables II through VIII in Chapter III was derived by the author, only the derivations of the important new describing functions are included in this paper (Appendices A and B). The following tables are included, therefore, for the scrutinizing reader who desires to check the derivations of the other describing functions.

Table XXIX

References where Derivations of the Conventional Describing Functions Used in this Study May Be Found.

Nonlinearity	Reference
Dead Zone	1:434
Saturation	1:435
Dead Zone + Saturation	1:436
Ideal Relay	9:457
Relay + Hysteresis	11:740
Relay + Dead Zone	9:458
Relay + Dead Zone + Hysteresis	9:459

Table XXX

References where Some of the Unconventional Describing Functions Used in this Study May Be Found.

Describing Function	Nonlinearity	Reference
New RMS	Saturation	3:1321
	Ideal Relay	2:382
	Relay + Dead Zone	2:382
Minimum Average Error	Ideal Relay	2:381

Appendix F

Analysis of the New RMS Describing Function

In Chapter III the new rms describing function is defined as

$$N = \frac{\left\{\frac{1}{\pi}\int_0^{2\pi}\left[y(t)\right]^2 \, d\omega t\right\}^{\frac{1}{2}} \angle -\phi}{X \angle 0^\circ} \tag{15}$$

where X = the amplitude of the sinusoidal input to the nonlinearity and y(t) = the actual output from the nonlinearity. By comparison with Eq (1) in Chapter I, Eq (15) indicates that the amplitude of the equivalent output sine wave from the nonlinearity has been chosen as

$$|Y| = \left\{\frac{1}{\pi}\int_0^{2\pi}\left[y(t)\right]^2 \, d\omega t\right\}^{\frac{1}{2}} \tag{49}$$

That is, the equivalent output sine wave has the same rms value as the actual output of the nonlinearity. If y(t) is an odd-harmonic, odd-periodic function, as is often the case, and is expanded in a Fourier Series, then Eq (49) becomes

$$Y = \left[\frac{1}{\pi}\int_0^{2\pi}(Y_1 \sin\omega t + Y_3 \sin 3\omega t + Y_5 \sin 5\omega t + \ldots.)^2 \, d\omega t\right]^{\frac{1}{2}}$$

$$= \left[\frac{1}{\pi}\int_0^{2\pi}(Y_1^2 \sin^2\omega t + 2Y_1Y_3 \sin\omega t \sin 3\omega t + 2Y_1Y_5 \sin\omega t \sin 5\omega t + \ldots + Y_3^2 \sin^2 3\omega t + 2Y_3Y_5 \sin 3\omega t \sin 5\omega t + \ldots + Y_5^2 \sin^2 5\omega t + \ldots.) \, d\omega t\right]^{\frac{1}{2}} \tag{50}$$

$$\text{but} \int_0^{2\pi} \sin m\omega t \sin n\omega t \, d\omega t = 0 \qquad \text{if } m \neq n \tag{51}$$

$$\text{and} \int_0^{2\pi} \sin^2 n\omega t \, d\omega t = \pi \tag{52}$$

$$\text{Therefore,} \quad |Y| = \left[\frac{1}{\pi}\left(Y_1^2\pi + Y_3^2\pi + Y_5^2\pi + \ldots.\right)\right]^{\frac{1}{2}}$$

$$= \left(Y_1^2 + Y_3^2 + Y_5^2 + \ldots.\right)^{\frac{1}{2}} \tag{53}$$

Stating the above analysis in words, the new rms describing function, in effect, takes as the amplitude of the equivalent output sine wave from the nonlinearity, the square root of the sum of the squares of all the Fourier coefficients in the Fourier Series expansion of the actual output of the nonlinearity.